



Tomas Bata University in Zlín

Faculty of Technology

Doctoral Thesis

Dialdehyde cellulose preparation, characterization and utilization as crosslinking agent for PVA

**Příprava, charakterizace a využití dialdehydu celulózy jako
síťovacího činidla pro PVA**

Author: **Ing. Lukáš Münster**

Study programme: Chemistry and Materials Technology (P2808)

Study course: Technology of Macromolecular Compounds (2808V006)

Supervisor: Assoc. Prof. Ing. *et* Ing. Ivo Kuřitka, Ph.D. *et* Ph.D.

Consultant: Mgr. Jan Vícha, Ph.D.

Zlín, August 2018

© Lukáš Münster, August 2018

ACKNOWLEDGEMENT

Foremost, I would like to express my deepest gratitude to my supervisor, Assoc. Prof. Ing. *et* Ing. Ivo Kuřitka, Ph.D. *et* Ph.D., for the continuous support during my doctoral study and research, for his patience, motivation, enthusiasm, and immense knowledge. His guidance and encouragement helped me in all the time of research and writing of this Thesis.

Besides my supervisor, my sincere thanks belong to my consultant, Mgr. Jan Vícha, Ph.D., for help with NMR analysis, valuable advices and fruitful discussions regarding the topic of this Thesis, and further widening of the knowledge and understanding beyond the scope of the topic.

My gratitude goes to all my colleagues and friends from the Centre of Polymer Systems who helped me throughout my doctoral study with special mention to Ing. Jiří Klofáč, Ing. Pavel Kucharczyk, Ph.D. and Ing. Milan Masař, for introduction into measurement techniques and help with experimental work.

Special thanks belong to my family for all the support, patience, encouragement and endless love.

This Doctoral Thesis was supported by CPS project no. CZ.1.05/2.1.00/03.0111, CPS+ project no. LO1504 and CPS – strengthening research capacity project no. CZ.1.05/2.1.00/19.0409. Furthermore, this work was supported by internal grant agency of TBU in Zlín projects no. IGA/CPS/2015/005, no. IGA/CPS/2016/006 and no. IGA/CPS/2017/007.

The financial support granted to my research work by the funding providers is partially addressed and acknowledged in the respective places in my published or submitted papers whenever the opportunity to do so was. Here, I would like to thank the Centre of Polymer Systems and the Faculty of Technology of the Tomas Bata University in Zlín for the financial support during my studies.

CONTENTS

ABSTRACT	1
ABSTRAKT	2
KEY WORDS/KLÍČOVÁ SLOVA	3
1. INTRODUCTION.....	4
2. CELLULOSE	7
2.1 Structure and properties	9
2.2 Derivatives	13
2.2.1 Oxidation induced derivatives	14
2.2.2 Applications of oxycellulose derivatives.....	16
3. DIALDEHYDE CELLULOSE	17
3.1 Preparation	17
3.2 Structure and properties	19
3.3 Applications of DAC	24
4. POLY(VINYL ALCOHOL) BASED HYDROGELS.....	25
4.1 PVA hydrogel formation.....	26
4.1.1 Physical routes	26
4.1.2 Chemical routes	27
4.2 Characterization and network parameters.....	28
4.3 Applications of PVA hydrogels	29
5. AIM OF DOCTORAL THESIS.....	31
6. EXPERIMENTAL	32
6.1 Materials.....	32
6.2 Sample preparation	33
6.3 Experimental methods	39
7. RESULTS AND DISCUSSION	44
7.1 Pilot study	44
7.1.1 Characterization of uncrosslinked PVA	44

7.1.2 FT-IR and TGA analysis of PVA/DAC xerogels (pilot study).....	45
7.1.3 PVA/DAC network parameters and macroscopic observation (pilot study).....	46
7.1.4 Summary of the pilot study	49
7.2 DAC study	50
7.2.1 Basic DAC characterization	51
7.2.2 Determination of solubilized DAC composition	58
7.2.3 Molecular weight distribution study of DAC – focused on aging	64
7.2.4 Study of DAC solubilization process	67
7.3 Hydrogel study	78
7.3.1 Characterization of PVA/DAC.....	78
7.3.2 Structural and functional characterization PVA/DAC.....	83
7.3.3 Correlation between measured characteristics of PVA/DAC and role of catalyst system.....	89
7.3.4 Comparative PVA crosslinking study of DAC and GA	94
8. CONCLUDING SUMMARY	102
9. SUMMARY OF CONTRIBUTIONS TO SCIENCE AND PRAXIS	106
REFERENCES.....	107
LIST OF FIGURES	127
LIST OF TABLES	132
LIST OF ABBREVIATIONS.....	134
LIST OF SYMBOLS	136
LIST OF UNITS	138
LIST OF PUBLICATIONS	140
CURRICULUM VITAE.....	142

ABSTRACT

Solubilized dialdehyde cellulose (DAC) obtained from alpha cellulose modification via simple oxidation by sodium periodate was prepared and characterized. Immediately after preparation, solubilized DAC was stabilized by low pH in order to suppress degradation. The influence of DAC solubilization and its aging under acidic conditions on DAC properties was analysed. Molecular mass distribution (GPC), reactive aldehyde group content (titrimetry), crystallinity (XRD), vibrational spectra (FT-IR), thermal stability (TGA) and structural composition (LC-MS, NMR, SEM) were of the main interest. Furthermore, DAC was utilized as a suitable crosslinking agent for poly(vinyl alcohol) (PVA). The reactive aldehyde groups of DAC formed on the C2 and C3 carbons of anhydroglucopyranose unit serve as crosslinking counterparts for hydroxyl groups of PVA under acidic conditions. Appropriate catalyst system must be introduced to ensure formation of crosslinked acetal/hemiacetal bridged network of hybrid PVA/DAC hydrogels. Initially, two concentrations of catalyst system and different drying temperatures were chosen and their influences on the PVA/DAC xerogel and hydrogel properties were investigated by several analytical methods (FT-IR, XRD, TGA, network parameters etc.). Next, fresh and aged acidic DAC and two chemically distinct catalyst systems were employed in the crosslinking of PVA. The crosslinking effectivity and efficiency of these crosslinking systems (crosslinker + catalyst) were investigated in the terms resulting PVA/DAC hydrogel properties, i.e. crystallinity (XRD) and stiffness (tensile testing) of the dried gel, furthermore structural and functional network parameters of swollen gels were characterized. Finally, comparison between DAC and glutaraldehyde (GA) crosslinker was carried out using broad range of these PVA crosslinkers with subsequent evaluation of network parameters of prepared PVA/DAC and PVA/GA hydrogels. Acidified DAC exhibited the capability to act as an effective crosslinker for PVA with the resulting hydrogel properties dependent on the choice of concentration of catalyst system and the drying temperature. Moreover, it was found that the properties of PVA/DAC are governed by the molecular weight of used DAC. The acidic condition retains DAC usability as a crosslinking agent even after 28 days from its preparation. It was found that DAC possesses exceptional crosslinking efficiency at very low concentrations compared to GA and enables formation of hydrogels of very high swelling capacity. This behaviour arises from DAC macromolecular character as it forms “two-phase” network topology containing regions of very high crosslink density adjacent to DAC chains embedded in a matrix formed by linear parts of PVA macromolecules.

ABSTRAKT

Byl připraven a charakterizován solubilizovaný dialdehyd celulózy (DAC) získaný modifikací alfa celulózy pomocí jodistanové oxidace. Za účelem potlačení degradace byl solubilizovaný DAC stabilizován nízkým pH ihned po jeho přípravě. Byl zkoumán vliv solubilizace a stárnutí v kyselém prostředí na vlastnosti DAC. Hlavními předměty zájmu byla zkoumání distribuce molekulových hmotností (GPC), obsahu reaktivních aldehydových skupin (volumetrie), vibračních spekter (FT-IR), tepelné stability (TGA) a strukturního složení (LC-MS, NMR, SEM). Dále byl DAC použit jako síťovací činidlo pro polyvinylalkohol (PVA). Reaktivní aldehydové skupiny DAC vytvořené na pozicích C2 a C3 anhydroglukopyranózové jednotky slouží jako síťovací protějšky k hydroxylovým skupinám PVA v kyselých podmínkách. K zajištění vzniku sítě hybridního PVA/DAC hydrogelu tvořeného acetalovými/hemiacetalovými můstky musí být zaveden vhodný katalytický systém. Zpočátku byl zkoumán vliv dvou vybraných koncentrací katalytického systému a zvolených teplot sušení na vlastnosti PVA/DAC xerogelů a hydrogelů pomocí několika analytických metod (FT-IR, XRD, TGA a parametry sítě). Poté se k síťování PVA použil kyselý roztok DAC o různém stáří společně se dvěma chemicky odlišnými katalytickými systémy. Síťovací efektivita a účinnost těchto různých síťovacích systémů (síťovadlo + katalyzátor) byly zkoumány z hlediska vlastností výsledných PVA/DAC hydrogelů, tj. krystalinity (XRD) a tuhosti (tahové zkoušky) vysušeného gelu, a dále strukturních i funkčních parametrů nabobtnalé sítě. Nakonec bylo provedeno srovnání mezi síťovacími činidly DAC a glutaraldehydem (GA) v širokém rozsahu jejich koncentrací s následným vyhodnocením parametrů sítě připravených PVA/DAC a PVA/GA hydrogelů. DAC udržovaný při nízkém pH vykazuje schopnost působit jako účinné síťovací činidlo pro tvorbu PVA hydrogelů o výsledných vlastnostech závislých na koncentraci katalytického systému a teplotě sušení. Bylo zjištěno, že vlastnosti PVA/DAC jsou řízeny molekulovou hmotností použitého DAC. Podmínky nízkého pH zachovávají použitelnost DAC jako síťovacího činidla i po 28 dnech od jeho přípravy. DAC vykazuje výjimečnou účinnost síťování PVA ve velmi nízkých koncentracích ve srovnání s GA a umožňuje tak tvorbu hydrogelů s velmi vysokou schopností bobtnání. Toto chování je projevem makromolekulárního charakteru DAC, jenž vytváří "dvoufázovou" topologii sítě obsahující oblasti s velmi vysokou hustotou zesíťování PVA v blízkosti řetězců DAC vložených do matrice tvořené lineárními částmi PVA makromolekul.

KEY WORDS/KLÍČOVÁ SLOVA

English

Cellulose; periodate oxidation; dialdehyde cellulose; solubilization; aging; glutaraldehyde; poly(vinyl alcohol); crosslinking; hydrogel; network parameters

Czech

Celulóza; jodistanová oxidace; dialdehyd celulózy; solubilizace; stárnutí; glutaraldehyd; polyvinylalkohol; síťování; hydrogel; parametry sítě

1. INTRODUCTION

Biopolymer-based materials are at the peak of interest for many scientists due to the growing demand of society to reach the goal of sustainable development via utilization of renewable and worldwide occurring substances with presumable lower impact on environment and living organisms. These materials benefit from their natural origin and find wide variety of applications in the areas of medical, packaging, food and agricultural sector. Biopolymer is by definition a macromolecular substance, which is naturally synthesized, often biodegradable and usually exhibits low toxicity. Cellulose, starch, chitosan, gluten or collagen meets this definition and therefore they are exhaustively used in a plethora of various fields. [1] These plant- and animal-based biopolymers commonly exhibit hydrophilicity, which imparts water retention capability and thus these materials are frequently used as additives or just as pure substances themselves. The valuable property of water retention emerges as result of presence of macromolecules containing hydrophilic side groups. If such macromolecules are joined in three-dimensional network, they are generally referred to as hydrogels [2]. Hydrogels should by definition possess (i) macromolecules of at least one polymeric substance joined by covalent bonds, and/or (ii) macromolecular entanglements resulting in physically crosslinked units, (iii) strong van der Waals interactions or hydrogen bonds between polymer chains, or (iv) crystallites composed of at least two macromolecular chains. [3]

Hydrogels can be prepared by the combination of appropriate biopolymer or biopolymer-based substance with synthetic polymer. Based on the natural origin of biopolymer component, these materials can be further employed in the field of biomedical sciences as they can mimic the living tissue structure; [4–6] or possess modified biodegradability profile. [7] Furthermore, if hydrogels are intended for utilization in pharmaceuticals they should exhibit low toxicity and biocompatibility so they can be used as wound dressing materials containing active substance for improved healing of wounds, various body implants such as cartilages, drug delivery systems with release profile dependent on external stimuli, scaffolds for better tissue regeneration and many others. [8–11]

Poly(vinyl alcohol) (PVA) is one of the synthetic polymers suitable for the preparation of hydrogels. There are several approaches how to achieve crosslinked PVA-based hydrogels utilizing different routes, which further determine physico-chemical properties of such material as well as the nature of formed polymer network. For example, PVA hydrogels can be obtained by physical crosslinking (reversible hydrogels) induced by cyclic freeze-thawing or high temperature/energy treatment [12]. However, such crosslinking process exhibits relatively poor definition of the chemical reaction mechanism although it is advantageous as no additive compound is needed. Next, the hydroxyl

groups of PVA enable formation of chemical crosslinks (permanent hydrogel) when various aldehydes, anhydrides or boric acid are used as crosslinking agents. [1, 12–14] The disadvantage of this approach lies in the relatively high toxicity of these low molecular crosslinkers. Particularly, it is their high reactivity and synthetic origin (except boric acid) that causes high cytotoxicity and enables readily penetration through various portals of entry into living organism. For this reason, the residues of such compounds must be removed from the hydrogel matrix prior to final application to prevent undesirable biological response.

Thus, to fulfil the requirements on the fabrication of non-toxic and biocompatible hydrogels suitable for pharmaceutical or medical applications, it is preferable to employ crosslinking agent based on or derived from biopolymers. This allows to obtain materials with low toxicity as well as to reduce the impact on environment and living organisms. Partial progress in this field was accomplished by introducing naturally available low toxic crosslinker Genipin. This substance is produced by the enzymatic extraction from the fruits of *Gardenia Jasminoides*. However, the drawbacks of its mass utilization can be found in its limited availability and therefore relatively high cost. [15] It is more desirable to perform specific derivatization of abundant and easily available biopolymers and thus introducing new functional groups on polymer backbone. One of many potential candidates for this purpose is cellulose as it offers broad possibility of modifications resulting in number of various derivatives. [16]

In the theoretical section of this Thesis, the literature review on the topic of cellulose and its oxidation, especially dialdehyde cellulose (DAC), was carried out. Furthermore, background of PVA hydrogel preparation, characterization and utilization is discussed. In the first part of experimental section, dialdehyde cellulose (DAC) prepared from alpha cellulose by simple sodium periodate oxidation of hydroxyl groups to aldehyde groups was utilized as a crosslinking agent for PVA. The results of this pilot study have shown potential of DAC towards these purposes. [17] DAC solution was blended with commercially available poly(vinyl alcohol), forming PVA/DAC hydrogels. Effects of two different concentrations of catalyst system based on the mixture of sulfuric acid, methanol and acetic acid were studied, as such mixture represent one possible catalyst system for crosslinking reactions of aldehyde moiety. [18] To optimize the process of PVA/DAC preparation, the influence of drying temperature on its physical properties was investigated. In the second part, insolubilized and solubilized form of prepared DAC was investigated with respect to crosslinking application. Furthermore, the process of DAC solubilization was investigated and the products were analysed during four weeks of its aging. Due to known DAC sensitivity towards alkaline environment, the DAC solution was kept under acidic condition for the first time. The last part of this Thesis deals with the broader study on application of DAC as a PVA crosslinking agent. This includes utilization of fresh and aged DAC with subsequent analysis of

properties of prepared PVA/DAC hydrogels. Moreover, two chemically distinct catalyst systems were introduced to initiate crosslinking reactions and their influence was evaluated. Next, in order of DAC crosslinking effectivity and efficiency assessment, this novel macromolecular crosslinking agent was utilized in broad concentration range and compared to commonly used low molecular crosslinker glutaraldehyde in the terms of network parameters and the properties of resulting xerogels and hydrogels.

2. CELLULOSE

Cellulose is undoubtedly the most abundant and widely used organic macromolecular substance in the world. It represents linear macromolecular chains consisting of D-anhydroglucopyranose units linked by β -1,4-glycosidic bonds. Cellulose occurs naturally in various species of higher vascular plants (seed hairs of cotton – 95 %; bast fibres of flax, hemp, sisal, jute and ramie – 60 to 80 %; wood – 40 to 55 %), lower non-vascular plants (algae, lichen and fungi) and other organisms like tunicates and bacteria. For this reason, it is identified as a renewable biopolymer, a substance synthesized by living organisms.

The presence of cellulose is often accompanied by several other natural substances including numerous saccharides, e.g. maltose and xylose; polysaccharides hemicellulose and lichenin and other macromolecular substances such as lignin. [19] The cellulose content of some of these important and industrially utilized sources is given in Table 1.

Table 1 Cellulose content of naturally occurring species. [19–22]

Source	Cellulose content (%)
Cotton	95
Flax (retted)	71
Flax (untreated)	63
Hemp	70
Sisal	73
Jute	71
Ramie	76
Softwood	40–44
Hardwood	43–47
Algae	20–30
Tunicates	3–48
Bacteria	37

Generally, it is presumed it makes up at least one third of all the vegetable matter in the world. Among above mentioned cellulose containing materials, there are two most important and commercially successful sources, wood and cotton seed hairs. The rest shows relative insignificant importance due to difficulties in collection, complicated isolation from non-cellulosic moieties or quality/quantity limitations. Subsequently, all of these factors negatively influence the final cost of cellulose. Figure 1 represents the flow of cellulose of wood and cotton origin through diverse converting operations into its chief end uses.

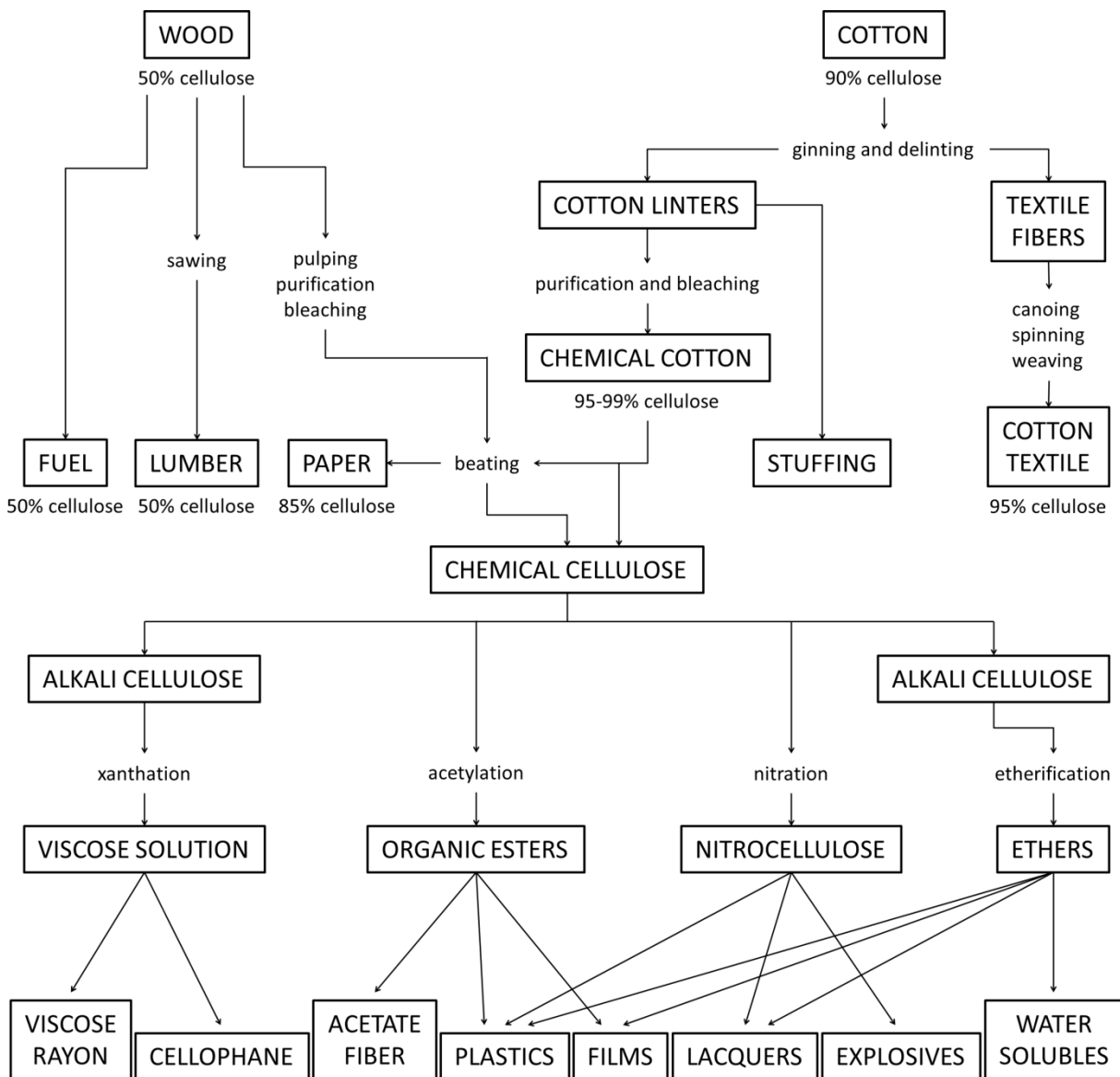


Figure 1 Converting operations of cellulose obtained from wood and cotton (adapted from Ott *et al.* 1954). [16]

Due to industrial importance of cellulose and its many derivatives it has been the subject of an enormous amount of investigation on its occurrence, formation, isolation and purification, chemical and physical structures and properties. From historical point of view, the term “cellulose” itself was coined for the first time by Anselme Payen (1838), the French agriculturist and pioneer in cellulose research who used this expression for sufficiently purified plant tissue. Other numerous researchers continued to use the term cellulose to describe plant cell wall material and their investigations further led to identification of basic principles of polymer chemistry. The advances in the research, identification and characterization of cellulose is best seen in the work of Emil Ott *et al.* (1954), which is considered as a magnificent omnibus summarizing historical evolution

of cellulose and cellulose derivatives research and is a valuable source of information on this topic. [16]

As this work is focused on the specific cellulose derivative, its characterization and application, only the most important properties and structural arrangements of cellulose will be mentioned in the following chapter.

2.1 Structure and properties

On molecular level, cellulose macromolecules consist of β -1,4-linked D-anhydroglucopyranose units (AGU) established in chair conformation. Figure 2 depicts molecular structure of cellulose with marked parts: (i) β -1,4-glycosidic bond, (ii) AGU, (iii) non-reducing end and (iv) reducing end of cellulose macromolecule and (v) cellobiose unit. [23] The last one mentioned is often identified as the fundamental unit because the most crystal structures of cellulose poses twofold helical conformation, [24] i.e. two AGUs per turn of helix. Similarly as for all 1,4-linked glucans, non-reducing and reducing end contains an unsubstituted hemiacetal and additional hydroxyl group at C4, respectively. [23]

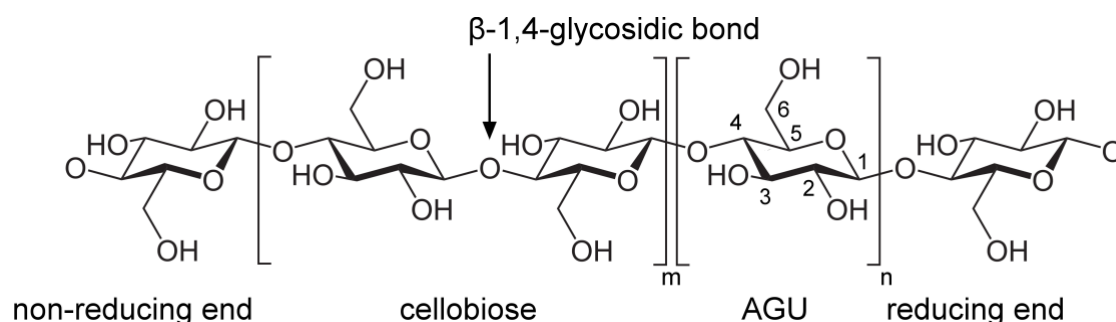


Figure 2 Representation of cellulose constituted of cellobiose units or AGUs (with atom numbering) via β -1,4-glycosidic bonds, non-reducing and reducing end of polymer. [Own resource.]

Another molecular level parameter relevant for the characterization of cellulose and polymers in general is the degree of polymerization (DP), an average number of monomeric units (n) in one macromolecular chain. DP of cellulose is strongly dependent on its source and treatment such as purification, milling etc. In general, processing of cellulose reduces the DP, thus regenerated cellulose possesses relatively low DP compared to that of native cellulose. The values of DP are ranging from 100 for cellulose powders to approximately 44 000 for green algae genus *Valonia*. [23] DP values of selected cellulose sources are mentioned in Table 2.

Table 2 Degree of polymerization of selected cellulose sources. [19, 23]

Cellulose	DP (n)
Wood of various species	6 000–10 000
Pulp	500–2 000
Sulfate pulp	950–1 300
Chemical pulp bleached	700
Cotton	10 000–20 000
Cotton linters bleached	1 000–5 000
<i>Valonia</i>	25 000–44 000
Bacterial cellulose	4 000–6 000
Ramie	10 000
Textile flax	9 000
Rayon	300–500
Cellophane	300
Cellulose acetate	200–350
Cellulose powder	100–300

From the supramolecular level point of view, pure cellulose has been identified in the number of different crystal polymorphs (type **I**, **II**, **III** and **IV**) defined by their unit cell parameters. [25]

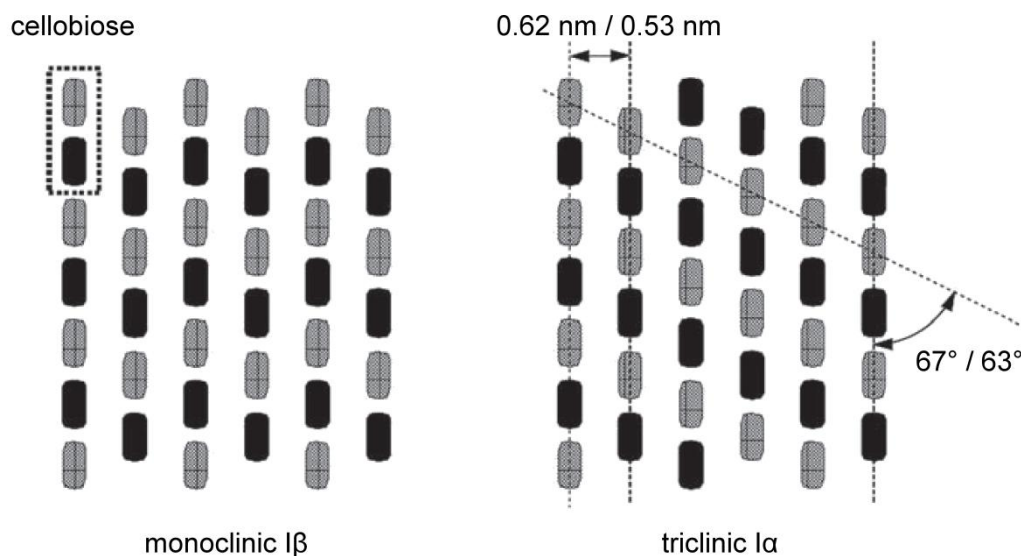


Figure 3 Allomorphs **Iα** and **Iβ** of cellulose polymorph type **I**, chain arrangements with distances and angles for 100/010 faces. [19, 26]

Type **I** exhibits distinctive X-ray pattern of unique crystalline lattice common for almost all sources of native cellulose. Moreover, type **I** can be further divided into two crystalline allomorphs **Iα** (monoclinic) and **Iβ** (triclinic), where **Iα** is metastable and can be converted into thermodynamically more stable **Iβ**.

[23] An example of occurrence of type **I α** is the group of freshwater algae *Glaucozystis* containing around 90 % of **I α** allomorph. On the other side, type **I β** is a domain of higher vascular plants such as ramie and cotton. [27] The difference between the crystal lattice of these two allomorphs can be seen in Figure 3.

Polymorph type **II** represents crystalline structure of cellulose, which underwent dissolution and precipitation (i.e. regeneration), or alkali treatment and subsequent washing (i.e. mercerization). Since type **II** is even more thermodynamically stable form of cellulose than type **I**, it is impossible to convert type **II** back to type **I**.

Fairly stable cellulose polymorph **III** can be formed by swelling of type **I** or type **II** (**III_I**, **III_{II}**) using amines or liquid ammonia with subsequent anhydrous removal of swelling agent. Type **III_I** is well-known, however type **III_{II}** is more or less hypothetical as nothing definite is known about it. [23]

The last recognized formation of crystal lattice of cellulose, type **IV**, can be obtained by annealing type **III** in glycerol. Again, it can be formed in two subclasses (**IV_I**, **IV_{II}**) depending on the input material (**III_I**, **III_{II}**). The strongly disordered structure of **IV_I** is somewhat similar to structure of type **I**. [23] Its presence has been reported in some plants. [28]

Cellulose polymorphism and the conversions between different crystal polymorphs is schematically depicted in Figure 4 along with the cell units proposed for types **I β** , **II**, **III_I**, and **IV_I** with units in angstroms (Å) and γ angle in degrees. It should be noted, that unit cell is the fundamental building block of a crystal defined by (i) three vectors of crystallographic axes (a , b , c) forming the edges of parallelepiped and (ii) angles between these vectors (α between b and c , β between a and c , γ between a and b). [23]

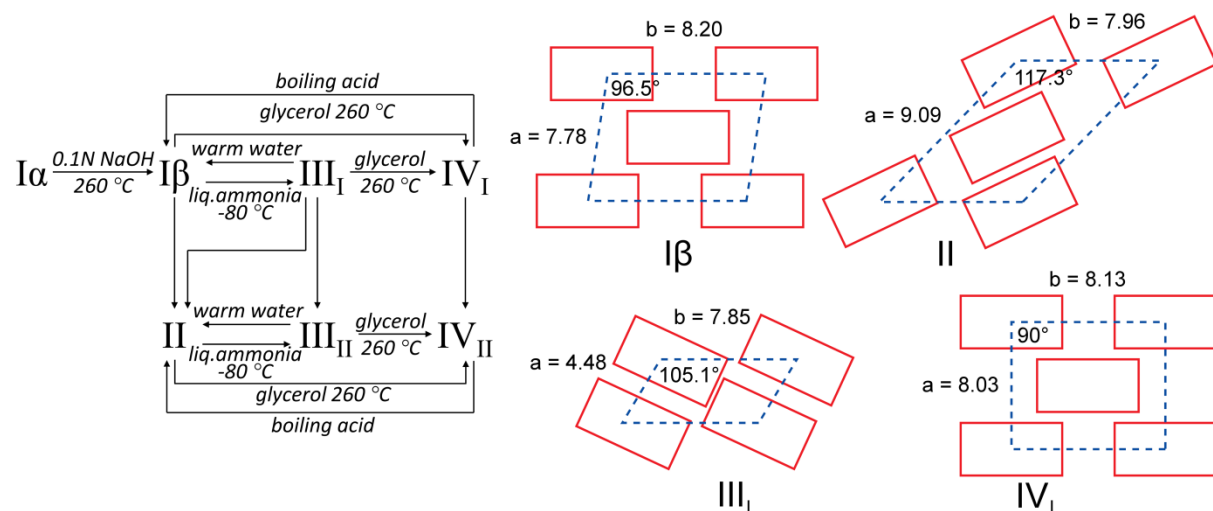


Figure 4 Cellulose crystal polymorphism and possible conversions between different types (left), [29] cell units for cellulose types **I β** , **II**, **III_I**, **IV_I**. The c dimension perpendicular to the drawing is ~ 10.31 – 10.38 Å. [30]

Table 3 X-ray diffraction estimated crystallinity of native and man-made cellulose sources. [31–33]

Cellulose	Crystallinity (%)
Higher plants	50–75
<i>Valonia</i>	90
Tunicates	80
Bacterial	40–63
Man-made	25–40

Closely related to the crystal lattice formation is the crystallinity of different sources of cellulose. Degree of crystallinity can reach relatively high values, especially for native cellulose of algal (*Valonia*) and animal origin (tunicates). Man-made cellulose generally exhibits lower crystallinity oppose to native cellulose. Some examples of crystallinity of different cellulose sources estimated by X-ray analysis are mentioned in Table 3. [31–33]

Finally, morphological level is defined as organization of crystals into microfibrils. Microfibrils consequently form fibrillary structures, layers, cell walls, tissues etc. [16, 19, 23] Width of microfibrils is ranging from 2–50 nm and strongly depends on the organism in which cellulose is synthesized. [34, 35]

Subsequently, molecular, supramolecular and morphological levels impart material properties of cellulose in the terms of mechanical, thermal and chemical behaviour. The mechanical properties of native cellulose fibres on macroscopic level are given in Table 4. The thermal properties of cellulose are summarized in Table 5.

Table 4 Native cellulose fibres tensile properties. [23]

Cellulose fibres	Elastic modulus E (GPa)	Tensile strength σ (GPa)
Flax	27–100	0.34–1.03
Jute	26–65	0.39–0.77
Ramie	60–128	0.40–0.94
Cotton	5–13	0.28–0.6
Wood	10–40	1

Besides the specific mechanical and thermal characteristics, cellulose possesses other typical properties such as hydrophilicity, chirality, biodegradability and relatively high chemical reactivity potential due to the donor ability of hydroxyl groups. In contrast to synthetic polymers, cellulose exhibits extraordinary polyfunctionality, high level of chain rigidity and sensitivity to hydrolysis and oxidation. [19]

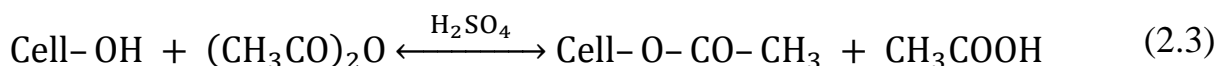
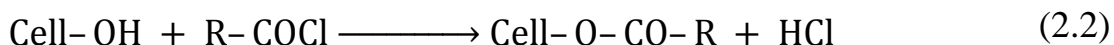
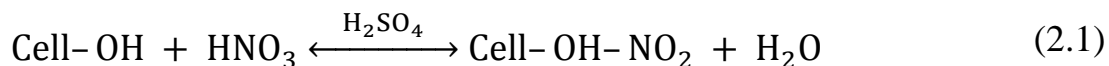
Table 5 Cellulose thermal properties data. [33, 36]

Thermal property	
Thermal decomposition	> 180 °C
Glass transition temperature (extrapolated)	230–245 °C
Ignition point	> 290 °C
Heat of combustion	17.46 kJ/g
Heat of crystallization	18.7–21.8 kJ/mol (glucose)
Specific heat	1.00–1.21 J/g.K
Heat of transition type I → II	38.1 J/g
Coefficient of thermal conductivity	0.076–0.256 W/m.K
Thermal decomposition	> 180 °C

2.2 Derivatives

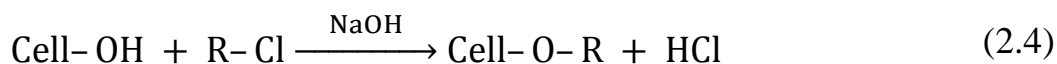
Arising from the presence of the three hydroxyl groups bonded on C6 (primary), C2 and C3 (secondary) positions in AGU (Figure 2), cellulose offers a broad variety of possible modifications via different derivatizations. These hydroxyl groups follow the rich alcohol chemistry base on which two derivatization routes are the most common, i.e. esterification (xanthanation, acetylation and nitration) and etherification. Products of these reactions find numerous commercial application as it is depicted in Figure 1.

Esterification of cellulose takes place in the presence of acid and dehydrating agent (equation 2.1) or acid/acyl chlorides (equation 2.2) or acid anhydrides (equation 2.3). [25, 33] In this manner, one can synthesize esters of inorganic acids (cellulose nitrate, sulphate and phosphate) and esters of organic acids (cellulose acetate, acetobutyrate and acetophthalate). Based on the degree of substitution, the physico-chemical properties of the products of these reactions differ drastically from those of cellulose, for example they are soluble in wide range of solvents. [23]



For the etherification of cellulose, Williamson ether syntheses can be successfully employed. These incorporate reactions of cellulose with alkyl halides in strong alkaline conditions (equation 2.4) or with alkylene oxides in weak alkaline conditions (equation 2.5). Another approach is to use acrylic or related unsaturated compounds via Michael addition (equation 2.6). [25, 33]

Methylcellulose, ethylcellulose, carboxymethylcellulose and hydroxyethylcellulose, hydroxypropylcellulose originate from reaction of cellulose with alkyl halides and alkylene oxides, respectively. An example of Michael addition is the reaction of acrylonitrile with cellulose providing cyanoethylcellulose. These cellulose derivatives find their application as food additives, anti-redepositing agents etc. [23]



In addition to above mentioned derivatizations, hydroxyl groups of cellulose can act as ligands in metal complexes or form addition compounds with acids and bases. Furthermore, hydroxyl groups of AGU can enter oxidation reactions. [23, 33] This will be discussed in next chapter.

2.2.1 Oxidation induced derivatives

For the long time the industrial processing (i.e. bleaching and pulping) of textile fibres and wood pulp was at the peak of interest for many scientists due to the need of cellulose damage prevention caused by oxidation. Within these processes, oxidation represents somewhat undesirable yet unavoidable side reaction. [23, 25, 33] In extreme case, cellulose can be broken down by complete oxidation to carbon dioxide and water. However, less drastic partial oxidation without cleavage of glycosidic bonds leads to fibrous solids generally referred to as oxycellulose. These partial oxidation processes of cellulose are considered as long-standing goal in cellulose chemistry, since they provide access to novel products and intermediates with valuable properties. In general, such materials are considered insoluble in water, although there are exceptions. [25, 33, 37]

The complexity of cellulose oxidation emerges from the (i) different reactivity of three available hydroxyl groups per AGU, (ii) different accessibility of regions of cellulose present in crystalline or amorphous form and (iii) choice of oxidizing agent. [23] This complexity results in a plethora of various possible products of oxidation, i.e. oxycellulose. However, the specific structure of each kind of oxycellulose is highly dependent on the nature of oxidant. [33] With respect to this fact, oxidizing agents can be divided into two groups, non-specific and specific oxidants.

Non-specific oxidizing agents (e.g. hypochlorite, ozone, hydrogen peroxide, persulfates, UV) favour formation of aldehyde, ketone and carboxyl groups in ratios given by reaction conditions such as concentration of reactants, pH, temperature and time. [33, 38–41] Specific oxidizing agents (e.g. sodium

periodate, sodium chlorite or sodium hypochlorite 2,2,6,6-tetramethylpiperidine-1-oxyl and sodium bromide catalysed oxidation) act with high selectivity towards reactive site and give rise to dialdehyde, carboxyl or dicarboxyl groups. [33, 37, 42, 43]

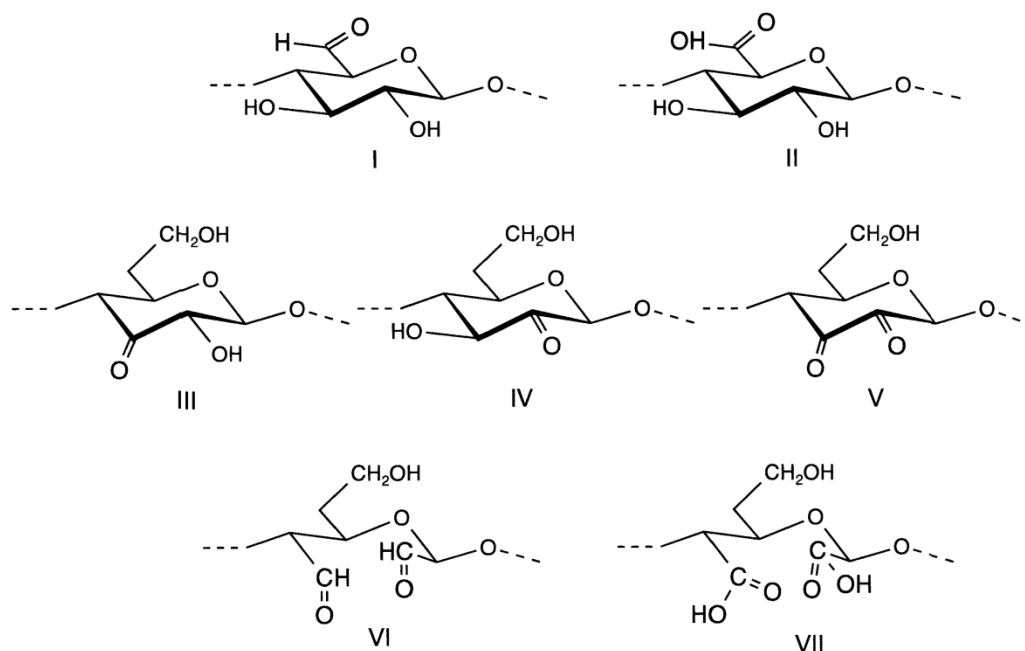


Figure 5 Possible structures of oxycellulose repeating units. [33]

The family of possible structural motives that can be present on oxycellulose is depicted in Figure 5. The structures are arranged according to the hydroxyl group classification.

Primary hydroxyl groups of AGU (see the top row in the Figure 5) can be oxidized to 6-aldehydecellulose (**I**) via elaborate photolysis of the 6-azido-6-deoxycellulose derivative. [44] Another oxidative modification of cellulose primary hydroxyl groups, which results in 6-carboxycellulose (**II**), can be achieved by reaction of cellulose and nitrogen dioxide in nonpolar solvent, [45] by utilizing phosphoric acid and sodium nitrile as the oxidizing agents [46] or by many others. [43, 47, 48]

The oxidation of secondary hydroxyl groups of AGU gives two distinctive types of oxycellulose. The first type without C2–C3 bond cleavage (see Figure 5 middle row) yields 2-keto- (**III**), 3-keto- (**IV**) or 2,3-diketo-cellulose (**V**). These types can be prepared using acetic anhydride, dimethylsulfoxide and paraformaldehyde [49] or perchloric acid with manganese (III+). [50] The second type is characterized by the cleavage of C2–C3 bond of AGU (see Figure 5 bottom row) giving rise to 2,3-dialdehydecellulose (**VI**), which can be further oxidized to 2,3-dicarboxycellulose (**VII**). The preparation of 2,3-dialdehydecellulose by periodate oxidation is considered as the most selective oxidative process of cellulose. [33, 42] Furthermore, 2,3-dialdehydecellulose

can enter secondary oxidation by sodium chlorite to obtain water soluble 2,3-dicarboxycellulose. [37] In the following chapter, applications of oxycellulose will be discussed.

2.2.2 Applications of oxycellulose derivatives

One of the most valuable properties of oxycellulose (especially 6-carboxycellulose) is its unique bioresorbability by human body. [51, 52] This fact predetermines the usage of oxycellulose in numerous applications in medical sector.

Since the success in 1950s clinical trials, when tests on oxycellulose proved its haemostatic properties, non-anaphylactic reaction in body with minimal tissue irritation and the ability to easily decompose to nontoxic products at the pH of blood, it was introduced to the market under different trade names such as SurgicelTM, OxycelTM, GelitacelTM or InterceedTM. [53, 54] For the medical application in human, it is manufactured in different forms such as powder, amorphous material or knitted fabric with defined content of carboxyl group in span of 16–24 %. [55] Due to the physical uniformity, regenerated cellulose is preferred as a source for oxycellulose over the native. [52]

Therapeutic applications include usage of oxycellulose as (i) haemostatic agent participating on blood coagulation, where the haemostasis is supported by decreasing pH of oxycellulose acting as an acid. [56–59] (ii) It is used as a material for wound dressing, which reduces protein-degrading proinflammatory interleukins as well as scavenger of reactive oxygen species and binder of excessive metal ions; [57, 59–61] (iii) antibacterial agent with potent action against invasion of pathogens, which is presumably caused by the effect of low pH; [58, 59] (iv) postoperative adhesion agent acting as a synthetic barrier preventing unwanted tissue growth between organs; [52, 62] (v) enterosorbent, if present in the form of salt, with antiulcerogenic effects in gastroenterology and detoxication therapy based on cation exchange. [59, 63, 64] Other pharmaceutical applications involve usage of 6-carboxycellulose or 2,3-dialdehydecellulose as a drug carrier, as a scaffold in tissue engineering or as a material suitable for enzyme immobilization. [65–70]

Besides the applications within medical sector, there are other possibilities how to utilize oxidized cellulose. For example, 2,3-dicarboxycellulose possesses interesting complexing properties with metal cations, which could be employed in phosphate-free detergents. [71] Other specific applications of oxidized cellulose, namely 2,3-dialdehydecellulose, will be discussed in Chapter 3.3.

3. DIALDEHYDE CELLULOSE

The oxidation of cellulose by periodate salts has been known for long time [72, 73] and has been recognized to follow the mechanism of Malaprade reaction, [74] which similarly occurs with periodate oxidation of various carbohydrates. [75] As has been mentioned earlier, this reaction is highly regioselective without significant side reactions, thus it has been widely used in structural analysis of various carbohydrate compounds. [76] Periodate oxidation is well established in commercial utilization of dialdehyde starch as a wet strengthening agent in paper industry. [77, 78] However, the periodate oxidation has not been largely industrially exploited for cellulose due to crystalline nature of this biopolymer. [79] Resulting product of periodate oxidation of cellulose is referred to as 2,3-dialdehydecellulose or simplified to dialdehyde cellulose, commonly abbreviated as DAC.

3.1 Preparation

One of the main advantages of DAC preparation lies in the relative simplicity of the process. This means that the conversion from cellulose to DAC may be controlled by the reaction time and can be conducted in a quantitative manner as can be seen in Table 6. [37, 80]

Table 6 DAC prepared by periodate oxidation of spruce pulp ($DP = 650$) with 0.25 M $NaIO_4$ at 60 °C. [33, 80]

Reaction time (hours)	2,3-dialdehyde cellulose			
	Yield (g)	Recovery ^a (%)	Conversion ^b	
			-CHO (mmol/g)	(%)
2	8.9	94	7.13 ± 0.03	57
4	7.8	82	7.75 ± 0.09	62
5	8.2	87	8.08 ± 0.06	65
6	8.7	92	9.29 ± 0.17	73
8	8.0	84	10.14 ± 0.90	81

^a Recovery: Quotient (x 100) of actual yield of polymer isolated to the theoretical weight of 2,3-dialdehydecellulose from 9.6 g of cellulose.

^b Determined according to [81].

In general, aqueous solution of sodium periodate ($NaIO_4$) is mostly used as the cellulose periodate oxidizing agent [82–84], although potassium periodate is also reported [85]. The choice of the source cellulose material entering periodate oxidation process has shown to be crucial and substantial when considering time of reaction, concentration of oxidizing agent and consequent percentage of

conversion of cellulose to DAC. [83, 84, 86] It is presumed, that crystallinity plays important role as the initial periodate oxidation of cellulose is largely limited to the readily accessible regions, i.e. the amorphous region, and therefore has been used to determine the accessibility of cellulose starting materials [87]. The kinetic study of periodate oxidation revealed at least three steps involving (i) rapid random oxidation of amorphous regions, (ii) slow oxidation of crystallites surface and (iii) very slow oxidation of crystalline cores [88]. Moreover, it is recommended to carry out this oxidation in dark and incorporate scavenger in reaction mixture to prevent radical-induced depolymerisation. [33, 89, 90] The mechanism of periodate oxidation of 1,4-linked glucans is shown in Figure 6.

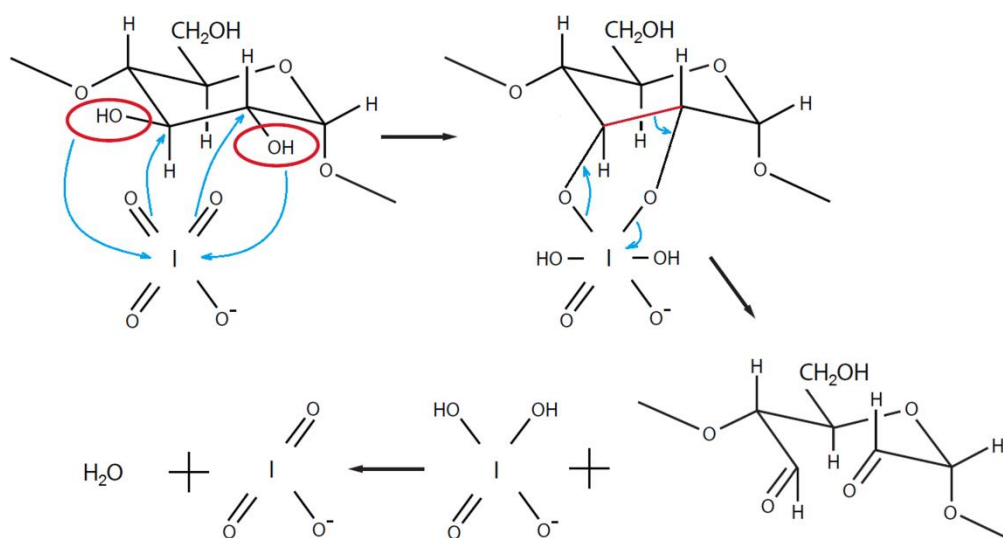
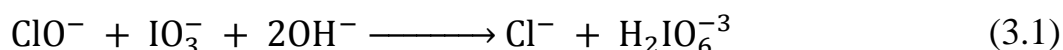


Figure 6 Mechanism of periodate oxidation of cellulose AGU. [91]

As can be seen in the reaction scheme in Figure 6, a waste product of periodate oxidation in form of weaker oxidizing iodate anion is developing next to the DAC product. However, it is possible to regenerate and recycle periodate from the waste products of oxidation by utilizing strong oxidizing agents such as sodium hypochlorite or ozone. [92, 93] The reaction of periodate regeneration via sodium hypochlorite runs under alkali conditions and is described in equation 3.1. [94]



Besides of mentioned preparation routes, advanced methods of DAC production were presented. For example, utilization of high temperatures and metal salts (e.g. lithium chloride) within periodate oxidation leads towards time and oxidant concentration reduction while achieving sufficient aldehyde content. Lithium chloride and other metal chloride salts probably reduce the amount of

inter- and intramolecular hydrogen bonds between cellulose chains. On the one hand, higher temperature speeds up reaction kinetics but on the other hand, too high temperature (over 75 °C) partially decomposes DAC. [95] Another example of advanced DAC preparation is the utilization of milling-induced periodate oxidation [96].

All together, these methods produce solid state DAC in various forms such as particles, microfibrils, beads etc. Nevertheless, it is possible to prepare aqueous solution of DAC of high degree of oxidation by the methods of prolonged heat assisted solubilization in water. Solubilized DAC can be afterwards utilized in solution-based processes. [97, 98]

3.2 Structure and properties

The mechanism of periodate oxidation (see Figure 6) shows the resulting molecular structure of DAC product. The secondary hydroxyl groups of AGU are converted to pair of aldehyde groups along with the cleavage of C2–C3 bond. However, it has been confirmed in the 1970s that the free aldehyde groups in DAC (**A** in Figure 7) are in very limited amount. This is not surprising because highly reactive aldehyde groups tend to stabilize them self. Instead of free aldehyde form, a mixture of hydrated form (**B**), hemialdal (**C**), and intra- and intermolecular hemiacetals (**D**, **E**) were proposed. [73] Complex composition of the DAC was later confirmed by solid-state NMR. [79] These possible structural arrangements of DAC are shown in Figure 7. [99]

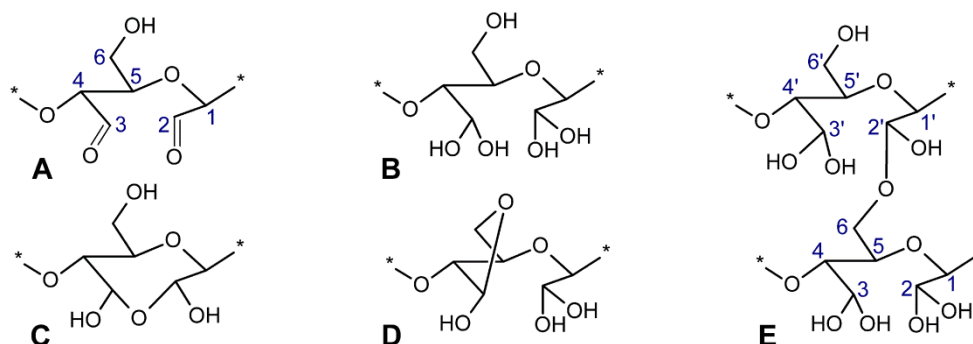


Figure 7 Possible structures of DAC: **A** – dialdehyde, **B** – hydrated dialdehyde, **C** – hemialdal, **D** – intramolecular hemiacetal, **E** – intermolecular hemiacetal.[99]

The reactive aldehyde group content can be determined by two different methods appearing the most in literature. The first method utilizes Schiff base reaction of aldehyde group with hydroxylamine hydrochloride resulting in formation of oxime (see Figure 8). [79, 95] The hydrochloric acid liberated from this reaction can be quantitatively assessed by titration. Therefore, the conversion of aldehyde to oxime can be easily determined by the consumption of alkali. [97, 100] The second method is related to the calculation of consumed periodate during oxidation. The amount of consumed periodate is determined by

spectroscopy from the linear relationship of absorbance of periodate ion at 290 nm band and its concentration in reaction media. [37, 101] Fully oxidized DAC contains 12.5 mmol of aldehyde groups per gram. [97]

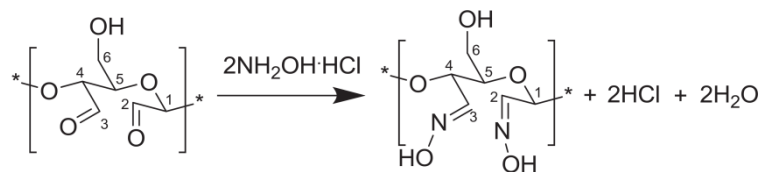


Figure 8 Schiff base reaction of aldehyde groups of AGU and hydroxylamine hydrochloride with subsequent formation of oxime. [95]

The changes in the chemical structure with the different degree of oxidation of DAC were analysed by infrared spectroscopy in detail by Kim *et al.* (2000). [79] Increasing the reaction time of periodate oxidation leads to the gradual increase of the degree of oxidation of DAC. This increase is reflected in recorded infrared spectra (see Figure 9), which shows gaining intensity of sharp band at 1740 cm^{-1} representing the carbonyl groups vibrations. Besides this specific band, another peak at 880 cm^{-1} , which can be assigned to the hemiacetal or hydrated form, appears with increasing level of oxidation. However, the amount of free aldehyde groups which could be determined by infrared spectroscopy is highly dependent on the state of measured sample. This is caused by high reactivity of aldehyde groups present in DAC, which are very sensitive to moisture, resulting in their immediate hydration as revealed by Spedding (1960). [75]

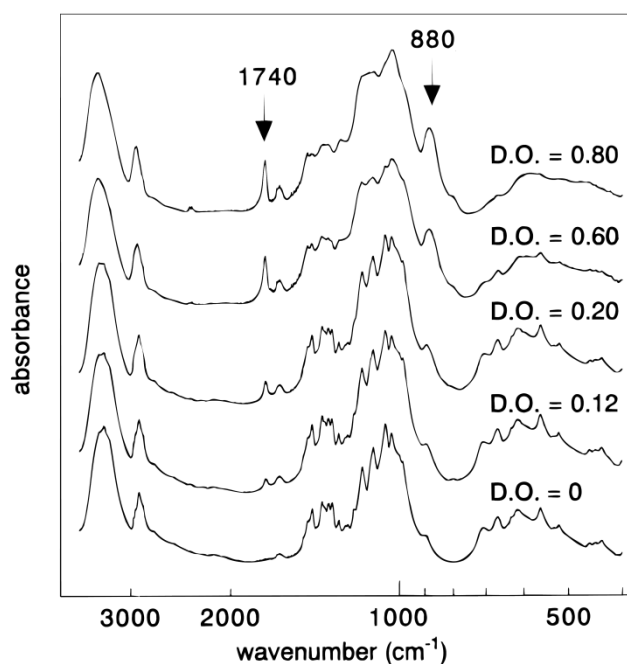


Figure 9 Infrared spectra of DAC different degree of oxidation (D.O.). [79]

Closely related to the reactive aldehyde group content (or more generally to the degree of oxidation or conversion) is the crystallinity of resulting derivatives. The scission of C2–C3 bond induced by the periodate oxidation results in the opening of the AGU ring which is further reflected in the destruction of otherwise ordered packing of cellulose chains. This fact is directly manifested in the crystalline behaviour of DAC of different degree of oxidation as it can be seen in the right part of Figure 10. [79, 101] As it was mentioned in section 3.1 focused on preparation of DAC, the periodate ions firstly attack the amorphous regions of cellulose. This rapid initial oxidation causes only minimal changes in crystalline structure. As the oxidation proceed through surface of crystalline domains, the crystallinity gradually decreases till the material becomes fairly amorphous.

In general, amorphous structures are less stable than crystalline forms of analogue compound. Hence, the decrease of crystallinity due to partial destruction of AGU units proceeds hand in hand with the loss of thermal stability. In other words, the higher is the degree of DAC conversion, the less thermally stable is the final product, although the oxidation process is not necessarily accompanied by the polymer chain shortening. Typical thermo-degradation experiment is illustrated in the left part of Figure 10. Many other cellulose derivatives show similar behaviour, i.e. shift of decomposition temperatures to lower values in comparison with the starting material. [102, 103]

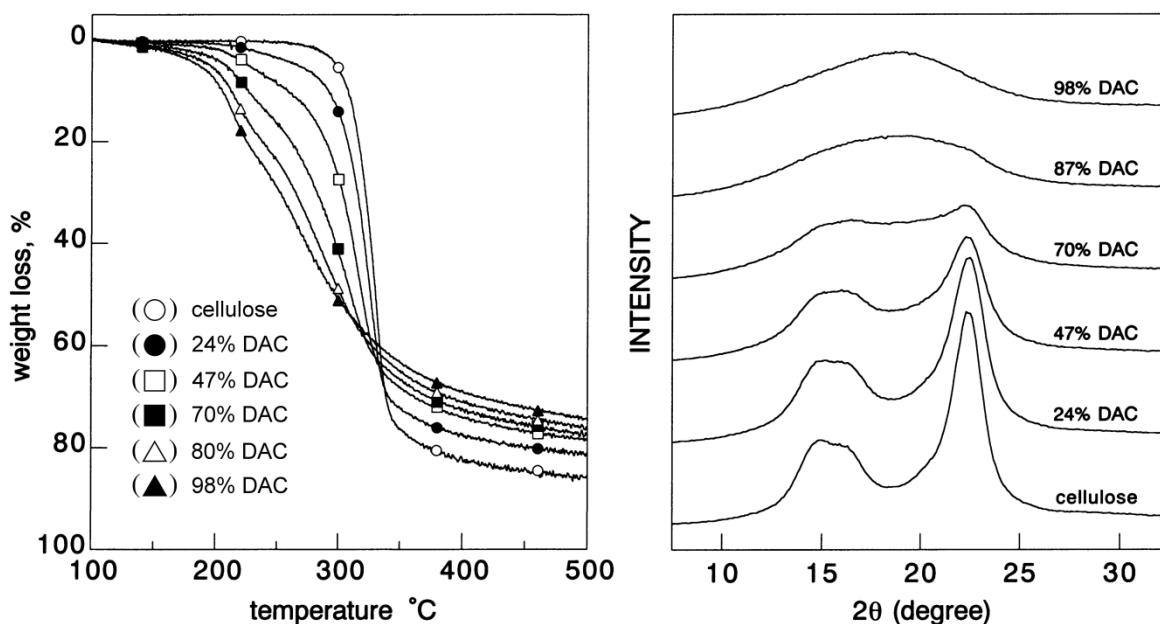


Figure 10 Dependence of degree of oxidation on X-ray diffraction profiles (left) and thermal stability. [101]

Another very important property, the stability of DAC in time, should be addressed before any consideration of practical use. The stability of DAC is related to the structure and reactive aldehyde group content that can change in time under defined storage conditions. When DAC is kept in non-dried state, the reactivity dramatically decreases to 68 % after only one week from preparation as has been reported by Sirviö *et al.* (2014) [104] Complex study on stability behaviour in time associated with the reactive aldehyde group content and molecular weight distribution of solubilized DAC prepared from microcrystalline cellulose was conducted by Kim *et al.* (2004). This research showed the gradual decrease of reactive aldehyde group content about 15 % as well as the steady decrease of molecular weight about 50 % after 3 weeks from preparation of fully oxidized DAC solubilized under various conditions. [97]

The solubilization processes of DAC used within the study of Kim *et al.* (2004) showed to have relatively low impact on the molecular weight of DAC prepared from microcrystalline cellulose Funacel SF (see Table 7). [97] However, the study of Sulaeva *et al.* (2015), which was mainly focused on the characterization of molecular weight of solubilized DAC from another source of microcrystalline cellulose Avicel PH-101 and cotton linters, showed somewhat contradictory results to those made by Kim *et al.* (2004). In brief, Sulaeva *et al.* (2015) reported that the solubilization process strongly affects the molecular weight of resulting solubilized DAC (50 % decrease of molecular weight after one hour of solubilization). [98] Their findings are summarized in Table 7.

Table 7 Mass average molecular weight (\bar{M}_w) values of source cellulose material and DAC after defined process of solubilization. [97, 98]

Source	\bar{M}_w source (kDa)	DAC sol. (time, temp.)	\bar{M}_w sol. DAC (kDa)	\bar{M}_w loss (%)
Funacel SF	42.7	4 h, 80 °C	41.2	3.5
		6 h, 80 °C	39.2	8.2
		1 h, 100 °C	42.0	1.6
		2 h, 100 °C	30.4	28.8
Avicel PH-101	40	1 h, ^a	19.7	50.8
Cotton linters	180	1 h, ^a	23.6	86.9

^a Not specified, heated at reflux.

DAC, whether solubilized or not, was reported to be rather unstable in time especially when kept in alkaline solution. [98, 105] The degradation processes identified as β -elimination, hemiacetal hydrolysis and benzil-benzilic acid rearrangements of DAC polymer analogue dialdehyde starch (see Figure 11) in alkaline environment were well described by Veelaert *et al.* (1997). [100]

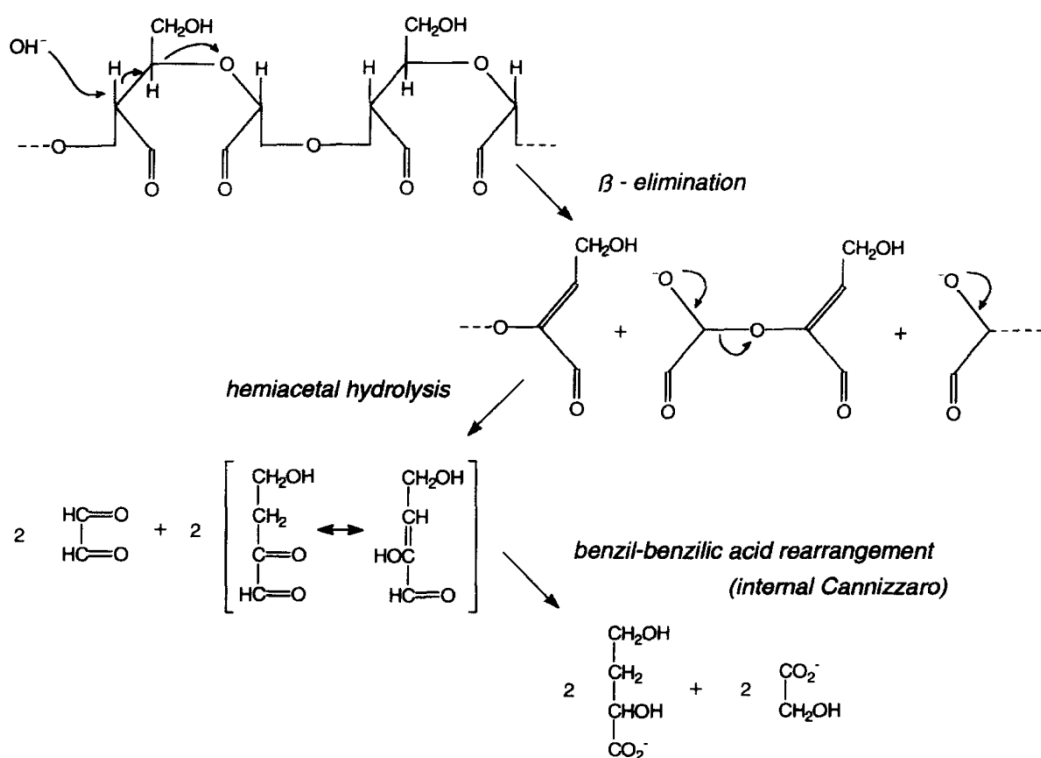


Figure 11 Example of dialdehyde starch degradation by the process of β -elimination. [100]

The later work of Potthast *et al.* (2009) showed similar degradation behaviour of partially oxidized DAC via β -elimination under alkaline conditions as shown in Figure 12. Based on the study of β -elimination processes, this research revealed that the low degrees of conversion from cellulose to DAC favour random formation of isolated oxidized AGUs. As the conversion increases, cluster-like oxidation becomes more dominant. [105]

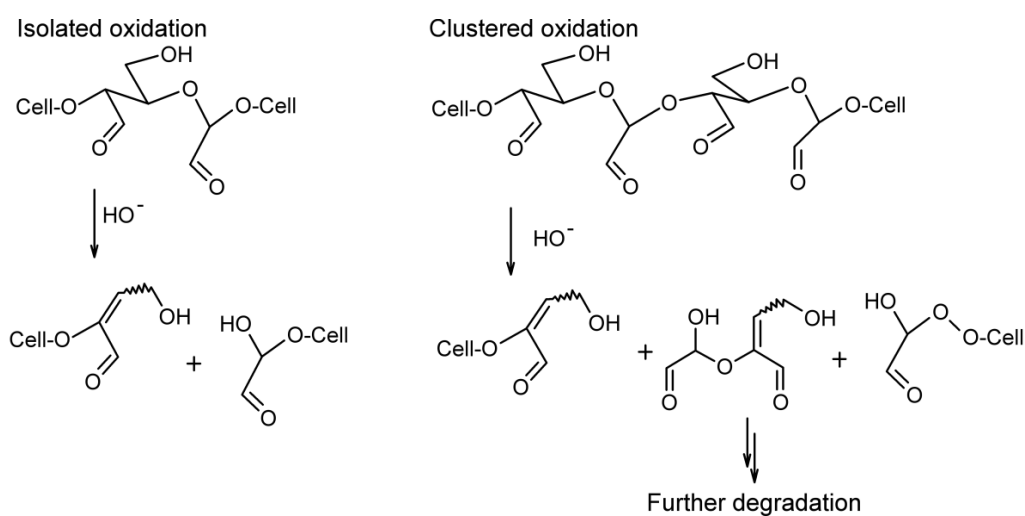


Figure 12 β -elimination degradation mechanism of DAC under alkaline conditions connected to the different degrees of DAC oxidation (left – lower degree of oxidation, right – higher degree of oxidation). [105]

Besides these interesting conclusions about the kinetics of periodate oxidation, the pH of DAC suspension or solution seems to be one of the key parameters when optimizing the stability.

3.3 Applications of DAC

The presence of highly reactive aldehyde groups on DAC backbone imparts its usage as cellulose based column packings in aqueous chromatography, [106–108] heavy metal ion and dyes absorbent, [37, 109, 110] flocculation agent, [111] protein immobilization material, [112–114] drug delivery carrier, [115–117] in tissue scaffold engineering, [118] or in graft copolymerization. [119]

Furthermore, the recent studies of solubilized DAC showed its potential as a suitable crosslinking agent for chitosan [120, 121]. Such combination of materials exhibits minimal cytotoxicity compared to chitosan crosslinked by glutaraldehyde. Besides, DAC itself displays 6–12x lower toxicity than commonly used crosslinking agent glutaraldehyde [120].

In general, aldehyde groups promise a broad follow-up chemistry as it can be modified to carboxylic acid, [37, 80, 109, 122, 123] primary alcohols, [80, 122] imines, [82, 101] or sulfonates. [124] Both DAC and its derivatives possess a great potential in high-end applications such as medical materials [120, 125] and biodegradable composites. [126]

4. POLY(VINYL ALCOHOL) BASED HYDROGELS

Hydrogels in general find their firm place in various areas, particularly in medical and agricultural sector, packaging industry etc. [3, 127, 128] From the historical point of view, innovation of hydrogel materials by Wichterle and Lím (1960) was the initial spark for utilization of these materials in numerous biomedical applications such as contact lenses or absorbable sutures. [2, 129] Later on, these efforts resulted in hydrogel microcapsules for cell engineering, novel dressing materials for burns and wounds healing and many others. [130, 131]

Hydrogels are by definition three-dimensional, hydrophilic, polymeric crosslinked network structures capable of absorbing large amounts of water. [132] Network of hydrogel is generally composed of homo- or copolymers, which is insoluble due to the presence of chemical or physical crosslinks. [133] The mechanism of network formation begins with soluble polymer of finite macromolecules dispersed in medial (sol). As the linking process proceeds, the solubility of polymer decreases giving rise to the infinite polymer network (gel). This phenomenon is referred to as sol-gel transition or gelation and can be further distinguished into chemical or physical gelation. The essential classification of hydrogels includes two categories:

(i) Permanent (chemical) hydrogel: covalently crosslinked network, which contains stable covalent bonds between macromolecules (besides the hydrogen bonds). The crosslink density and polymer-water interaction parameter defines their equilibrium swollen state. [134, 135]

(ii) Reversible (physical) hydrogel: molecular entanglements, secondary forces such as ionic, hydrogen bonding or hydrophobic interactions are responsible for the network formation. The change in physical conditions or application of stress causes disruption of these reversible interactions. [134, 135]

Besides above mentioned categorization, hydrogels can be classified on the base of their other properties such as degradability, response to external stimuli, ionic charge and many others summarized in Table 8. [8]

The most important characteristic feature of hydrogel is the water retention capacity. The absorbed water can be further divided into (i) primary bound water, by definition the first water molecules to hydrate the most polar, hydrophilic groups present in the matrix of hydrogel. As the hydrophilic groups are hydrated, the network swells and exposes hydrophobic groups, which are also interacting with water molecules. This leads to the so-called (ii) secondary bound water. The sum of primary and secondary bound water is described as (iii) total bound water. Furthermore, due to the osmotic force of hydrogel network towards infinite dilution, the network imbibes additional free water reaching the equilibrium swelling level. [136]

Table 8 Classification of hydrogels based on their properties. [8]

Hydrogels		
Crosslinking	<ul style="list-style-type: none"> • Physical • Chemical 	
Response	<ul style="list-style-type: none"> • Chemically responsive • Biochemically responsive • Physically responsive 	<ul style="list-style-type: none"> • pH, glucose • Antigen, enzyme, ligands • Temperature, pressure, light, electric/magnetic
Physical properties	<ul style="list-style-type: none"> • Smart • Conventional 	
Preparation	<ul style="list-style-type: none"> • Copolymeric • Homopolymeric • Interpenetrating 	
Source	<ul style="list-style-type: none"> • Natural, • Synthetic • Hybrid 	
Degradability	<ul style="list-style-type: none"> • Biodegradable • Non-biodegradable 	
Ionic charge	<ul style="list-style-type: none"> • Cationic • Anionic • Non-ionic 	

4.1 PVA hydrogel formation

Poly(vinyl alcohol) (PVA) is undoubtedly one of the most frequent and used material for hydrogel applications as it possesses valuable properties such as biocompatibility, biodegradability, relatively low toxicity and it is possible to blend it with a broad range of synthetic polymers or biopolymers. [11] Above mentioned properties are particularly favourable in applications of medical sector. Furthermore, crosslinked PVA possesses good chemical, thermal and mechanical stability which imparts its use in packaging, waste water treatment etc. [12] The specific applications are closely related to the methods of preparation, which can be generally divided to two approaches of hydrogel formation, i.e. physical and chemical routes.

4.1.1 Physical routes

There are several physical crosslinking methods how to prepare PVA hydrogel. Principally, this type of approach has the undeniable advantage in omitting any kind of crosslinking agent. However, the crosslinking process is

rather poorly defined in the term of chemical reaction mechanism. Hydrogels prepared using physical routes exhibit somewhat lower mechanical properties in swollen state and physical crosslinks are not as strong and stable as chemical. [12, 128, 137] The physical routes of PVA crosslinking include:

(i) Freeze-thaw induced crystallization. The crosslinking of PVA is induced by formation of crystalline regions by cyclic heating and freezing (-20/+25 °C), these regions then act as physical crosslinks. [138]

(ii) Heat treatment. The crosslinks are created via prolonged heating. For example, 30–80 minutes at 120–175 °C is suitable for manufacturing reverse osmosis membranes. [139] Partial degradation due to higher temperatures produces unsaturation, chain scission and thus chemical crosslinks. [12]

(iii) Irradiation. Utilizing sources of radiation such as ^{60}Co on cast films from PVA result in their crosslinking. [140] Radiation induced crosslinking exhibit looser, more open structure. [12]

4.1.2 Chemical routes

Characteristic feature of all chemical crosslinking routes is the utilization of crosslinking agent. The crosslinking is achieved by the reaction of functional hydroxyl groups of PVA and crosslinking agents such as aldehydes (formaldehyde, glutaraldehyde, acrolein etc.), [140, 141] di- tri- and polycarboxylic acids, [142] anhydrides, [143] alkoxysilanes [144] and many others. [12, 145–147] The common characteristic for these crosslinking agents is the synthetic origin and subsequent high toxicity. Thus, the resulting hydrogels should be intensively washed prior to use in medical sector. An example of PVA crosslinking reaction with glutaraldehyde is depicted in Figure 13. [128]

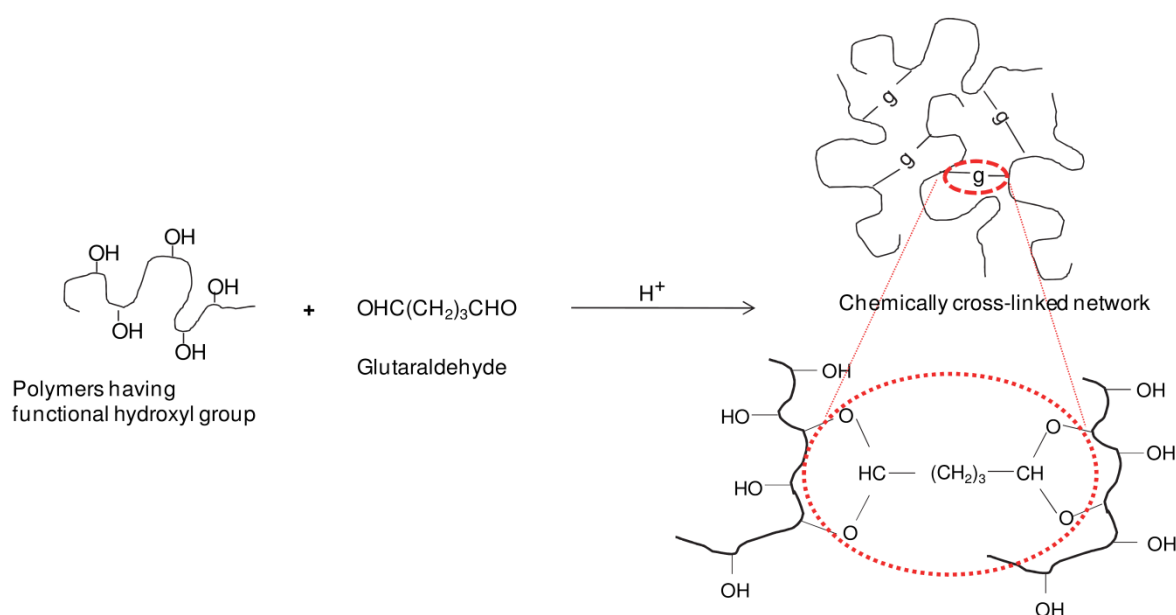


Figure 13 Crosslinking reaction of PVA using glutaraldehyde. [128]

4.2 Characterization and network parameters

The evaluation of properties of hydrogels is often expressed by the network parameters. These include molecular weight between crosslinks (\bar{M}_c) and crosslink density (ρ_c), which can be calculated with the aid of equilibrium swelling theory suggested by Flory and Rehner (1943). [148] The crucial and the most important parameters of network are expressed in the following equations:

(i) Percentage of swelling, where M_t is the weight of swollen polymer at time t , and M_0 is the initial weight of washed and dried hydrogel. [128]

$$\text{Percentage of swelling (\%)} = \frac{M_t - M_0}{M_0} \times 100 \quad (4.1)$$

(ii) The equilibrium water content (EWC), describing maximum amount of water absorbed by hydrogel. M_s is the weight of sample swelled at equilibrium conditions and M_0 is the weight of dry washed hydrogel. [149]

$$\text{EWC (\%)} = \frac{M_s - M_0}{M_s} \times 100 \quad (4.2)$$

(iii) Gel fraction, where M_0 refers to the weight of dried hydrogel after extraction of soluble fraction in hydrogel and M_{init} is the weight of dry and unwashed hydrogel. [128]

$$\text{Gel fraction (\%)} = \frac{M_0}{M_{\text{init}}} \times 100 \quad (4.3)$$

(iv) Average molecular weight between crosslinks (\bar{M}_c), where \bar{M}_n is the number average of molecular weight of initial uncrosslinked polymer, \bar{v} is the specific volume of polymer, V_1 is the molar volume of water, $V_{2,s}$ is the polymer volume fraction, and χ_1 is the polymer-solvent interaction parameter. [148]

$$\frac{1}{\bar{M}_c} = \frac{2}{\bar{M}_n} - \frac{\left(\frac{\bar{v}}{V_1}\right) \left[\ln(1 - V_{2,s}) + V_{2,s} + \chi_1 (V_{2,s})^2 \right]}{\left[(V_{2,s})^{\frac{1}{3}} - \frac{V_{2,s}}{2} \right]} \quad (4.4)$$

(v) Polymer fraction ($V_{2,s}$), where M_s/M_0 is the weight swelling ratio of swollen hydrogel at equilibrium, ρ_p is the polymer density, and ρ_w is the density of water. [150]

$$V_{2,s} = \left[1 + \frac{\rho_p}{\rho_w} \left(\frac{M_s}{M_0} - 1 \right) \right]^{-1} \quad (4.5)$$

(vi) Crosslink density (ρ_c). [151]

$$\rho_c = \frac{1}{\bar{v}M_c} \quad (4.6)$$

4.3 Applications of PVA hydrogels

There are myriad of specific applications of crosslinked PVA hydrogels in many various fields. The properties of PVA hydrogels are often tailored by addition of other synthetic polymer or biopolymer.

The work of Kamoun *et al.* (2014) summarizes the wound dressing applications of PVA based hydrogel combined with numerous natural and synthetic polymers including sodium alginate, dextran, starch, chitosan, polyethylene glycol, poly(N-vinylpyrrolidone) and many others. [11]

Several other important applications of PVA hydrogels are within the medical sector. Their applicability arises from the biocompatibility and low protein adsorption. The review on the utilization of PVA hydrogels by Baker *et al.* (2012) outlines the most widespread usage of this material in soft contact lenses, tissue adhesion barriers, artificial cartilages, orthopaedic applications and other medical devices. [10]

Another valuable source on the usage of PVA hydrogels in the form of membranes designed for variety of water treatment applications is the work of Bolto *et al.* (2009). These applications include micro-, ultra- and nano-filtration, reverse osmosis, pervaporation etc. It offers deep insight into the possible methods of PVA crosslinking and its subsequent specific applications. [12]

One cannot forget the packaging industry, where the crosslinked PVA finds it applications, for example in combination with gelatine or pectin. [127]

Besides above mentioned reviews, there are number of reports in the Web of Science database (WoS) in recent years (2013–2017) regarding the characterization and utilization of PVA-based hydrogels. These can be divided in several topics such as the most cited articles relevant for:

Medical sector applications:

- PVA/cellulose nanowhiskers (CNWs) freeze-thawed hydrogels with controlled porosity, morphology and barrier properties suitable for wound dressing application [152].
- Freeze-thaw prepared PVA/sodium alginate hydrogel containing sodium ampicillin with improved antibacterial activity and hemocompatibility useful as wound dressing material [153].

- Carboxyl-modified PVA/chitosan hydrogel with enhanced mechanical properties, low cytotoxicity and haemolytic potential, sustained release profile of gentamicin sulfate suppressing bacterial proliferation. Thus, this material could be effectively used for wound protection [154].
- PVA impregnated bacterial nano-cellulose (BNC) composites with improved mechanical properties, water permeability and enhanced compliance applicable as suitable materials for blood vessels [155].

Water treatment applications, namely phosphate/dye/heavy metal adsorbents and sensors:

- Hydrogels with improved dye adsorption capacity (via physisorption and chemisorption) tuned by the incorporation of amphiphilic graphene oxide in PVA hydrogel network, which increases chain mobility and adds new functional groups to the polymer matrix [156].
- Reusable high capacity PVA/gelatine hydrogel beads crosslinked by boric acid utilized for Pb^{2+} removal driven by chemisorption with ion-exchange mechanism [157].
- PVA reusable hydrogel beads crosslinked by boric acid in the presence of aluminium chloride containing aluminium ions in the network structure suitable for phosphate removal [158].
- PVA/poly(acrylic acid) (PAA) hydrogels usable for sensing of Ni^{2+} . When such material exposed to heavy metal ion, there is a change of hydrogel degree of crosslinking reflected in the change of refractive index measurable as phase shift in the interferogram [159].

Self-healing and shape memory hydrogels:

- Borax crosslinked PVA hybrid hydrogels containing nano-fibrillated cellulose (NFC) with enhanced material stability and the ability of hydrogen bonds re-formation without external stimuli when such hydrogel broken apart [160].
- PVA/tannic acid (TA) hydrogels with memory shape behaviour due to strong H-bonding interaction between PVA and TA and excellent mechanical properties [161].
- PVA/graphene oxide memory shape nanocomposite with strong H-bonding interaction between PVA and graphene oxide [162].

Gas separation application:

- Separation membranes composed of diethanolamine (DEA) impregnated PVA crosslinked by glutaraldehyde cast on supportive polytetrafluoroethylene (PTFE) layer. Membranes prepared using different amount of crosslinker were utilized in gas separation experiments for CO_2/CH_4 with reasonable permselectivities in comparison with uncrosslinked membranes [163].

5. AIM OF DOCTORAL THESIS

The current work deals with research and development of a biopolymer-based crosslinking agent for polymers containing hydroxyl groups on their backbone. Cellulose derivative and poly(vinyl alcohol) were selected as the starting materials. The aim of the Thesis was study of dialdehyde cellulose preparation, characterization and its utilization as a crosslinking agent for PVA. It was defined according to challenge identified with respect to the studied field, performed literature review and preliminary experiences.

Particularly, the aim includes preparation of DAC by a suitable technique, optimization of the method of its preparation, study of its structure, properties and aging, and its applicability as crosslinker in the preparation of PVA hydrogels. Furthermore, this study includes an optimization of the crosslinking process with respect to the properties of final hydrogel material and a comparative crosslinker study, in which the properties (namely network parameters) of hydrogel materials prepared using DAC are compared to those of hydrogels prepared using common crosslinking agent (glutaraldehyde).

This aim may be achieved by accomplishment of the following objectives:

- Research of cellulose oxidation to prepare its reactive derivative (namely DAC) with potential use as a crosslinking agent for PVA.
- Elucidation of structure of prepared DAC via suitable analytical methods, particularly in solution.
- Research of stability (including eventual stabilization if discovered) of prepared DAC in its application form (i.e. solution) in time. Characterization of changes in the structure with aging.
- Development of a crosslinking system, namely choice and suitability of crosslinking catalysts, process parameters (i.e. drying temperatures) and evaluation of their influence on properties crosslinked materials.
- Investigation of crosslinking capability of fresh and aged crosslinking agent and influence of catalyst choice on material properties of resulting hydrogels.
- Comparative study on PVA crosslinking utilizing common crosslinking agent (i.e. glutaraldehyde) and DAC under equal conditions, evaluation of crosslinking efficiency of used crosslinkers on resulting hydrogel properties in the terms of network parameters comparison.

6. EXPERIMENTAL

For the sake of clarity, sections of Experimental part, Results and Discussion part and Concluding Summary part of this Thesis are divided into:

- (i) “Pilot study” – initial study regarding the suitability of DAC as a crosslinking agent for PVA and experimental setup of hydrogel preparation using different process parameters. These include catalyst system concentration and the investigation of drying temperature influence on resulting hydrogel properties.
- (ii) “DAC study” – preparation and characterization of DAC via suitable methods, investigation of its stability and structure during aging. Study of DAC solubilization process under different conditions.
- (iii) “Hydrogel study” – utilization of solubilized DAC of different age accompanied by incorporation of two chemically distinct catalyst systems in the crosslinking reactions of PVA. Use of various concentration of fresh solubilized DAC or glutaraldehyde under equal conditions as crosslinkers for different types of PVA. Characterization and comparison of properties of all of the prepared hydrogels.

6.1 Materials

6.1.i Pilot study

Commercially available material Mowiflex TC 232 (Kuraray Specialities, Europe GmbH), density $\rho_p = 1.3 \text{ g/cm}^3$, $\bar{M}_n = 23\,500 \text{ g/mol}$ (estimated by GPC), was used as a source of PVA for initial testing. Dialdehyde cellulose (DAC) was prepared from alpha cellulose (Sigma Aldrich, Co.) by periodate oxidation using sodium periodate (NaIO_4) (PENTA, Czech Republic). Ethylene glycol (PENTA, Czech Republic) was used for the decomposition of residual periodate salt. All of the chemicals used in crosslinking reactions and subsequent analysis of product were of analytical purity (p.a.) and were used without further purification. These include 96% sulfuric acid (H_2SO_4), 99.8% methanol (CH_3OH), sodium hydroxide (NaOH), 35% hydrochloric acid (HCl) (PENTA, Czech Republic), and 99.8% acetic acid (CH_3COOH), hydroxylamine hydrochloride (Sigma Aldrich, Co.). Demineralized water was used throughout the experiment. [17]

6.1.ii DAC study

Powdered microcrystalline alpha cellulose (Sigma Aldrich Co.) of DP = 672 [164] was used as a cellulose source material. NaIO_4 , ethylene glycol, NaOH (PENTA Czech Republic) and hydroxylamine hydrochloride, sodium chlorite

(NaClO₂) and CH₃COOH (Sigma Aldrich Co.) were of analytical purity (p.a.) and used as received without further purification. Demineralized water was used throughout the experiment. [99]

6.1.iii Hydrogel study

Two sources of poly(vinyl alcohol) (PVA) were used. The first source, Mowiflex TC 232 (Kuraray Specialities Europe GmbH), 83 % hydrolysis (estimated by NMR), density $\rho_p = 1.3 \text{ g/cm}^3$, $\bar{M}_n = 23\,500 \text{ g/mol}$ (estimated by GPC), was utilized in the study of crosslinking via fresh and aged DAC as well as in the comparative crosslinker study. The second source, Mowiol 84–86% hydrolysed (Sigma Aldrich Co.), $\rho_p = 1.3 \text{ g/cm}^3$, $\bar{M}_n = 27\,500 \text{ g/mol}$ (estimated by GPC), was employed only in the comparative crosslinker study along the first one. Alpha cellulose (Sigma Aldrich Co.) served as the source material entering the periodate oxidation via NaIO₄ (PENTA, Czech Republic). The termination of this oxidation reaction resulting in dialdehyde cellulose (DAC) was achieved by the addition of excess of ethylene glycol (PENTA, Czech Republic). The degree of DAC oxidation (conversion) was determined on the base of consumption of NaOH (PENTA, Czech Republic) in alkalimetric titration of the resulting by-product (HCl) of oxime reaction between DAC and hydroxylamine hydrochloride (Sigma Aldrich Co.). The other chemicals used in PVA crosslinking reaction, including 35% HCl, 96% H₂SO₄, 99.8% CH₃OH (PENTA, Czech Republic), 99.8% CH₃COOH and 50% water solution of glutaraldehyde (Sigma Aldrich Co.), were of analytical purity (p.a.) and used as received without further purification. Demineralized water was used throughout the experiment. [91]

6.2 Sample preparation

6.2.i Pilot study

In the first step, oxidized cellulose was prepared analogically to the literature. [97] 10 g of alpha cellulose was suspended in 250 mL of aqueous solution containing 16.5 g of NaIO₄. To obtain DAC of high degree of oxidation, reaction was stirred in dark for 168 hours at laboratory temperature. Periodate oxidation was stopped by adding 10 mL of ethylene glycol. DAC product was rinsed on filter to remove residues of periodate reaction and in never-dried state transferred to three-necked flask equipped with reflux and stirrer. DAC sample was diluted with 250 mL of water and the flask was immersed in water bath heated up to 80 °C for 7-hour solubilization. Completely solubilized DAC was rapidly cooled and purified by centrifugation to remove insolubilized material negligible in amount. Resulting supernatant was dialysed and transferred into 250mL volumetric flask (stock solution), where it was kept until usage as a crosslinking agent for PVA. Weight concentration of DAC in solution was

assessed from the recovery of solids after drying of defined volume of DAC solution at 100 °C.

In the second step, PVA/DAC aqueous mixtures containing 2 wt% of crosslinking agent (solubilized DAC) were prepared by dissolving 4.9 g of PVA (Mowiflex TC 232) and subsequent addition of exact volume of DAC solution containing 0.1 g of solubilized DAC. Total volume of such mixture was 70 mL.

In the third step, catalyst system composed of 10vol% CH₃COOH, 10vol% CH₃OH, 10vol% H₂SO₄ was introduced. Two sets of PVA/DAC mixtures with different concentration of catalyst system were prepared. Specific amount of each component per PVA/DAC set is described in Table 9. [17]

Table 9 Catalyst system composition and volume in different sets of PVA/DAC mixtures.[17]

Components of catalyst system	PVA/DAC set 1	PVA/DAC set 2
10 vol% CH ₃ COOH (buffer)	3 mL	0.75 mL
10 vol% CH ₃ OH (quencher)	1.5 mL	0.5 mL
10 vol% H ₂ SO ₄ (catalyst)	1 mL	0.25 mL

PVA/DAC aqueous mixtures containing different amount of catalyst system were cast on plates of 15 cm in diameter to form thin films. These films were dried at different temperatures till constant weight. For determination of network parameters, PVA/DAC samples from each set were intensively washed and subsequently dried at 30 °C until constant weight. The designation of samples prepared under different condition (i.e. drying temperature, different amount of catalyst system) is mentioned in Table 10. [17]

Table 10 PVA/DAC samples designation based on different amount of catalyst system and different drying temperatures.[17]

Drying temperature (°C)	PVA/DAC set 1		PVA/DAC set 2	
	unwashed	washed	unwashed	washed
90	1-90-U	1-90-W	2-90-U	2-90-W
60	1-60-U	1-60-W	2-60-U	2-60-W
30	1-30-U	1-30-W	2-30-U	2-30-W

6.2.ii DAC study

The periodate oxidation of alpha cellulose was further optimized (time of reaction, change of solubilization volume etc.) when compared to the process of DAC preparation in the pilot study. Such optimization reduces reaction time while maintaining the product properties. In brief, 16.5 g of NaIO₄ was

dissolved in 250 mL of water with subsequent addition of 10 g of alpha cellulose. This reaction mixture was stirred at 750 rpm in dark (closed container) at laboratory temperature for 72 hours. [97, 99, 101] At the end of the reaction time, reaction was stopped by decomposing residual periodate by the addition of 10 mL of ethylene glycol.

The raw DAC product (insolubilized DAC suspension) was thoroughly washed on a filter and in a never-dried state transferred into a three-neck flask equipped with external stirrer and reflux cooler. Raw DAC was diluted by adding of 200 mL of water and pH of such suspension was recorded (pH = 6). Next, the flask was immersed in water-bath heated up to 80 °C and stirred at 350 rpm for 7-hour solubilization. After rapid cooling, solubilized DAC was purified by centrifugation at 15 000 g for 10 minutes with subsequent dialysis of supernatant against demineralized water for 12 hours. After dialysis, solubilized DAC was transferred and diluted by water into 250mL volumetric flask with resulting pH of the solution of 3.5 ± 0.1 which remained constant during whole experiment (DAC stock solution). Weight concentration of DAC in solution was assessed from the recovery of solids after drying of defined volume of DAC solution at 100 °C. Such dried samples were kept in desiccator for further analysis of solubilized-dried DAC.

Hereby prepared solubilized DAC stock solution sample was examined in the terms of its stability and structure during 28 days of aging study. The specimens from this sample were designated by their time of aging, i.e 1 day old (fresh), 14 and 28 days old. [99]

Due to somewhat contradictory results regarding the DAC solubilization mentioned by Kim *et al.* (2004) [97] and Sulaeva *et al.* (2015) [98] (see Table 7), solubilization process was investigated in details here. For this reason, raw DAC was converted into its water soluble derivative, sodium salt of 2,3-dicarboxy cellulose (Na-DCC). This was achieved by the reaction of raw DAC with NaClO₂ in the presence of CH₃COOH according to Maekawa *et al.* (1984) [37]. In brief, composition of such reaction mixture was set with the respect to the molar ratio of reactants in following amount 1 mole -CHO : 4 moles of NaClO₂ : 2 moles of CH₃COOH. This reaction was performed on an aliquot part of raw DAC suspension (pH = 6) prior to solubilization. The other aliquots of the same sample were solubilized employing above described process varying solubilization time from 30 minutes to 7 hours. [99] Subsequently, all aliquots were filtered separately using 0.2 μm filters and the separated solids as well as filtrates were analysed.

This aliquot-solubilization experiment was repeated using raw DAC suspensions, whose pH was set to values 3.5, 5 and 7.5 by diluted HCl or NaOH solution prior to their solubilization. Such approach enables comprehensive evaluation of the influence of DAC solubilization and initial pH setup of DAC suspensions on molecular weight of final product and the process as a whole. Within this aliquot-solubilization experiment, the change of filtrate pH and

solubilized DAC molecular weight were investigated with the respect to the solubilization time. Raw DAC particle morphology during these solubilization experiments was also analysed.

In contrast to conventional heating method used for DAC solubilization, microwave assisted solubilization (MWS) was employed for raw DAC suspensions of different initial pH as described above. Typically, 50 mL of raw DAC suspension was transferred into 100mL flat bottom flask equipped with reflux cooler and placed in open-vessel microwave-oven laboratory system MWG1K-10 operated at 800 W and 2.45 GHz (Radan, Czech Republic) for 1 hour. Completely solubilized DAC samples were filtered using 0.2 μm filter and analysed.

Finally, all DAC samples solubilized utilizing 7-hour solubilization via conventional heating and 1-hour MWS were rapidly cooled using ethanol ice, freeze-dried and analysed.

The designation of samples within this solubilization study along the crucial parameters of solubilization process is noted in Table 11.

Table 11 Designation of DAC samples within solubilization study distinguished by the solubilization time, used method of heating and initial pH of raw DAC suspension.

Method	Conventional heating			
Solubilization (hours)	pH			
	3.5	5	6	7.5
0.5	W05-s	X05-s	Y05-s	Z05-s
	W05-f	X05-f	Y05-f	Z05-f
1	W1-s	X1-s	Y1-s	Z1-s
	W1-f	X1-f	X1-f	Z1-f
3	W3-s	X3-s	Y3-s	Z3-s
	W3-f	X3-f	Y3-f	Z3-f
5	W5-s	X5-s	Y5-s	Z5-s
	W5-f	X5-f	Y5-f	Z5-f
7	W7-s	X7-s	Y7-s	Z7-s
	W7-f	X7-f	Y7-f	Z7-f

Method	Microwave assisted solubilization (MWS)			
Solubilization (hours)	pH			
	3.5	5	6	7.5
1	mw-W	mw-X	mw-Y	mw-Z

Samples marked as “s” refer to the solid phase DAC separated by filtration after solubilization.

Samples marked as “f” refer to the filtrate solution of DAC after solubilization.

6.2.iii Hydrogel study

The exact method of DAC preparation and solubilization is described above (see part “6.2.ii DAC study”).

After the solubilization of DAC, preparation of PVA crosslinked samples using aged DAC was carried out. In the first step, PVA/DAC mixtures containing 1 wt% of crosslinker (solubilized DAC) were prepared by dissolution of 4.95 g of PVA (Mowiflex TC 232) in 70 mL of demineralized water with subsequent addition of exact volume of 1 day old (fresh) DAC solution containing 0.05 g of solubilized DAC. To induce formation of crosslinked network, acidic catalyst must be introduced.

For this reason, two chemically distinct types of acidic catalyst systems (one of identical composition as in “6.2.i Pilot study” used for “PVA/DAC set 2” in Table 9) were selected and added to the mixture of polymer and crosslinker forming two types of PVA/DAC blends. These blends/catalyst systems are referred as series/type A and B in following text. The composition of used catalyst systems along with the volume used per sample is noted in Table 12. The same experimental setup and process of sample preparation was repeated using aged DAC (14 and 28 days old). [91]

Table 12 Composition and volume per sample of catalyst systems used for crosslinking of PVA using fresh and aged DAC. [91]

Catalyst system type A	Catalyst system type B
1.33M HCl (1.5 mL)	10vol% H ₂ SO ₄ (0.25 mL)
	10vol% CH ₃ OH (0.5 mL)
	10vol% CH ₃ COOH (0.75 mL)

For further investigation of crosslinking ability and effectivity of DAC, conventional crosslinking agent glutaraldehyde (GA) was chosen for comparison. Equal amounts of DAC or GA were employed for crosslinking of two PVA source materials (Mowiflex TC 232 and Mowiol 84–86% hydrolysed). For this reason, it was necessary to experimentally assess the reactive aldehyde group content for both of used crosslinking agents (DAC and GA). This was achieved with the aid the oxime reaction between crosslinker and hydroxylamine hydrochloride (see Figure 8) with subsequent alkalimetric titration by 1N NaOH. The consumption of standard solution revealed reactive aldehyde group content of 11.7 ± 0.3 mmol/g for fresh DAC and of 11.1 ± 0.5 mmol/g for 50 % GA solution. These values were reflected in the sample preparation in following manner. For example, PVA/DAC hydrogel sample crosslinked using 1 wt% contained 0.05 g of DAC. This DAC crosslinker weight corresponds to the amount of 585 ± 13 μ mol of reactive aldehyde groups (n_{-CHO}) used for crosslinking of this specific sample. To achieve comparable crosslinking using GA, the same amount of reactive n_{-CHO}

per sample must be used. Thus, equivalent PVA/GA hydrogel sample to the one prepared by DAC was crosslinked using 46.6 μL of GA 50% solution. Such approach was applied in the entire comparative crosslinker study, which encompassed use of DAC crosslinker in the concentration range from 0.0625 to 5 wt% and equivalent amount of GA. For the sake of simplicity, only catalyst system type A (1.33M HCl, 1.5 mL per sample) was used for the preparation of PVA/DAC and PVA/GA blends.

PVA/DAC blends prepared using 1 wt% of fresh and aged DAC and two distinct catalyst systems as well as the PVA/DAC and PVA/GA blends within comparative crosslinker study were cast on 20×10 cm frame and dried at 30 °C. Subsequently, these xerogel samples were intensively washed in order to remove uncrosslinked material components and again dried at 30 °C. PVA/DAC xerogel/hydrogel samples prepared using 1 wt% of fresh and aged DAC were analysed by several analytical methods described below. PVA/DAC and PVA/GA hydrogel samples prepared within comparative crosslinker study were analysed only in the terms of their network parameters. Designation of all PVA/DAC and PVA/GA hydrogel samples is noted in Tables 13 and 14. [91]

Table 13 PVA/DAC samples prepared using aged DAC. [91]

DAC age (days)	PVA/DAC blend A	PVA/DAC blend B
1	A01	B01
14	A02	B02
28	A03	B03

Table 14 PVA/DAC and PVA/GA samples prepared using different PVA source and different crosslinker (DAC or GA). Equal conditions are expressed by the amount of reactive group ($n_{\text{-CHO}}$) per sample. [91]

$n_{\text{-CHO}}$ per sample (μmol)	DAC crosslinker			GA crosslinker		
	DAC (wt%)	PVA/DAC		GA (μL)	PVA/GA	
		Mowiflex	Mowioli		Mowiflex	Mowioli
2920	5	DTC-A	DSA-A	233	GTC-A	GSA-A
1750	3	DTC-B	DSA-B	240	GTC-B	GSA-B
877	1.5	DTC-C	DSA-C	69.9	GTC-C	GSA-C
585	1	DTC-D	DSA-D	46.6	GTC-D	GSA-D
146	0.25	DTC-E	DSA-E	11.6	GTC-E	GSA-E
73.1	0.125	DTC-F	DSA-F	5.8	GTC-F	GSA-F
36.6	0.0625	DTC-G	DSA-G	2.9	GTC-G	GSA-G

6.3 Experimental methods

6.3.i Pilot study

FT-IR analysis. Infrared spectroscopic analysis was conducted on input uncrosslinked PVA (Mowiflex TC 232), unwashed and washed PVA/DAC samples from both prepared set (1 and 2) and for every sample dried at different temperature (30 °C, 60 °C, 90 °C).

Infrared spectra were collected using IR spectrometer Thermo Scientific Nicolet 6700 FT-IR equipped with ZnSe-diamond crystal (ATR mode) in span of 750–4000 cm^{-1} . (resolution: 4, number of scans: 64, suppression of atmospheric gases enabled). [17]

TGA analysis. Thermogravimetric curves were recorded for input uncrosslinked PVA (Mowiflex TC 232) and for crosslinked PVA/DAC samples dried using different temperature. Only washed xerogel samples were analysed. Thermogravimetric measurements were conducted using TA Instruments TGA Q500 thermogravimeter equipped with platinum pan. The temperature range was set from 30 °C to 1000 °C, heating rate 10 °C/min. Weight of all samples was kept the same (5 ± 0.1 mg). Inert gas in ratio 40:60 mL/min (balance:sample) was used during measurements. [17]

Network parameters. Base on the swelling behaviour of all of the of prepared PVA/DAC samples within this pilot study, network parameters (see Chapter 4.2) were calculated. These parameters include percentage of swelling, equilibrium water content (EWC), gel fraction, average molecular weight of macromolecules between crosslinks (\bar{M}_c) and crosslink density (ρ_c). To determine gel fraction, PVA/DAC samples were weighted in dry unwashed state and subsequently intensively washed in demineralized water for several weeks. After washing process, samples were dried at 30 °C till constant weight. From all of the washed and dried PVA/DAC samples, specimens of 3 cm in diameter were cut. The weight of specimens was recorded. Next, these specimens were immersed and shaken in demineralized water for 24 hours. After this period of time they were weighted in their swollen state. [17]

Macroscopic observation. All of the prepared PVA/DAC samples were compared based on their macroscopic observation. [17]

6.3.ii DAC study

FT-IR and XRD analysis. Spectral analysis of input alpha cellulose and its periodate oxidized derivative in the form of raw (insolubilized) DAC and solubilized DAC was carried out. In order of DAC analysis via these methods, samples were dried at 100 °C according to previous literature [97]. Instrument and the setup were identical as in the pilot study.

X-ray diffraction analysis was conducted on the same materials as mentioned above. For this purpose, PANalytical XPert PRO X-Ray diffractometer in span of diffraction angles 5–95 2θ degree was used. $\text{Cu}_{K\alpha 1}$ was used as a source of radiation. [99]

TGA analysis. Thermogravimetric analysis (TGA) was conducted on insolubilized as well as on fresh and aged solubilized-dried DAC samples. Instrument and the experimental setup were identical as in the pilot study. [99]

Reactive aldehyde group content. Prepared DAC was analysed in the terms of its reactive aldehyde group content. This analysis was conducted on raw (insolubilized) and freshly solubilized DAC (1 day old) as well as on the aged solubilized samples (14 and 28 days old). Weight concentration of DAC in solution was assessed from the recovery of solids after drying of defined volume of each sample at 100 °C. Determination of reactive aldehyde group content was conducted on 0.1 g of DAC present in solution or suspension. Typically, 0.1 g of each DAC sample was diluted to fixed volume by water and 0.01M hydrochloric acid was used to set pH = 4.00. DAC samples were subsequently mixed with solution of hydroxylamine hydrochloride (0.43 g in 20 mL of water, 0.01M NaOH was used to set pH = 4.00). Such mixtures were stirred at 100 rpm for 24 hours at laboratory temperature in closed containers. The conversion of aldehyde to oxime was determined by the consumption of 0.1N NaOH. [97, 99, 100]

Viscosity and density measurements. The viscosity and density was measured for fresh and aged DAC solutions. These properties were measure using Anton Paar microviscometer Lovis 2000 ME and Density meter DMA 5000 M at 25 °C. [99]

LC-QTOF MS analysis. High performance liquid chromatography (HPLC) analysis of solubilized DAC samples (fresh and aged) were performed on 1260 Infinity LC system (Agilent Technologies). Chromatographic separation of the sample components was carried out on a Zorbax Extend-C18 (2.1 × 50 mm, 1.8 μm) column at a flow rate of 0.3 mL/min. The mobile phase consisted of 0.1% formic acid in water and acetonitrile (isocratic flow, 70:30). The sample injection volume was 1 μL . Detection was performed with a quadrupole Time of Flight mass spectrometer (6530 Q-TOF, Agilent Technologies) employing an electrospray ion (ESI) source. The mass spectrometer was operated with capillary voltage 3000 V. Data was recorded and processed using the MassHunter software v. B.05.01 (Agilent Technologies). [99]

NMR spectroscopy. Nuclear magnetic resonance (NMR) spectra of solubilized fresh and aged DAC sample solutions of pH 3.5 ± 0.1 were recorded

in mixture of 90% H₂O and 10% D₂O at 25 °C utilizing Bruker Avance III HD 700MHz NMR spectrometer equipped with triple-resonance cryoprobe optimized for ¹³C detection. In order to differentiate between CH and CH₂ resonances, gradient-enhanced multiplicity-edited ¹H–¹³C HSQC experiment with J_{H-C} coupling constant set to 145 Hz was used. The C3/H3, C4/H4 and C5/H5 signals were assigned to corresponding C6/H6 resonances using ¹H–¹H TOCSY, ¹H–¹³C HSQC and ¹H–¹³C HMBC (ⁿJ_{H-C} = 10 Hz) experiments with standard setup. Based on the combination spectra of ¹H–¹³C HMBC and ¹H–¹H ROESY, the corresponding C1/H1 and C2/H2 resonances were identified. Isolated signals of diastereotopic protons from CH₂ groups are marked as H^a and H^b. The assignment of signal was carried out on the 1 day old (fresh) sample, which was further investigated after 14 and 28 days from preparation by ¹H and ¹³C NMR spectra. Signal intensities were estimated based on 1D ¹³C spectra due to a number of overlapping signals in ¹H spectra. Thus, to minimize the influence of various proton counts in the vicinity of carbon atoms to the intensity of ¹³C signals, only signals from the identical atoms/groups (CH₂) were compared. The populations of discussed moieties (structural arrangements of DAC) are expected to be reflected in signal intensities at least on semi-quantitative manner. [99]

GPC analysis. Gel permeation chromatography (GPC) analysis was performed on diluted samples of stock DAC solution (dilution factor = 10). Chromatographic system Waters HPLC Breeze equipped with Waters 2424 ELS detector (temperature of drift tube 60 °C) and Shodex OHpack SB-806M HQ (300 x 7.8 mm x 8µm, column *T* = 30 °C) column was used. Mobile phase was 0.05M ammonium carbonate water solution. Pullulan polysaccharide calibration kit SAC-10 (Agilent Technologies, Inc.) in a span of *M_p* 180–100 000 g/mol was utilized for calibration. Obtained data were processed and evaluated using Empower Pro software.

Waters 2414 refractive index (RI) detector was employed in the case of the solubilization study. This study included the analysis of the resulting molecular weight of solubilized DAC using solubilization process (i) under different initial pH conditions and solubilization time and (ii) via utilization of non-conventional heating by microwave assisted solubilization (MWS). Furthermore, RI detector was used in the investigation of molecular weight of DAC water soluble polymer derivative sodium 2,3-dicarboxy cellulose. Besides the use of this different detector, the experimental setup and conditions (column, mobile phase, etc.) were identical as mentioned above. [99]

SEM analysis. Scanning electron microscopy (SEM) was utilized for imaging of input alpha cellulose and DAC materials. These include solid state DAC samples obtained by filtration and lyophilised filtrate solutions of DAC both from solubilization study. For this purpose, field-emission scanning electron

microscope (FE-SEM) FEI Nova NanoSEM 450 (FEI, Czech Republic) operated at 5kV acceleration voltage was utilized.

6.3.iii Hydrogel study

Solid-state ^{13}C NMR. Cross-polarization/magic-angle-spinning carbon-13 nuclear magnetic resonance (CP/MAS ^{13}C NMR) spectra were recorded for uncrosslinked PVA (Mowiflex TC 232) and PVA/DAC samples prepared using fresh and aged DAC. For this purpose, powdered samples suitable for this analysis were prepared utilizing ultra-centrifugal mill Retch ZM 200 equipped with 0.12 mm trapezoid-holed ring sieve. To prevent thermal degradation during high speed milling (10 000 rpm), samples were nitrogen-cooled prior the milling procedure. Finely ground powders were collected and stored several days in desiccator until analysis.

Bruker Advance 500MHz spectrometer operated at 500.13 MHz (^1H) and 125.77 MHz (^{13}C) equipped with 4 mm solid-state dual (BB-1H) CP/MAS probe was used for the CP/MAS ^{13}C NMR acquisition of spectra at laboratory temperature. Rotor spin frequency was set to 10 kHz with 4 s relaxation time. Crystalline α -glycine was selected as secondary reference to the ^{13}C NMR chemical shifts ($\delta_{st} = 176.03$ ppm for carbonyl carbon) [165]. According to previous studies [166], spectra of above mentioned samples were measured using contact time of 1 ms in order to achieve the best signal-to-noise ratio. The exponential fit of carbon signal decay was used for the determination of $T_{1\rho}(^1\text{H})$ values of PVA and PVA/DAC samples as a function of contact time (from 1 to 8 ms). The $T_{1\rho}(^{13}\text{C})$ values were calculated using exponential fit of the carbon signal decay as a function of the variable ^{13}C spin-lock time in the span of 0.5–7 ms following the cross-polarization time fixed to 1 ms in the case of all samples. [91, 167]

XRD analysis. X-ray diffraction analysis was conducted on input uncrosslinked PVA (Mowiflex TC 232) and PVA/DAC xerogels crosslinked via fresh and aged DAC. For this purpose, Rigaku MiniFlex600 X-ray diffractometer equipped with $\text{Co}_{K\alpha}$ ($\lambda = 1.789 \text{ \AA}$) radiation source and $\text{K}\beta$ line filter was used in the span of diffraction 5–95 2θ angles. [91]

Tensile measurements. Mechanical properties of uncrosslinked PVA and PVA/DAC xerogels samples prepared using fresh and aged DAC were analysed according to the standard EN ISO 37 (621436) on tensile testing apparatus M350 5CT (Labor Chemie, Czech Republic). The sets of specimens were prepared from the cast uncrosslinked PVA thin film and PVA/DAC xerogels in lengths of 35 mm and tempered at 25 °C and 40 % humidity. These specimens were initially strained at rate 1 mm/min to 7.5 % strain for Young's modulus estimation. The strain rate was then increased to rate of 50 mm/min. [91]

TGA analysis. Thermogravimetric analysis (TGA) was carried out on uncrosslinked PVA and PVA/DAC xerogel samples crosslinked by fresh and aged solubilized DAC. Besides washed PVA/DAC xerogels, unwashed PVA/DAC xerogels were analysed as well. Instrument and the experimental setup were identical as in the pilot study.

Network parameters. PVA/DAC hydrogel samples prepared using aged DAC as well as samples prepared within comparative crosslinker study (i.e. utilizing DAC and GA crosslinkers for two types of PVA) were evaluated and compared in the terms of their network parameters. In order to assess these parameters, disc specimens of diameter 8 mm were cut from above mentioned unwashed xerogel samples. Such specimens were intensively washed and swelled for one week. Swollen samples were then dried at 30 °C and placed in desiccator. High precision balance was used for weighing of these specimens before and after each step. The data was subsequently used for the calculation of network parameters defined by the equilibrium swelling theory suggested by Flory and Rehner, 1943 (see chapter 4.2). [148] The network parameters include percentage of swelling, equilibrium water content (EWC), gel fraction, average molecular weight of macromolecules between crosslinks (\bar{M}_c) and crosslink density (ρ_c). [91]

7. RESULTS AND DISCUSSION

7.1 Pilot study

The scope of the pilot study was to test the hypothetical suitability of DAC as a crosslinking agent for PVA. This assumption arises from the presence of aldehyde groups ($-\text{CHO}$) in DAC and hydroxyl groups ($-\text{OH}$) in PVA, which possibly leads to the formation of acetal or hemiacetal bridges between these macromolecular compounds under acidic conditions. Furthermore, influence of two different concentrations of acid catalyst systems (see Table 9) on PVA/DAC hydrogel properties was investigated. As the formation of crosslinked network is presumed to take place during drying of PVA/DAC blend and dehydration of DAC, the drying temperature was varied as one of the key process parameters in PVA/DAC hydrogel preparation. This pilot study served as a starting point for further investigation of DAC and its utilization as PVA crosslinker.

7.1.1 Characterization of uncrosslinked PVA

FT-IR and TGA analysis of uncrosslinked PVA. Untreated PVA was analysed by FT-IR spectroscopy and TGA analysis for subsequent comparison with its DAC crosslinked form. FT-IR spectrum (Figure 14 part **I**) shows peaks related to the presence of hydroxyl and acetate groups on PVA backbone. There can be found inter- intramolecular O–H stretching vibrations manifested by a broad band at 3240 cm^{-1} , symmetric and asymmetric stretching of alkyl groups CH_2 with peaks at 2939 cm^{-1} and 2909 cm^{-1} , vibrations of vinyl acetate groups (from non-hydrolysed PVA) C–O and C=O with band in the span of $1735\text{--}1710\text{ cm}^{-1}$, C=C end group vibrations at 1520 cm^{-1} peak, CH_2 bending (1427 cm^{-1}), O–H and C–H wagging (1374 cm^{-1}), CH_2 wagging (1325 cm^{-1}), C–O–C vibrations (1243 cm^{-1}), C–O stretching vibrations of PVA crystalline sequences (1141 cm^{-1}), C–O stretching and O–H bending vibrations of PVA amorphous sequences (1090 cm^{-1}), CH_2 bending and rocking (920 cm^{-1} , 830 cm^{-1}). [147–149] Figure 14 (parts **IIa** and **IIb**) shows the results from TGA analysis of uncrosslinked PVA with distinct peak weight loss rates at around $190\text{ }^\circ\text{C}$, $327\text{ }^\circ\text{C}$ and $437\text{ }^\circ\text{C}$. [17]

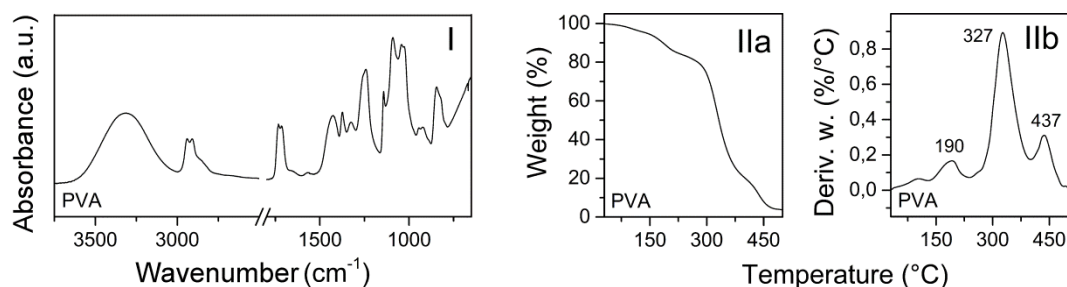


Figure 14 FT-IR spectrum (part **I**) and TGA thermogravimetric curves (parts **IIa** and **IIb**) of uncrosslinked PVA (Mowiflex TC 232). [17]

7.1.2 FT-IR and TGA analysis of PVA/DAC xerogels (pilot study)

FT-IR analysis of PVA/DAC. In general, the differences between IR spectra of uncrosslinked PVA (Figure 14 part I) and prepared PVA/DAC xerogels (Figure 15) can be seen in the relative weakening of intensity of the bands at 3240 cm^{-1} (O–H stretching) and $1735\text{--}1710\text{ cm}^{-1}$ (C–O and C=O vibrations). The lower intensity at 3240 cm^{-1} is caused by slight reduction of hydroxyl group amount possibly due to formation of acetal or hemiacetal bridges as a result of crosslinking via DAC. The second observed decrease for the bands at $1735\text{--}1710\text{ cm}^{-1}$ could be explained as the result of acid hydrolysis originating from the presence of introduced acid catalyst. In other words, the addition of acid catalyst system composed of H_2SO_4 , CH_3OH and CH_3COOH possesses not only function as mediator of crosslinking reaction of PVA via DAC, it also most likely influences the degree of hydrolysis of PVA. The evidence of acid hydrolysis of PVA was noticeable as a strong odour reminiscent of acetic acid during drying of PVA/DAC blends (regardless of the drying temperature). [17]

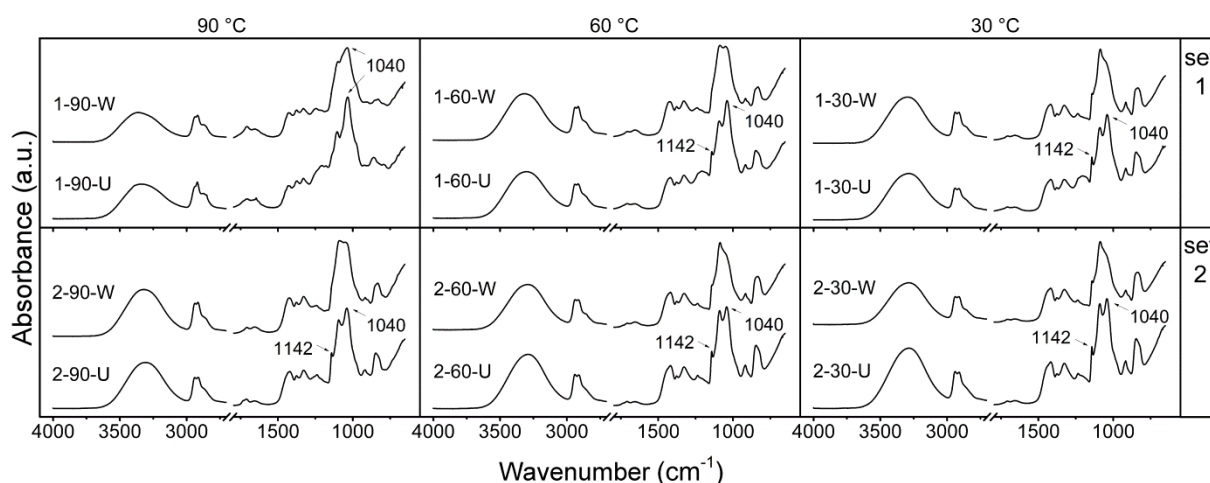


Figure 15 FT-IR analysis of PVA/DAC xerogels prepared within pilot study. [17]

The difference in IR spectra of PVA/DAC xerogel samples prior and after washing are manifested in the change of intensity of two bands, namely 1142 cm^{-1} and 1040 cm^{-1} . The decrease of the band at 1142 cm^{-1} in all of the washed samples signals removal of uncrosslinked crystalline phase of PVA in the process of washing. The other noticeable change, absence of band at 1040 cm^{-1} in all of the washed samples (except 1-90-W) can be explained as removal of glycerol, which has a role of softener in untreated PVA (Mowiflex TC 232) as it is compounded with PVA by manufacturer. Based on the macroscopic observation, the samples 1-90 are probably heavily degraded because of the high temperature of drying and the redundant high amount of catalyst. This causes slightly different trends observed in IR spectra of 1-90 samples. [17]

TGA analysis of PVA/DAC. All PVA/DAC xerogel samples within pilot study were analysed and compared using TGA (see Figure 16). The recorded thermogravimetric curves revealed increasing thermal stability ascending from sample 2-90-W, 2-60-W to 2-30-W. Thus, the higher drying temperatures decrease thermal stability profile of the samples prepared using lower concentration of catalyst system (PVA/DAC set 2). When higher catalyst system concentration is used (PVA/DAC set 1), the different and non-linear thermal stability dependence on used drying temperature is apparent from the recorded thermogravimetric curves. For the samples 1-60-W and 1-30-W within PVA/DAC set 1 is the thermal stability more or less similar. The last sample from this set (1-90-W) exhibited somewhat increased thermal stability behaviour. Analogously to the disclosure in FT-IR spectroscopy, thermal behaviour of this sample is strongly influenced by the redundant catalyst system and high drying temperature. Such experimental setup used in the case of this specific sample may cause possible degradation and/or formation of unsaturated bonds along the PVA macromolecules increasing the thermal stability. [17]

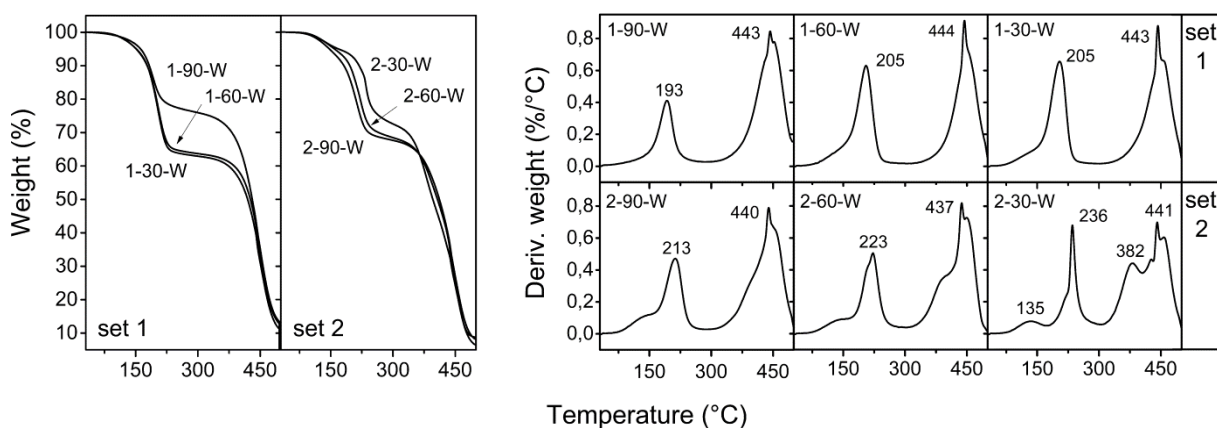


Figure 16 TGA analysis of PVA/DAC xerogels prepared within pilot study. [17]

7.1.3 PVA/DAC network parameters and macroscopic observation (pilot study)

Network parameters. According to the equations given in the Chapter 4.2 the network parameters of crosslinked PVA/DAC hydrogel samples were calculated. The average molecular weight of macromolecules between crosslinks (\bar{M}_c) and crosslink density (ρ_c) were calculated with the aid of equilibrium swelling theory. These network parameters require exact definition of following variables: density of polymer $\rho_p = 1.3 \text{ g/cm}^3$; specific volume of polymer $\bar{v} = 0.7692 \text{ cm}^3/\text{g}$; density of water at 25 °C $\rho_w = 0.99705 \text{ g/cm}^3$; molar volume of water $V_l = 18.0477$; number average molecular weight of PVA Mowiflex TC 232 $\bar{M}_n = 23\,500 \text{ g/mol}$ (estimated by GPC); polymer-solvent interaction parameter for PVA and water $\chi_l = 0.464$ [150]. The resulting network parameters are noted in Table 15 and Figure 17.

Table 15 Network parameters, i.e. swelling capacity, equilibrium water content (EWC), gel fraction, average molecular weight between crosslinks (\bar{M}_c) and crosslink density (ρ_c), calculated for PVA/DAC hydrogel samples prepared within pilot study.

#	Swelling (%)	EWC (%)	Gel Fraction (%)	\bar{M}_c (g/mol)	ρ_c (mmol/cm ³)
1-30	129.0	56.3	83.7	410	3.2
1-60	109.5	52.3	85.1	310	4.3
1-90	48.4	32.6	81.0	80	16.7
2-30	140.6	58.4	84.8	490	2.7
2-60	144.3	59.1	85.2	510	2.6
2-90	108.3	52.0	88.7	300	4.4

There are similar trends within network parameters of hydrogels regardless of the tested catalyst system concentrations (PVA/DAC set 1 and set 2). However, these trends are closely related to drying temperature. On the one side, the swelling capacity, average molecular weight between crosslinks \bar{M}_c and equilibrium water content EWC exhibit decrease with the increasing drying temperature. On the other side, crosslink density ρ_c and gel fraction (with the exception of 1-90 sample) increases dramatically when higher drying temperatures are used.

All these trends are visible especially for the PVA/DAC set 1 (higher concentration of catalyst system). For set 2 the tendencies are less pronounced (see Figure 17). The explanation to this can be found in the possible crosslinking induced by thermal degradation. In other words, as the drying temperature rises, degradation of polymer/crosslinker most likely produces crosslinking hotspots and thus denser network of crosslinks (higher ρ_c) can be formed. Such network is defined by shorter macromolecules between these crosslinks (lower \bar{M}_c) and subsequently by decreased swelling capacity and EWC.

To summarize, if higher concentration of catalyst system is used (set 1), the dependence of network parameters on the increase of the drying temperature is much more pronounced. In contrast to this, utilization of lower concentration of catalyst system leads to samples with essentially identical network parameters up to drying temperature 60 °C. Thus, the combination of high concentration of catalyst system along with the use of high drying temperature produces highly crosslinked samples. However, the gel fraction of such material (namely sample 1-90) decreases steeply oppose to expected behaviour. This observation implies significant degradation of 1-90 caused by the excess of catalyst system and relatively high drying temperature. These assumptions were partially confirmed by FT-IR, TGA and by simple macroscopic observation of prepared samples (see following page).

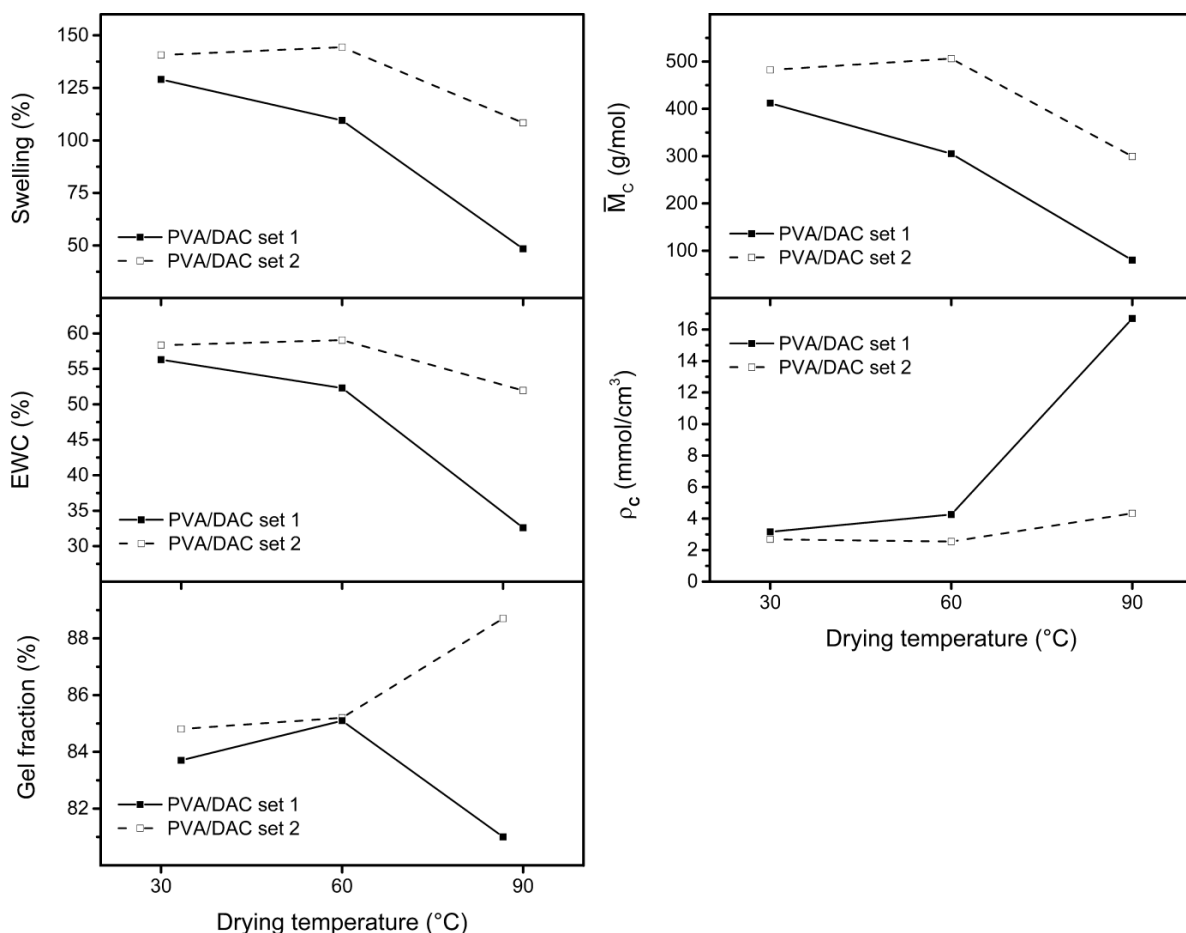


Figure 17 PVA/DAC network parameters dependence on drying temperature and used concentration of catalyst system (pilot study). The lines connecting points in the right graph are only guides for eyes.

Macroscopic observation. The influence of drying temperature and the concentration of catalyst system is best seen via macroscopic observation. Figure 18 depicts the PVA/DAC sample specimens prior washing, washed and swelled specimens, and washed and dried specimens. Increase of the catalyst system amount hand in hand with increase of drying temperature results in visible degradation of PVA/DAC samples manifested by colour change. [17]

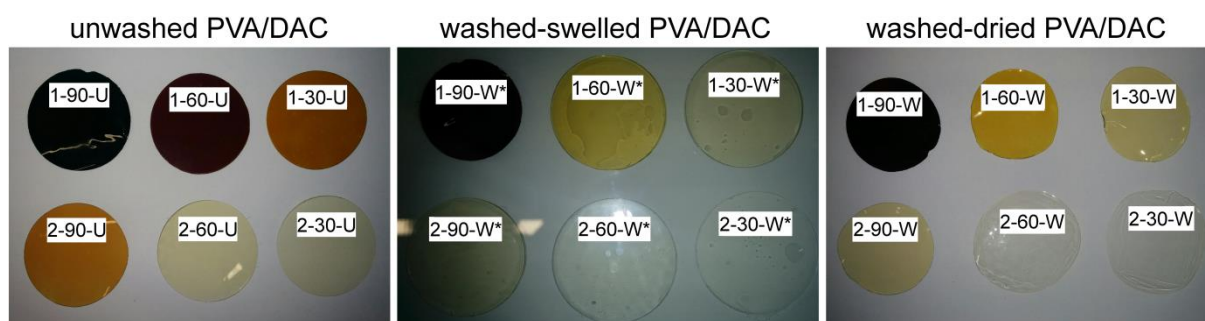


Figure 18 Macroscopic observation of PVA/DAC xerogels prepared within pilot study. [17]

7.1.4 Summary of the pilot study

The results from pilot study showed DAC applicability as a crosslinking agent for PVA. The properties of prepared PVA/DAC samples can be modified by the choice of process parameters such as catalyst concentration or drying temperature. However, to obtain degradation-free hydrogel materials, it is advisable to utilize lower concentration of catalyst system along with drying temperatures up to 60 °C. [17]

Following text is focused on detail analysis of DAC structure, properties and their changes in time, which are believed to have direct influence on intended crosslinking application.

7.2 DAC study

The main goals of DAC study are to (i) determine and compare basic properties and characteristic of the insolubilized and solubilized product of periodate cellulose oxidation, to (ii) characterize solubilized DAC in the terms of its structure, structural changes and stability within chosen timeframe while maintaining low pH of DAC solution and to (iii) investigate the DAC solubilization process and its influence on properties of DAC while modulating parameters of such process.

Basic characterization includes confirmation of aldehyde group presence using adequate absolute methods (such as IR spectroscopy); concomitantly indirect methods such as XRD allowing observation of crystallinity loss as a result of anhydroglucopyranose rings opening; and essentially important evaluation of the efficiency the oxidation reaction in the terms of degree of oxidation or conversion expressed in the reactive aldehyde group content.

The structure of DAC on molecular and supramolecular level defines its physico-chemical properties. Furthermore, there is a reasonable assumption that specific structural arrangement of DAC itself, or the changes induced for example by its aging, will further influence its potential as a crosslinking agent. As have been mentioned in the earlier text regarding the DAC structure and properties (chapter 3.2), presence of highly reactive aldehyde group results in complex composition of DAC. Some structural arrangements were already given (see Figure 7); nevertheless, Figure 19 [99] depicts expanded proposals of theoretical and possible DAC structures. These include DAC bearing free aldehyde groups (**A**) and wide variety of its hydrated forms, i.e. fully hydrated form (**B**), hemialdal form (**C**), intra- and intermolecular hemiacetal DAC forms (**D–G**).

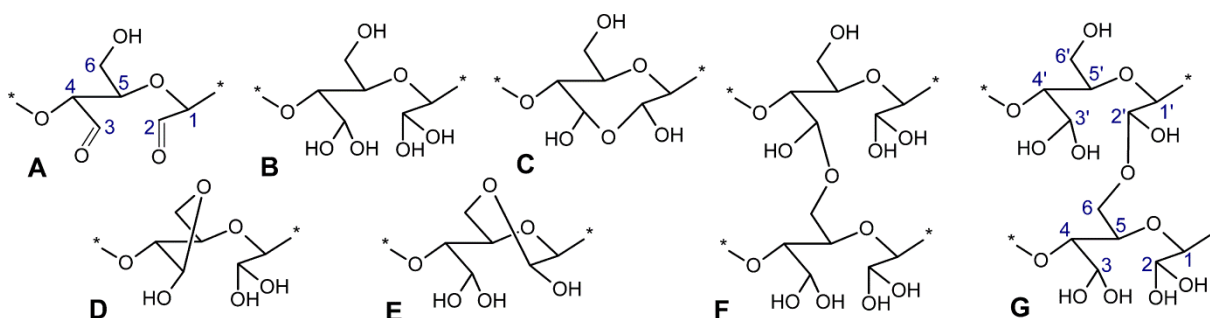


Figure 19 Possible structural arrangements of DAC. A – dialdehyde, B – fully hydrated dialdehyde, C – hemialdal, D – intramolecular hemiacetal with C3–O–C6 bond, E – intramolecular hemiacetal with C2–O–C6 bond, F – intermolecular hemiacetal with C6–O–C3' bond, G – intermolecular hemiacetal with C6–O–C2' bond. Intermolecular hemiacetals F and G may also contain hemialdal unit C in their structure (not shown). [99]

Besides the complexity of possible structural arrangements, the DAC solubilization process has shown to be intriguing topic of research as there are somewhat contradictory reports about its influence on DAC degradation. [98] To evaluate degradation potential of solubilization, insolubilized DAC aliquot was transformed into easily dissolvable derivative Na-DCC [37] prior the solubilization and analysed in terms of molecular weight distribution. This initial step also gives information whether the periodate oxidation promotes degradation or maintains high selectivity. Other aliquots of raw DAC were solubilized utilizing different time of solubilization (0.5–7 hours) to investigate this process in detail. For this reason, each DAC aliquot was characterized in the terms of pH, molecular weight, amount of solubilized content, insolubilized particle morphology etc.). Moreover, the same aliquot-solubilization experiments were repeated utilizing different initial pH of raw DAC (3.5–7.5). These pH-dependent aliquot-solubilization experiments were carried out based on the knowledge of pH sensitivity of DAC and structurally similar compound (i.e. dialdehyde starch, DAS). Besides the conventional heating used during solubilization, microwave assisted solubilization was employed and resulting products were analysed in the solubilized as well as in the dried and freeze-dried state.

The following sections are focused on the detailed description of DAC. The results and conclusions drawn in this chapter are further broadened and utilized in the next chapter “7.3 Hydrogel study” dealing with the DAC application as a crosslinking agent.

7.2.1 Basic DAC characterization

Basic characterization methods were applied to analyse prepared DAC and compare it to the input cellulose material. IR spectroscopy was employed to investigate the presence of reactive aldehyde groups formed on DAC as a result of periodate oxidation of input cellulose material. The process of periodate oxidation disrupts ordered macromolecular packing, thus the crystallinity of resulting DAC was studied by XRD. Furthermore, thermal stability and reactive aldehyde group content of different DAC forms (insolubilized vs. solubilized) as well as of the fresh and aged solubilized-dried DAC samples were evaluated using TGA. Finally, viscosity and density of the prepared DAC solutions was analysed.

FT-IR analysis. Spectral analysis was conducted on source cellulose material and its periodate oxidized derivative DAC present in two forms, raw (insolubilized) and solubilized-dried DAC (see Figure 20). The IR spectra of both forms of DAC exhibit similar bands as cellulose. The difference between cellulose and DAC is manifested by the presence of C=O vibrational band at 1730 cm^{-1} serving as the evidence of –CHO groups formation on DAC backbone. There is also noticeable relative intensity increase of the band at

875 cm^{-1} indicating increased amount of hemiacetal structures (C–O–C) in both forms of DAC when compared to cellulose. These DAC typical bands are well known and were reported earlier, [97, 168–170] however it is not possible to assess of exact amount of –CHO functional groups as they tend hydrate when exposed to moisture. [73] The last observed phenomena in the spectral analysis of DAC is the broadening of peak shoulder in the span of 1150–1200 cm^{-1} obscuring vibrational bands of asymmetric and symmetric stretching of C–O–C otherwise visible for unmodified cellulose. These two bands can be resolved in the spectrum of crystalline cellulose where only one kind of C–O–C groups exists, while several hemiacetal or acetal groups exist in DAC. Another reason for this broadening may be the presence of adsorbed water molecules arising from ambient humidity, which may influence the vibration frequency by formation hydrogen bonds blurring thus observed peaks.

IR spectra of raw and solubilized-dried DAC are more or less identical with only one difference in slightly higher intensity of absorption band of hemiacetal group vibration (C–O–C) at 875 cm^{-1} for solubilized-dried DAC sample. The possible reason of higher amount of hemiacetal groups of this form of DAC manifested by the increased intensity can be explained as the influence of sample preparation process. In other words, DAC was initially solubilized (possible formation of intra- and intermolecular hemiacetal structures) and subsequently dried from water solution. This drying process could further favour the formation of potentially more stable hemiacetal forms of DAC (see Figure 19 D–F). [99]

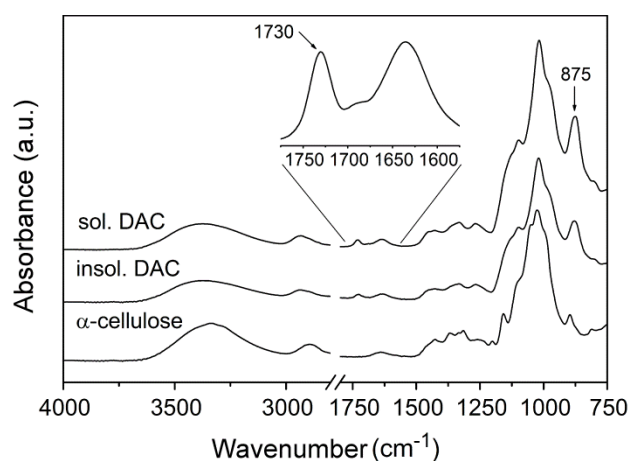


Figure 20 FT-IR spectra of source cellulose, insolubilized and solubilized-dried DAC. [17, 99]

Besides the sample of solubilized-dried DAC prepared from fresh DAC stock solution (1 day old), similar DAC samples were prepared using 14 and 28 days old solubilized DAC and analysed by IR spectroscopy as well. However, they did not show significant difference when compared to freshly solubilized-dried DAC. For this reason, they are not shown in the Figure 20. [99]

XRD analysis. X-ray diffraction analysis of source cellulose material and two forms of prepared DAC (insolubilized and solubilized-dried DAC) were analysed. Diffractograms of these samples are shown in Figure 21. As expected, relatively sharp patterns observed for alpha cellulose (diffraction peaks at 16.3, 22.4 and 34.6 $2\theta^\circ$) were shifted to broad signals after periodate oxidation to DAC (diffraction peaks at 20.0 and 43.0 $2\theta^\circ$). This is consistent with amorphization of original material as reported in the literature. [101] Based on the recorded diffractograms of both forms of DAC, the loss of crystallinity (from 25 % of input cellulose to approximately 7 % of prepared DAC) can be attributed to the destruction of otherwise ordered macromolecular packing of AGUs. The shift of diffraction peaks implies phase change from close-packed crystalline structure of cellulose to mostly amorphous structure of DAC, which is induced by the partial deterioration of AGU (scission of C2–C3 bond) during periodate oxidation and polymer periodicity decrease. [99]

The diffraction patterns observed for insolubilized and solubilized-dried DAC were identical (see Figure 21). Similarly to the results of FT-IR spectroscopy, XRD analysis of fresh and aged solubilized-dried DAC samples have also exhibited negligible differences.

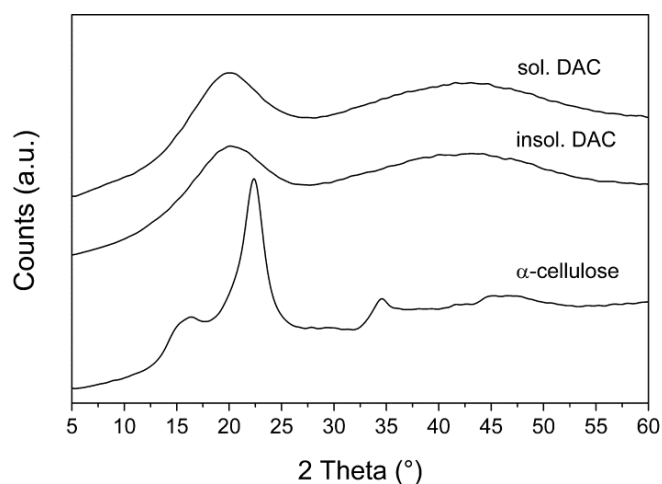


Figure 21 XRD analysis of source cellulose, insolubilized and solubilized-dried DAC. [17, 99]

Summary of FT-IR and XRD analyses. The characterization via FT-IR and XRD analysis of insolubilized (raw) and solubilized-dried DAC samples of different age showed almost identical patterns in recorded infrared spectra and XRD diffractograms. With the respect to the analytical power of used characterization methods, these results imply that relatively stable DAC product on qualitative level was obtained regardless of its solubilization conditions and aging. The only difference between insolubilized and solubilized-dried DAC was noticeable in IR spectra manifested in the somewhat higher intensity of the absorption band indicating higher amount of hemiacetal groups in solubilized-

dried DAC samples. This observation can be explained as a result of more stable hemiacetal structure formation during drying of solubilized DAC. If the raw DAC has higher porosity than solubilized-dried DAC and absorbs more humidity, another explanation of this phenomenon is possible. Competition between hemacetalization and hydration can result into slight suppression of the respective band intensity. [99]

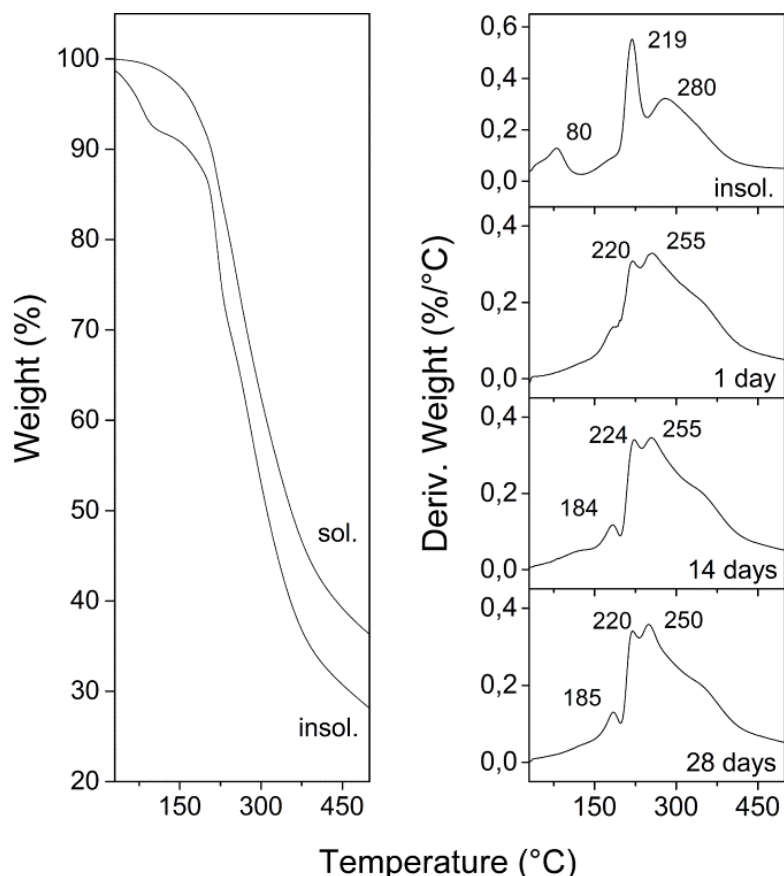


Figure 22 Thermogravimetric curves recorded for insolubilized DAC sample and aged solubilized-dried DAC samples.[99]

TGA analysis. Thermal behaviour of insolubilized as well as fresh and aged solubilized-dried DAC samples was investigated with the aid of thermogravimetric analysis (TGA). As the thermoanalytic curves of all aged solubilized-dried DAC samples were similar, only one example is shown (see Figure 22 left part). Nevertheless, differences between aged DAC samples are clearly visible in the graphs plotting the dependence of derivative weight loss on temperature (Figure 22 right part). [99]

In contrast to the previous spectral analysis of different DAC forms, there are noticeable differences between insolubilized and solubilized-dried DAC in the thermal stability profile (see Figure 22). In general, insolubilized form of DAC

exhibits well defined and almost separate peaks in weight loss rate at 219 and 280 °C, which can be most likely assigned to thermal degradation of different molecular weight fractions. Another significant peak in weight loss rate present at 80 °C probably belongs to the water evaporation process as the dry insolubilized DAC is by nature in the form of powder of relatively high porosity. On the other side, thermal stability profiles of the solubilized-dried DAC samples exhibit overlap of several peaks in weight loss rate, regardless of the DAC age (Figure 22 right part). Observation of such thermogravimetric profile change is not surprising given the prolonged solubilization process of DAC (7 hours at 80 °C), and can be considered as an indirect evidence of pro-degradation character of solubilization as reported by Sulaeva *et al.* (2015). [98] In other words, solubilization probably results in thermal degradation/fragmentation of DAC macromolecules into different molecular fractions further emerging in broader polydispersity. The influence of solubilization process under various conditions is discussed in detail in the section 7.2.4. [99]

The thermogravimetric curves of aged solubilized-dried DAC samples showed quite similar patterns with some minor changes in the intensity of peaks in weight loss rate (see Figure 22 right part). The first characteristic peak around 184 °C is unambiguously present in the thermal profile of 14 and 28 days old DAC samples and is also slightly visible as a small shoulder in thermogravimetric curve of fresh DAC. As this peak in weight loss rate is manifested at quite low temperature there is an assumption that it belongs to the low molecular fraction of DAC, which evolves in time of aging and thus is not present as distinct peak in the thermogravimetric curve of fresh DAC. The other peaks in weight loss rate at around 220 and 250 °C are present for all of the aged solubilized-dried DAC samples. There is visible modest shift of these peaks to higher temperatures (224 and 255 °C) recorded for 14 days old DAC sample and subsequent formation of shoulder at around 350 °C for both 14 and 28 days aged DAC samples. Such thermal behaviour is presumably associated to formation of intermolecular hemiacetals between DAC macromolecules, which imparts higher temperature stability of such samples. [99]

Reactive aldehyde group content. Insolubilized (raw), fresh and aged solubilized DAC samples were analysed in the terms of reactive aldehyde content. This quantitative analysis, in which the aldehyde content was determined by alkalimetric titration (1N NaOH), showed identical reactive aldehyde content of both insolubilized and solubilized (1 day old) DAC forms (10.97 ± 0.08 mmol/g). This value of reactive aldehyde group content corresponds to 88% degree of oxidation/conversion of cellulose to DAC (aldehyde content of fully oxidized cellulose 12.5 mmol/g). [99]

The fresh solubilized DAC was left to age at laboratory temperature and the reactive aldehyde group content was again determined after 14 and 28 days from

DAC preparation. Figure 23 shows the evolution of the reactive aldehyde content in the mentioned timeframe. The noticeable decreasing trend of this quantity is not surprising as it has been observed in previous works. [97, 104] However, there are some important differences when comparing result from current and previous studies.

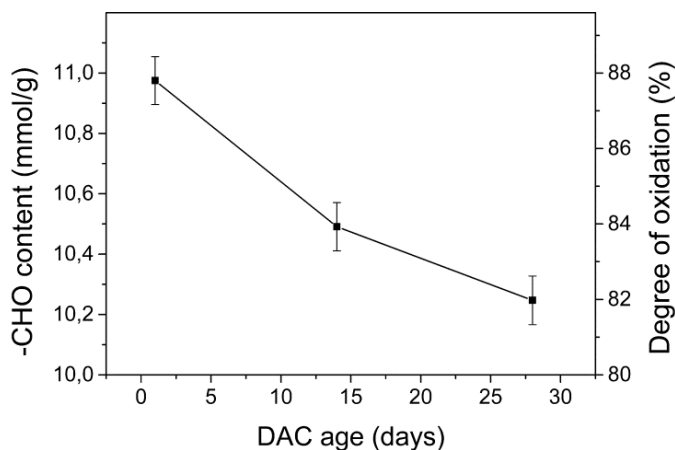


Figure 23 Reactive aldehyde group content and degree of oxidation of prepared solubilized DAC estimated over period of 28 days of DAC aging. The lines connecting points in the right graph are only guides for eyes. [99]

In the current study, the loss of aldehyde group content was estimated to be roughly around 7 % after 28 days from DAC preparation. In contrast to this, in the study of Kim *et al.* (2004) regarding the stability of solubilized DAC, the decrease in reactive aldehyde group content of similarly prepared DAC was approximately 15 % after 21 days [97]. The other study made by Sirviö *et al.* (2014) involved analysis of insolubilized DAC as an intermediate for 2,3-dicarboxy cellulose preparation. Such raw DAC was stored in never-dried state at 4 °C showed 32 % loss of reactive aldehyde group content between first and second week from DAC preparation. Based on this observation, Sirviö *et al.* strongly advise to prepare fresh DAC every time.

The considerably slower rate of aldehyde group content loss in current work can be explained by the suppression of negative degradation processes occurring at basic pH values. This assumption is based on the works of Veelaert *et al.* (1997) and Potthast *et al.* (2009) in which the influence of pH and temperature on stability of DAS and DAC was investigated, respectively. [100, 105] As has been noted earlier in the text (chapter 3.2), the degradation processes in periodate oxidized polysaccharides solutions or suspensions kept under alkaline conditions follow the mechanisms of β -elimination, internal and external Cannizzaro reactions as shown in Figures 11 and 12. To reduce these undesirable reactions and thus increase the stability of solubilized DAC, low pH was maintained in the current study. This pH setup possibly leads to the inhibition of hemiacetal hydrolysis and benzyl-benzilic acid type rearrangements.

Support for this hypothesis can be found in the previous works. The increased rate of aldehyde group content loss in the study carried out by Kim *et al.* (2004) was most likely caused by the neutral pH of solubilized DAC after dialysis. [97] Sirviö *et al.* (2014) did not discuss pH of raw DAC suspension at all. However, there is a reasonable expectation that employed repeated washing process of prepared raw DAC by distilled water resulted in a pH value close to neutral. Such conditions may favour the pronounced aldehyde group content loss. [104]

Summary of the TGA and reactive aldehyde group content studies. To suppress possible β -elimination degradation processes occurring at higher pH in DAC and analogue compounds, pH 3.5 ± 0.1 of DAC solution was maintained whole time. This experimental setup leads towards slower decrease of aldehyde group content. TGA revealed different thermal stability between insolubilized and solubilized-dried DAC of different age resulting from possible degradation during solubilization and aging.

Viscosity and density measurement. Viscosity (dynamic, kinematic) and density values were recorded for the DAC solution of different age and are given in Table 16. The noticeable decreasing trend of dynamic and kinematic viscosity of DAC solution with its age can be explained as the result of DAC chain scission and generation of lower molecular fractions. This conclusion correlates with TGA measurements. Fragmentation process influences the viscosity much more than potential DAC recombination (intermolecular hemiacetal formation), which should increase the viscosity. The values of DAC solution density remained constant during the observed timeframe of aging. [99]

Table 16 Viscosity and density values of fresh and aged DAC solutions. [99]

Time (days)	Dynamic viscosity (mPa.s)	Kinematic viscosity (mm²/s)	Density (g/cm³)
1	1.459	1.443	1.01049
14	1.414	1.400	1.01047
28	1.395	1.380	1.01049

Summary of characterization of DAC by basic analytical methods. Discussed analytical methods revealed essential properties of both insolubilized and solubilized (fresh and aged) DAC forms. However, they do not convey or uncover more detailed information about the exact molecular structure and composition of DAC. More elaborate and subtle analysis was necessary to clarify these issues. Furthermore, as a result of the interest in DAC applicability in solution-based processes, following text regarding the analysis and characterization of composition and structure is focused to solubilized form of DAC maintained at low pH.

7.2.2 Determination of solubilized DAC composition

To elucidate composition and molecular structure of solubilized DAC, HPLC analysis and NMR study was carried out on DAC fresh and aged samples. For possible structural arrangements of DAC, the reader is referred to Figure 19 again.

LC-QTOF MS analysis. HPLC analysis with detection performed by Q-TOF mass spectrometer was utilized for solubilized fresh and aged DAC, which showed two types of molecular peaks in obtained high resolution mass spectra. Observed signals can be divided and assigned to (i) different forms of DAC and to (ii) fragments of DAC degradation.

Regarding the signals of possible DAC structures, the first observed peak at 159.0299 m/z belongs to the form of DAC bearing free aldehyde groups (**A** in Figure 19). This signal had approximately the same intensity in all solubilized DAC samples spectra regardless of the DAC aging. The second peak detected at 177.0405 m/z corresponds to the partially hydrated DAC unit in the intramolecular hemiacetal and/or hemialdal form of DAC (**C**, **D** or **E** in Figure 19). This signal was clearly visible in the spectrum of fresh solubilized DAC sample as well as in the mass spectra collected for aged DAC samples, although with considerably lower intensity. The last observed signal at 371.0988 m/z was assigned to DAC in the form of intermolecular hemiacetal structures (**F** or **G** in Figure 19). The intensity of this peak was on the noise level in the spectrum of the fresh DAC. However, intensity of this signal increased with the age of DAC.

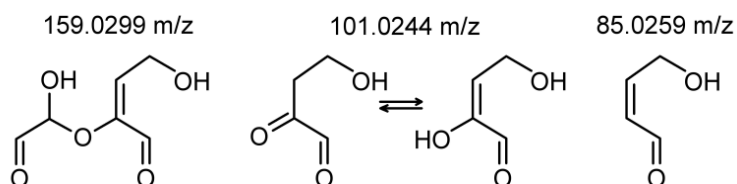


Figure 24 Possible molecular structures of DAC fragments suggested by Veelaert *et al.* (1997) [100] and Potthast *et al.* (2009) [105] observed at noted m/z values in HPLC analysis.

The β -elimination models of fragmentation of DAS and DAC reported by Veelaert *et al.* [100] and Potthast *et al.* [105] schematically represented in Figures 11 and 12, were compared with results from HPLC, and some of suggested DAC fragments were detected. These fragments were found at 159.0299, 101.0244 and 85.0295 m/z in mass spectra of all DAC sample regardless of the sample aging. The molecular structures of these fragments are depicted in Figure 24. At this point it should be noted, that the first mentioned fragment observed at 159.0299 m/z possesses the same m/z value as **A** form of

DAC, although their molecular structures are different. The signal intensity at this peak is probably sum of both of these entities. The other two bands found at 101.0244 and 85.0295 m/z are subsequent products of further DAC fragmentation. However, the presence of these relatively low molecular fragments can be caused by secondary fragmentation induced by the ionization and not as a result of DAC degradation. Besides mentioned signals, quite large number of other bands manifested by high m/z values was observed. This is not surprising, as macromolecular compound such as DAC forms larger and presumably very complex fragments which are difficult to analyse in the exact terms of their composition. However, based on the obtained mass spectra, very high molecular fragments (m/z values up to 2 500) were observed only for aged DAC samples.

Thus, HPLC equipped with Q-TOF mass spectrometer confirmed the presence of several DAC forms. The free aldehyde form (**A**) was detected in all of analysed solubilized DAC samples in spite of their age. The overall presence of this band is presumably due the tendency of hydrated DAC forms to easily lose -HO^- and -H^+ . In other words, the presence of DAC form **A** manifested by respective band could also arise due to the measurement-induced dehydration of otherwise hydrated DAC forms. Moreover, quite strong intensity of respective band in all of the DAC samples mass spectra may be also partially caused by the presence of DAC fragment with the same summary formula, which can be also induced by ionization and not as a result of DAC degradation as noted earlier.

Furthermore, partially hydrated and/or intramolecular hemiacetal forms of DAC (**C**, **D** or **E**) were manifested by relatively strong signal of respective m/z value in the fresh sample. The noticeably lower intensity, combined with higher m/z value signals in the mass spectra of aged DAC samples implies formation of intermolecular hemiacetal forms (**F** or **G**) of DAC.

These results correlate to some extent with TGA analysis, although they draw somewhat limited picture regarding the exact structural arrangements of prepared solubilized DAC. For this reason, more detailed NMR analysis of DAC structure was performed for fresh and aged DAC solutions.

NMR analysis of fresh DAC. As expected, NMR spectra of DAC solutions were quite complex, featuring a large number of signals arising from different spin systems.

In contrast to the findings obtained by HPLC analysis, only very weak aldehyde group ^{13}C signals at 191.4 ppm and 189.9 ppm were detected for fresh (one-day old) DAC solution. However, none of these signals can be attributed to free aldehyde groups of oxidized AGU, as was determined from ^1H - ^{13}C HMBC (heteronuclear multiple bond correlation) spectra analysis. Detected ^{13}C aldehyde signals correlate with ^1H resonances at 150.9/6.42 (149.9/6.48) ppm and 142/4.49 (133/4.29) ppm. NMR chemical shift ranges of these resonances do not match those of oxidized AGU. [79, 123] However they agree with

resonances describing side product of cellulose periodate oxidation in the form of 2,3-diketoglucopyranoside enol derivative with double bond between C3 and C4, originally reported by Röhrling *et al.* (2002). [171] No other signals corresponding to aldehyde groups were detected. [99]

Despite the absence of free aldehyde groups originating from DAC, ^{13}C signals of CH_2 groups from ^1H - ^{13}C HSQC (heteronuclear single quantum coherence) spectra can be assigned to several chemically distinct forms of DAC units. However, as a result of low signal intensity and signal broadening induced by the changes in neighbouring DAC chain groups, some resonances cannot be unambiguously assigned to specific DAC domains. Based on spectral-characteristic features, the assignment of the most intensive signals resulted in identification of four structural arrangements of DAC units. These moieties along with their ^1H and ^{13}C NMR chemical shifts are listed in the Table 17. [99]

Table 17 Different DAC forms C, D (involving two sub-forms noted as D I and D II) and G with the ^1H and ^{13}C NMR chemical shift assignment in ppm. [99]

Moiety	Atom	1	2	3	4	5	6 ($6^a/6^b$)
C	^1H	4.85	5.22	5.29	3.86	4.22	3.82/3.73
	^{13}C	96.6	85.3	86.6	70.1	65.4	60.6
D I	^1H	4.61	4.83	5.41	4.21	4.56	4.20/3.95
	^{13}C	96.7	90.5	99.6	80.8	75.9	69.5
D II	^1H	4.68	5.05	5.35	4.22	4.46	4.06/-*
	^{13}C	96.7	90.8	94.4	76.3	74.1	70.2
G	^1H	4.77	5.25	5.22	3.71	4.33	4.16/3.55
	^{13}C	95.4	85.2	87.0	70.1	66.2	57.7
	$^1\text{H}'$	4.85	4.88	5.22	4.55	3.95	3.90/-*
	$^{13}\text{C}'$	95.4	88.1	90.5	75.6	67.4	65.0

For atom numbering see Figure 19 caption.

* H6^b signal not observed.

The first two distinct forms of DAC, noted as **D I** and **D II**, were identified as intramolecular hemiacetals based on the two ^{13}C NMR CH_2 groups (C6) signals observed at 69.5 and 70.2 ppm, see Table 17. When compared these C6 signals to those of related cellulose derivatives such as 2,3-dicarboxycellulose (C6 = 62.3 ppm) [79] or cellulose 2,3-acetate (C6 = 58.5 ppm) [172], both forms **D I** and **D II** possess highly deshielded C6 atoms.

Furthermore, the exact DAC structure elucidation continued with analysis of 2D NMR spectra. The graph in Figure 25 shows results of experiments employing heteronuclear multiple-bond correlation and multiplicity edited heteronuclear single quantum correlation.

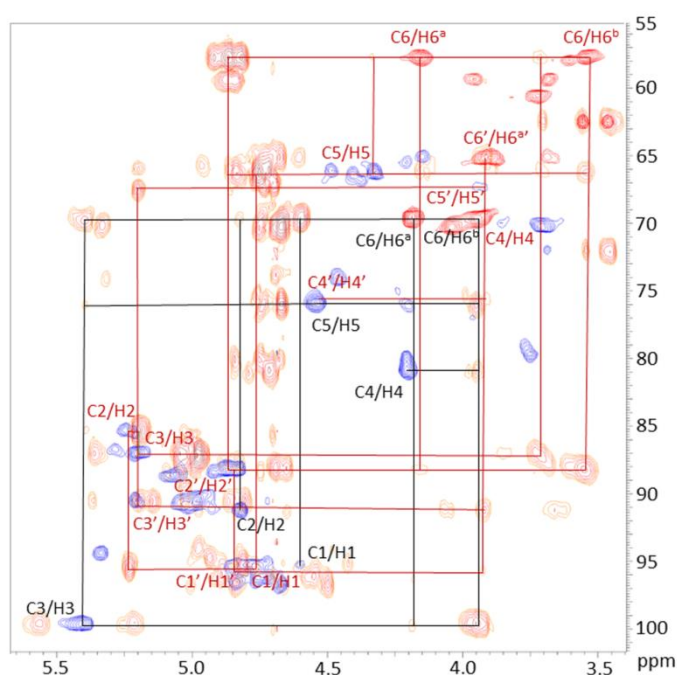


Figure 25 Portion of ^1H - ^{13}C HMBC (pale red) and multiplicity-edited ^1H - ^{13}C HSQC spectra (CH signals in blue, CH_2 signals in deep red). The $^{13}\text{C}/^1\text{H}$ correlations for **D I** are highlighted in black, for **G** in red. [99]

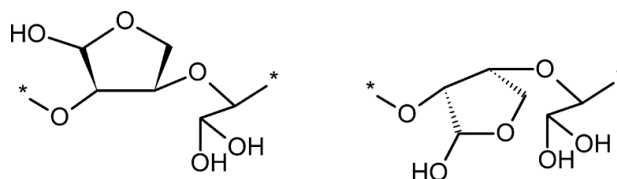


Figure 26 Suggested structures of **D I** and **D II** conformational isomers of DAC form **D**. [99]

Analysis of HMBC spectra of **D I** (highlighted black in Figure 25) and **D II** forms of DAC showed strong correlation of C6/H3 signals. This observation corresponds to three-bond coupling oppose to common described weaker four-bond coupling. Along with the considerably deshielded C3/H3 resonances (**D I** = 99.6/5.41 ppm, **D II** = 94.4/5.35 ppm), these results imply formation of furanoid-like five-membered C3–O–C6 hemiacetal rings of structural arrangement very close to **D** form of DAC depicted in Figure 19. The explicit nature of DAC forms **D I** and **D II** can be estimated only indirectly via ^{13}C NMR chemical shifts comparison. There is a noticeable increase about 5 ppm in the C3 and C4 and about 1.8 ppm in C5 chemical shifts of **D I** form when compared to **D II**. These differences imply conformation/geometry changes located on these carbon atoms giving rise to two possible conformational isomer units. In other words, intramolecular hemiacetal bonds C3–O–C6 might be formed with the respect to the plane of former AGU, i.e.

“above” and “below” the former AGUs plane (see Figure 26). If this assumption is correct, DAC chain can be composed of such conformational isomer units (**D I** and **D II**) differentiating by the spatial orientation of formed furanoid rings with the respect to the plane of former AGU. [99]

The third DAC form, manifested by somewhat shielded C6 ^{13}C NMR signal at 57.7 ppm, was recognized as DAC intermolecular hemiacetal **G**. Besides the signals at 87.0/5.22 ppm, 70.1/3.71 and 66.2/4.33 ppm (assigned to C3, C4 and C5, respectively), this C6 signal also correlates with signal at 88.1/4.88 ppm referring to connection with C2'/H2' of second DAC unit, see Figure 25. Furthermore, substitution on C6 is reflected in low ^{13}C NMR chemical shift of C4 (in this case 70.1 ppm), as was reported for similar C6-substituted derivatives of cellulose. [172] Additionally, there is noticeable correlation between C3/H3 resonance and C2/H2 resonance assigned to the signal at 85.2/5.25 ppm. This observation indicates the presence of seven-membered hemialdal ring formed by C3–O–C2 bond (**C** in Figure 19) connected to second DAC unit via C6. The rest of the signals of **G** form mentioned in the Table 17 were tentatively assigned (i) on the base of correlation between C2'/H2' and C1'/H1' signals in HMBC spectra or (ii) on a rather weak correlation signal between C1'/H1' and signal at 65.0/3.90 ppm (assigned to C6/H6^a). [99]

The last identified DAC form, exhibiting signal of CH₂ group at 60.6 ppm, possesses quite similar NMR chemical shifts as C6-joined intramolecular hemiacetal DAC unit noted as **G** (Table 17). However, there is no evidence of inter- or intramolecular correlation of C6' and its resonance appears to be about 3 ppm more deshielded. On the other side, three-bond C3–O–C2 coupling is undoubtedly observable. Based on these facts, recorded signals were assigned to hemialdal DAC form **C**. As a result of low intensity and relatively strong signal overlap, it is very difficult to evaluate the rest of the signals. Nevertheless, the signal at 59.4 ppm corresponding to C6 correlates with resonances at 90.6/5.02 and 88.1/4.88 ppm. According to the chemical shift, the first one mentioned can be assigned to C3/H3. Then, the C6 signal at 59.4 ppm is most likely associated with the formation of intermolecular hemiacetal. However, the exact nature of DAC form containing this C6–O–C3' bond cannot be straightforwardly determined. It could be present within **F** moiety, or different **G** form, for instance bearing hydrated aldehyde groups instead of hemialdal. [99]

In a broader perspective, analysed fresh DAC solution was comprised mostly from several C6-bonded hemiacetal forms. This observation is not surprising as the majority of C2 and C3 vicinal hydroxyl groups were converted to highly reactive aldehyde groups, and with C4 and C1 hydroxyl groups being engaged in the DAC chain, the hydroxyl group on C6 is the most favourable and perhaps the only spot allowing the hemiacetal reaction. DAC tends to form intramolecular hemiacetals rather than intermolecular hemiacetal structures joining separate DAC macromolecules. This observation can be likely ascribed to entropic reasons. [173] Regarding the exact structural composition of fresh

solubilized DAC based on the obtained and evaluated NMR data, the only favoured intramolecular C6-bonded hemiacetal is the **D** from (present in two different conformational isomers **D I** and **D II**). The chemical shifts referring to the second proposed intramolecular hemiacetal form **E** were not observed. The other dominant DAC form was found to be the intermolecular hemiacetal containing C6–O–C2' bonded moiety **G** (with C6-bonded ring in the form of hemialdal). Besides these C6-bonded hemiacetal DAC structures, the last identified DAC form is represented by 2,3-hemialdal **C**. The other proposed structural arrangements of DAC, namely free dialdehyde **A** and hydrated **B** form, were not confirmed. [99]

NMR analysis of solubilized DAC aging. The same solubilized DAC sample was left to age for 14 and 28 days under defined conditions (pH = 3.5, laboratory temperature, kept in dark) and analysed in the identical manner as the fresh solution. One of the most important observations within this is that no new signals appeared in the NMR spectral analysis as the aging of DAC proceeded. However, based on change of the observed signals integral intensities, the population of distinctive species estimated from ¹³C NMR spectra varied. [99]

According to the signal intensities, the most abundant DAC form in the fresh (one-day old) solution was **D I**, accompanied by slightly decreased signal intensity recorded for **D II** and **G** forms (both ~60 % of signal intensity of **D**). Another DAC form manifested by the CH₂ group signal at 59.4 ppm (further unspecified intermolecular hemiacetal) exhibit roughly 30 % intensity of **D**. Even weaker signal intensity (~20% of **D I**) was observed for DAC hemialdal form **C**.

The differences regarding the **D I** and **D II** signal intensities in the whole timeframe of DAC aging experiment were negligible. The signal intensities representing DAC forms **G** and **C** increased about 5 % over one-month period. The main portion of this signal increase was noticed within first 14 days of DAC aging. In contrast to these observations, signal belonging to the unspecified intermolecular hemiacetal (59.4 ppm) intensified by more than 10 % after two weeks. After this period, its signal intensity began to gradually decrease. This evolution of intermolecular hemiacetal signal intensity is consistent with the changes of molecular weight distribution analysed by gel permeation chromatography as discussed in the following part of the text.

To summarize, the investigated pH stabilized DAC solution did not exhibit formation of new chemical structures or specific degradation products. Presence of fragments during HPLC study is thus not a result of DAC aging as confirmed by NMR study. Instead of DAC degradation during its storage, the DAC aging process is characterized by changes in populations of inter- and intramolecular hemiacetals, which correlate with the result obtained in thermogravimetric and viscosimetric measurements and is manifested in other properties such as molecular weight discussed below. [99]

7.2.3 Molecular weight distribution study of DAC – focused on aging

In order to estimate the molecular weight distribution of solubilized DAC and the effect of its stabilization by low pH, gel permeation chromatography (GPC) was employed. This method principally gives comprehensive, yet relative (using standard), knowledge about molecular weight distribution of DAC macromolecules. Therefore, it is a primary method for studies of polymer degradation, in this case aging in solution.

GPC analysis of solubilized DAC aging. The samples of DAC fresh (one-day old) and aged (14 and 28 days old) solution stabilized by the low pH were analysed in the terms of their molecular weight distribution using gel permeation chromatography (GPC). Resulting chromatograms are plotted in the graph in Figure 27. As the aging of DAC proceeds, the changes in the molecular weight distribution are noticeable even by naked eye. For instance, there is relatively strong increase in molecular weight of DAC sample aged for 14 days (the whole distribution curve shifts virtually to higher molecular weights) which is followed by slight decrease (the distribution curve shifts to lower molecular weights again) after 28 days from DAC preparation. Moreover, as the aging time reaches 28 days, a broad peak at around 200 g/mol starts to be noticeable. This indicates presence of low-molecular weight fraction in the DAC solution. [99]

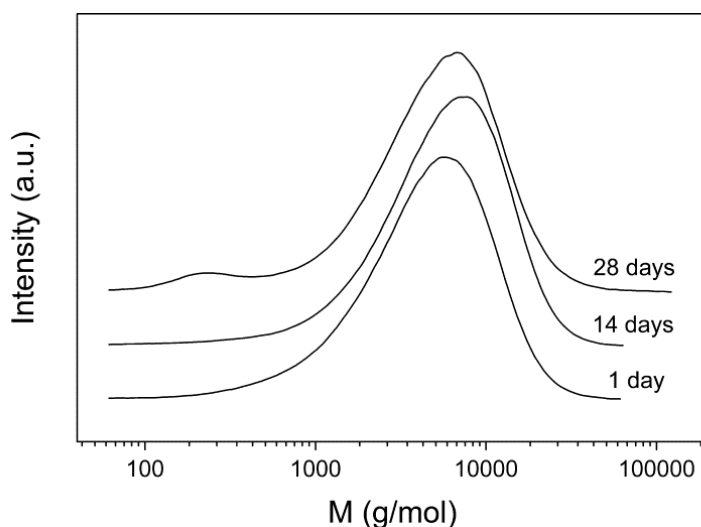


Figure 27 GPC chromatograms recorded for solubilized DAC of various age. The distribution curves are vertically shifted for better clarity. [99]

The summary of results obtained from GPC is given in Table 18. These include evaluation of typical molecular weight distribution moments differentiating by the statistical method of their calculation.

Table 18 GPC recorded data for DAC solutions in different aging time, where \bar{M}_n is the number average molecular weight; \bar{M}_w is the weight (mass) average molecular weight, M_p is the peak molecular weight, \bar{M}_z is the third moment of molecular weight and PDI is the index of polydispersity (\bar{M}_w/\bar{M}_n). [99]

Time (days)	\bar{M}_n (g/mol)	\bar{M}_w (g/mol)	M_p (g/mol)	\bar{M}_z (g/mol)	PDI (-)
1	2 600	6 100	5 500	10 200	2.36
14	3 100	7 400	7 000	12 000	2.38
28	2 000	6 900	6 700	13 200	3.46

The first moment, known as number average molecular weight (\bar{M}_n), is equal to the arithmetic mean of the number of particular macromolecules, which can be calculated using equation 7.1:

$$\bar{M}_n = \frac{\sum M_i N_i}{\sum N_i} \quad (7.1)$$

Where M_i is the molecular weight of particular polymer species; N_i is the number of moles of such species. In the case of fresh solubilized DAC, the \bar{M}_n was estimated to value 2 600 g/mol. As the aging reaches 14 day from DAC preparation, there was noticeable increase of \bar{M}_n roughly about 19 % ($\bar{M}_n = 3 100$ g/mol). After 28 day of aging, opposite trend was apparent as the \bar{M}_n dropped to 2 000 g/mol, which is 13 % below the value estimated for the sample of fresh solubilized DAC (see Table 18). These observations indicate two competing processes present within DAC solution. With the respect to previous result from HPLC and NMR analysis, the first process was identified as the formation of larger molecular DAC structures via (i) intermolecular hemiacetalization, i.e. connection of individual DAC macromolecules by C6–O–C2'(C3') linkage and/or via (ii) joining of the DAC macromolecules on their terminal reactive sites. Regardless of the precise nature of this recombination process, it results in relatively significant increase in \bar{M}_n . In contrast to this, the second process comprises of splitting of DAC chains into smaller molecular fragments most likely by the β -elimination mechanisms, which further leads to the lowering of \bar{M}_n . The first process is dominant after 14 days, which is reflected in the highest \bar{M}_n value recorded for 14 days-aged solubilized DAC sample. However, the rate of DAC recombination slows down after this period (possibly due to larger mass of recombined DAC macromolecules) and the second process identified as cleavage of lower molecular mass fragments prevails. This assumption is manifested by the lowest \bar{M}_n value estimated for 28 days aged DAC sample. Furthermore, as these two competing processes of DAC, recombination and scission, run under different rates and presumably

independently on each other during whole observed timeframe of DAC aging, the resulting polydispersity index (PDI, \bar{M}_w/\bar{M}_n), defining the uniformity of molecular mass distribution, increases with the age of DAC (from 1st day PDI = 2.36, up to 28 days PDI = 3.46, see Table 18). [99]

The second moment of molecular weight is defined as the weight (mass) average molecular weight (\bar{M}_w). Based on the equation (7.2) used for calculation, this parameter favours larger molecules over the smaller ones. In other words, bigger macromolecules will be of higher contribution to value of this parameter.

$$\bar{M}_w = \frac{\sum M_i^2 N_i}{\sum M_i N_i} \quad (7.2)$$

Similarly as in the case of \bar{M}_n , the considerable increase of \bar{M}_w was observed for solubilized DAC sample after 14 days of aging. The \bar{M}_w of DAC increased about 18 %, from 6 100 g/mol (fresh DAC) to 7 400 g/mol (14 days old DAC). As the aging of solubilized DAC proceeds to 28 days, slight decrease in \bar{M}_w value is noticeable (6 900 g/mol, i.e. 7% decrease relative to 14 days old DAC solution, see Table 18). These results well correlate with conclusions drawn in the NMR part. However, they are in stark contrast to the results of previous study made by Kim *et al.* (2004). The authors reported about 50 % loss of \bar{M}_w after 3 week from DAC preparation. In current study, most of the experimental parameters in DAC preparation were identical (type of source material, oxidation stoichiometry, solubilization conditions etc.). [97] The only significant difference is the utilization of lower pH setup (pH = 3.5 ± 0.1) of solubilized DAC in current work. Based on these observations the pH of DAC solution seems to be one of the most important parameters influencing the kinetics of DAC degradation and thus stability when considering its long term storage. [99]

Another molecular weight defining parameter is the third moment of molecular weight (\bar{M}_z). According to the equation (7.3) used for the calculation of this parameter, the largest molecular fractions contribute to the value of \bar{M}_z the most.

$$\bar{M}_z = \frac{\sum M_i^3 N_i}{\sum M_i^2 N_i} \quad (7.3)$$

Slightly different behaviour in the evolution of \bar{M}_z was observed when compared to previous changes of \bar{M}_n and \bar{M}_w during DAC aging. As can be seen in the Table 18, there is significant increase of this parameter value over 28 days after DAC preparation from 10 200 g/mol up to 13 200 g/mol (~29 % relative to \bar{M}_z of fresh DAC) with slightly more faster increase in \bar{M}_z after first 14 days of aging. This fact implies that recombination process of DAC macromolecules described earlier occurs during whole observed timeframe of DAC aging. [99]

In contrast to the recombination behaviour, the adverse process of DAC chain scission can be determined from the changes in the peak molecular weight (M_p), which defines the most abundant molecular weight fraction. The M_p value of fresh DAC was estimated to 5 500 g/mol with subsequent increase to 7 000 g/mol after 14 days and gradual decrease to 6 700 g/mol after 28 days of aging (see Table 18). Based on the measured data, the initial M_p increase reflects the recombination process while its modest decrease at the end of studied aging timeframe signifies the DAC chain scission process, which prevails over the recombination as the DAC aging proceeds. This subsequent increase in the rate of macromolecular domains cleavage after 14 days of solubilized DAC aging is further supported by the decrease of \bar{M}_n value as well as the formation of low molecular DAC fragments manifested by the peak at 220 g/mol in the chromatogram of 28 days aged DAC (see Figure 27). [99]

Outlined, both described processes of (i) intermolecular hemiacetal formation and (ii) chain scission/fragmentation occur simultaneously and are competitive to each other during investigated timeframe of DAC aging. The recombination process is characteristic for the first 14 days of DAC aging. After this aging period, the fragmentation process becomes dominant. Observed changes in all of the molecular weight moments (\bar{M}_n , \bar{M}_w and \bar{M}_z) along with M_p and PDI correlate well with results obtained in NMR part and are further supported by conclusions based on the evaluation of viscosimetric and thermogravimetric measurements in the section 7.2.1. From this point of view, the term “stabilization by low pH or in acid condition” has to be understood. Polymer degradation is a process primarily connected with the deterioration of molecular weight of its macromolecular chains. This can proceed as degradation of its polymerization degree by chain scission (or depolymerization) or it can result into crosslinking and rapid increase of the molecular weight. In contrast to previously reported fast degradation of solubilized DAC, results in this presented aging study confirmed that this can be avoided both in terms of reasonable deceleration of the loss of functional aldehyde groups content in DAC as well as in preventing rapid changes of DAC’s molecular weight. However, it does not mean that the system is “petrified” and no changes occur during the shelf-life; the opposite is true. It was convincingly shown, that solubilized DAC is a living system with two competing processes of intermolecular combination and intramolecular fragmentation which make it applicable with some reservations for four weeks but further extensions of its shelf time cannot be made.

7.2.4 Study of DAC solubilization process

The solubilization process of DAC is a crucial step for its subsequent utilization in solution-based processes such as crosslinking. Thus, it is important to evaluate influence of such process on the structure and properties of resulting DAC in solution. As has been mentioned in the previous text, there are some

contradictory conclusions regarding the effects of solubilization (see section 3.2). In brief, the first study carried out by Kim *et al.* (2004) focused on DAC solubilization process varying different parameters, i.e. temperature and time [97]. It showed negligible influence of such process on the molecular weight of resulting solubilized DAC (less than 10% decrease of \bar{M}_w compared to input material even after prolonged solubilization at relatively high temperature). In contrast to this, results of the second study made by Sulaeva *et al.* (2015) revealed quite severe DAC degradation during of solubilization process using more or less the same experimental setup (up to 50 % loss in solubilized DAC \bar{M}_w relative to input material). [98]

The following text is focused on the characterization of molecular weight, pH and solubilized content evolution during solubilization process. Furthermore, as the DAC stability is considered to be pH sensitive, different initial pH setups of solubilization were also investigated as well as non-conventional heating via microwave assisted solubilization (MWS). Obtained products of these solubilization processes in the form of residual insolubilized solids or DAC solutions were dried or lyophilised and imaged by scanning electron microscopy. This principally gives information about the progress of solubilization from the particle-dissolution kinetic.

GPC study of solubilization process. Entire process of DAC solubilization analysis is schematically depicted in the Figure 28.

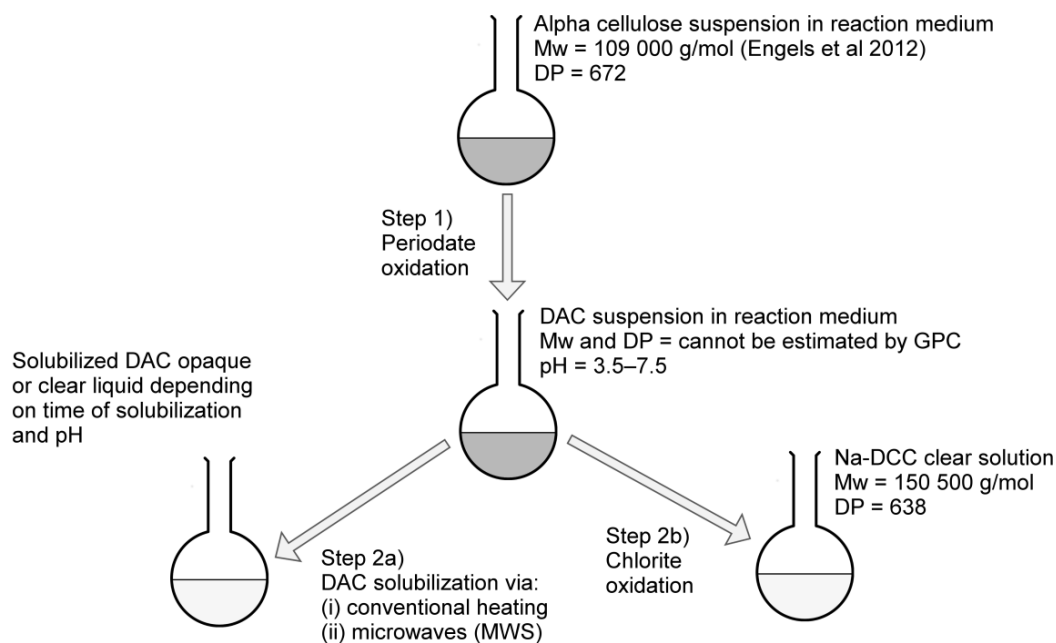


Figure 28 DAC solubilization analysis scheme; step 1) – cellulose periodate oxidation resulting in insolubilized DAC suspension; step 2a) – solubilization of insolubilized DAC at different initial pH setup via (i) conventional heating and (ii) microwave assisted solubilization (MWS); step 2b) – chlorite oxidation of aliquot part of insolubilized DAC in order to estimate its \bar{M}_w . [99]

First of all, to rule out the degradation during periodate oxidation and simultaneously confirm high selectivity of this reaction, molecular weight of original cellulose materials as well as insolubilized DAC were compared. Weight average molecular weight of input cellulose material (alpha cellulose supplied by Sigma Aldrich) was taken from the work of Engels *et al.* (2002); $\bar{M}_w = 109\,000$ g/mol (DP = 672) [164]. In order to obtain \bar{M}_w of insolubilized DAC, its easily dissolvable derivative Na-DCC was prepared by chlorite oxidation according to Maekawa *et al.* (1984) using aliquot part of prepared insolubilized DAC. [37] Subsequent molecular weight analysis carried out using Waters 2414 refractive index (RI) detector showed \bar{M}_w of 150 500 g/mol (DP = 638). The degree of polymerization of prepared insolubilized DAC is roughly about 5 % lower compared to original cellulose and thus the periodate oxidation can be considered as non-degradative derivatization as it exhibits minor influence with the respect to chain scission.

The rest of prepared insolubilized DAC suspension (pH = 6) was subsequently transferred into solubilization apparatus and analysed in the terms of solubilized content, pH, \bar{M}_w and PDI during the standard solubilization process described in section 6.2 part “DAC study”. The results are given in Table 19.

Table 19 DAC solubilization analysis carried out at initial pH = 6 (standard pH setup). [99]

Initial pH (-)	#	Solub. time (hour)	Solub. content (mg/mL; %)	pH (-)	\bar{M}_w (g/mol)	PDI (-)
6	Y05-f	0.5	1.67; 3.2	4.5	1 600	1.6
	Y1-f	1	8.32; 15.5	4.1	9 100	2.6
	Y3-f	3	18.81; 35.5	3.5	10 700	2.55
	Y5-f	5	31.74; 60	3.2	10 600	2.75
	Y7-f	7	51.25; 96.8	3.4	9 100	2.39

As can be seen from the data obtained during DAC solubilization analysis (Table 19), the solubilization produces quite small DAC macromolecules (sample Y05-f, 1 600 g/mol, PDI = 1.6) and steep drop of pH takes place (pH = 4.5) during first half an hour of this process. The solubilized DAC content in this initial sampling data point was estimated to about 3.2 % which further rapidly increases as the solubilization time proceeds. After only one hour, solubilized fraction (Y1-f) of DAC exhibited \bar{M}_w of 9 100 g/mol and large increase in polydispersity index (PDI = 2.6). The process continued with release of low molecular DAC polymer fragments (DP about 60) from the residual insolubilized DAC particles without significant change of PDI. It seems that the

solubilization goes simultaneously with degradation of DAC chains and can be ascribed to the scission of macromolecular DAC fragments loosen from the gradually dissolving solid phase of insolubilized DAC particles as schematically depicted in Figure 29.

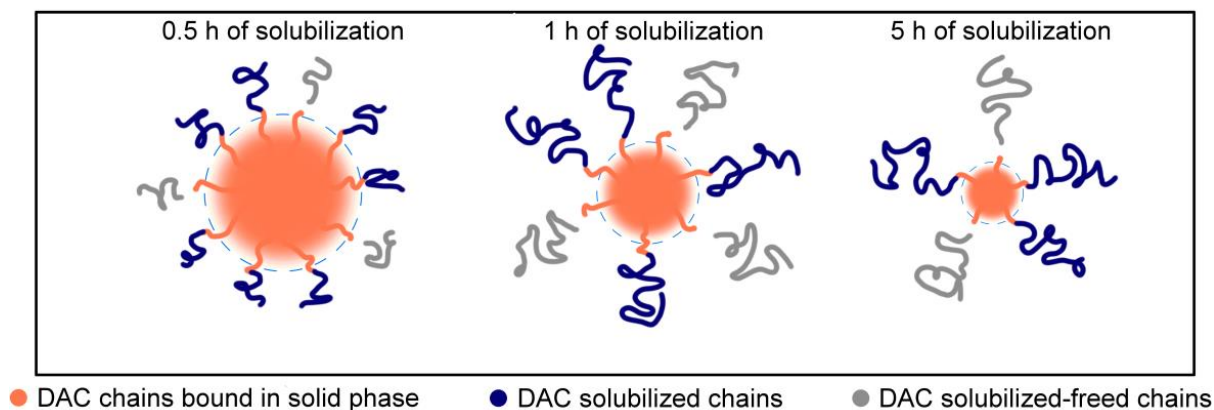


Figure 29 Schematic representation of DAC solubilization with the respect to its time, size of insolubilized DAC phase and size of macromolecular fragments.

After 7 hours, the process of DAC solubilization is nearly complete (sample Y7-f, 96.8 % of material solubilized) resulting in almost clear DAC solution exhibiting \bar{M}_w of 9 100 g/mol, PDI of 2.39 and pH value of 3.4. Observed shift of the DP value from 638 of insolubilized DAC to DP of 58 estimated for fully solubilized DAC testifies to severe degradative character of solubilization to nearly oligomer level. These results thus confirm the findings of DAC degradation after solubilization made by the group of Sulaeva *et al.* (2015) and disprove the earlier study carried out by Kim *et al.* (2004). [97, 98] The slight discrepancy of measured value of \bar{M}_w within this solubilization study and \bar{M}_w value of fresh DAC noted in the section 7.2.3 “Molecular weight study of DAC” was most likely caused due to the utilization of two different GPC detectors due to changes in the instrumentation in the GPC setup. Nevertheless, the trends in molecular weight evolution during aging of DAC sample prepared in solubilization study were identical.

DAC solubilization using different initial pH. Since the known fact about the DAC sensitivity toward pH of its environment, DAC solubilization analysis was conducted in equivalent manner as in previous case (pH = 6) using different initial pH setup (pH = 3.5; 5 and 7.5). Diluted solutions of HCl or NaOH were utilized for this purpose. The recorded changes in solubilized content, pH, \bar{M}_w and PDI during these pH-modified solubilization processes are noted in the Table 20.

Table 20 DAC solubilization analysis under different initial pH.

Initial pH (-)	#	Solub. time (hour)	Solub. content (mg/mL; %)	pH (-)	\bar{M}_w (g/mol)	PDI (-)
3.5	W05-f	0.5	0; 0	3.5	-	-
	W1-f	1	0.45; 0.8	3.8	6 600	1.89
	W3-f	3	0.57; 1.1	3.5	6 800	1.89
	W5-f	5	0.76; 1.4	3.5	6 900	2.03
	W7-f	7	1.27; 2.4	3.6	6 900	2.03
5	X05-f	0.5	1.48; 3.1	3.8	1 800	1.64
	X1-f	1	7.32; 15.2	3.5	8 500	2.58
	X3-f	3	12.67; 26.2	3.5	9 800	2.45
	X5-f	5	28.1; 58.2	3.5	10 700	2.55
	X7-f	7	45.54; 94.3	3.6	9 400	2.47
7.5	Z05-f	0.5	10.97; 22	4.5	1 400	1.56
	Z1-f	1	33.13; 66.4	4.4	6 600	2.44
	Z3-f	3	44.05; 88.3	3.8	6 500	2.83
	Z5-f	5	45.44; 91.1	3.5	5 000	2.38
	Z7-f	7	49.12; 98.4	3.6	4 300	2.26

The lowest initial pH setup of insolubilized DAC suspension (pH = 3.5, samples containing “W”) maintained close to the set value during entire solubilization analysis. However, DAC under such pH condition is nearly insoluble as only 2.4 % were solubilized after 7 hours. As a result of high portion of DAC solid phase the solutions exhibited high turbidity. Aside the low solubilization efficiency, such low pH setup produces solubilized DAC of more or less equal molecular weight ($\bar{M}_w \sim 7\ 000$ g/mol) during whole process. These observations can be explained as a result of stabilizing effect of low pH on DAC and possibly decreased polymer-solvent interaction and suppression of chain scission as discussed above.

Another investigated initial pH of value 5 (samples marked as “X”) exhibits quite similar evolution of quantities (solubilized content, \bar{M}_w and PDI) as in standard setup (initial pH = 6). Nevertheless, there is noticeable decrease in the solubilization rate compared to standard setup, which correlates with the effect seen in the solubilization under pH of 3.5.

The last studied initial solubilization pH setup of 7.5 (samples containing “Z”) testifies pro-degradative behaviour of alkaline pH on DAC as the solubilization proceeds very fast from the very beginning (22 % solubilized DAC after half an hour). After only one hour, there is about 66 % material solubilized and the \bar{M}_w value is on the peak (6 600 g/mol). After 3 hours, the

DAC is more or less completely solubilized and \bar{M}_w starts to slowly decrease along with the solution yellowing. At the end of solubilization, \bar{M}_w of strong yellow solubilized DAC was estimated to be 4 300 g/mol.

To summarize, the solubilization process is strongly influenced by the initial pH of system. As the pH is set at low value (pH = 3.5), the solubilization rate considerably slows down and DAC fragments exhibit homogeneous distribution of \bar{M}_w during all stages of this process. Increasing the initial pH to slightly acidic or close to neutral values (pH = 5 or 6) results in faster and complete solubilization after 7 hours. Further increase of initial pH to basic region increases substantially the solubilization rate but causes strong degradation via β -elimination mechanism. One common observation is identical for all solubilization processes regardless of the initial pH value. It is the tendency to reach pH around value of 3.5 at the end of solubilization. DAC may (i) presumably act as a buffer or (ii) there may be evolution of unspecified organic acid in the degradation cascade, which stabilizes the balance between degradation and recombination around this specific value.

Microwave assisted solubilization of DAC (MWS). Different approach towards DAC solubilization using microwave heating (one hour under reflux) was employed. MWS was carried out on insolubilized DAC suspensions of different initial pH (similarly as in the case of solubilization via conventional heating). Results are summarized in Table 21.

Table 21 DAC MWS solubilization analysis under different initial pH.

Initial pH (-)	#	Solub. time (hour)	Solub. content (mg/mL; %)	pH (-)	\bar{M}_w (g/mol)	PDI (-)
3.5	mw-W	1	48.25; 98	3.4	6 100	2.26
5	mw-X	1	49.04; 97.8	3.6	4 400	2.32
6	mw-Y	1	47.9; 98.3	3.6	4 500	2.37
7.5	mw-Z	1	48.66; 98.4	4.3	2 200	1.83

Complete solubilization was achieved after just one hour utilizing MWS of insolubilized DAC suspensions differentiating by initial pH. The effect of initial pH on DAC stability is more pronounced for MWS than for conventional heating. As the initial pH of DAC suspension grows, the resulting solubilized DAC after MWS exhibits lower molecular mass. However, it is possible to employ this alternative heating method to obtain high yields of solubilized product in very short amount of time.

SEM analysis of DAC solubilization products. To obtain deeper knowledge about the effect of periodate oxidation of cellulose from the material point of view, micrographs of original cellulose powder material and insolubilized dried DAC were taken by SEM. As can be seen from representative images in Figure 30, the size and shape of original cellulose and insolubilized DAC particles are more or less identical. The surface morphology on the other hand is fairly different. It is most likely caused by the oxidation process which requires diffusion of the oxidizing agent into the cellulose microcrystals, thus causing swelling and oxidation of the swollen material which begins from the surface. A small material loss is experienced (presumably due to some degraded hence readily soluble fraction from the surface) during almost complete 72h periodate oxidation which never results in 100 % yield of oxidized material. Obtained insoluble but swollen material is then washed, collected and dried which imparts the specific morphology to the surface of the insolubilized material.

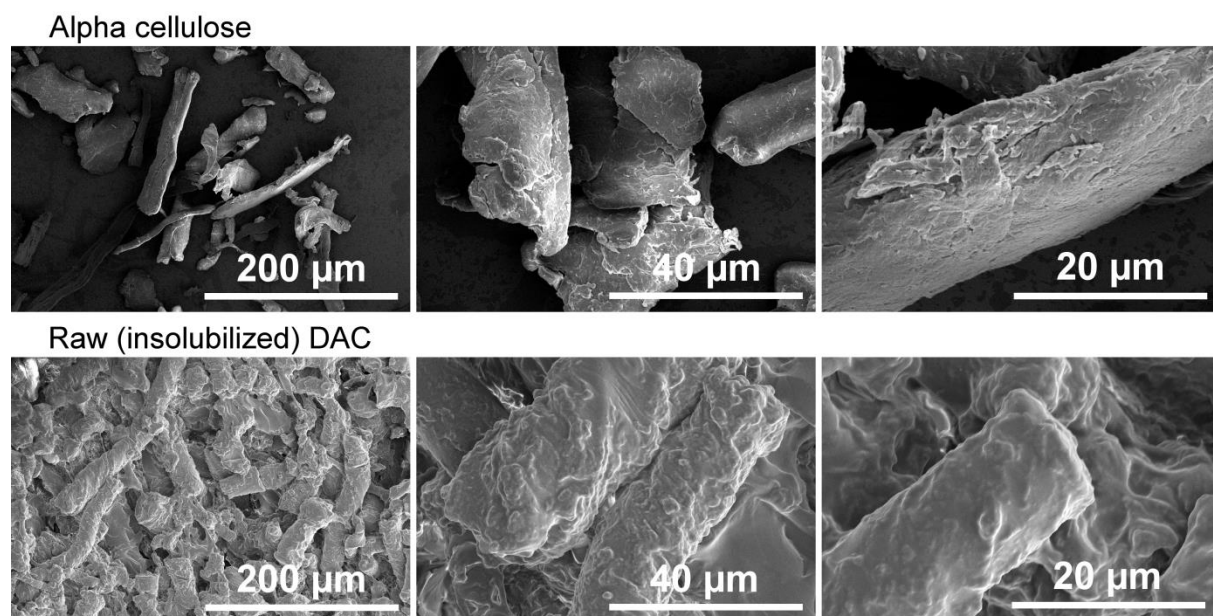


Figure 30 SEM micrographs of original cellulose and insolubilized DAC.

These initial observations were followed by a time lapse study which was carried out on the insolubilized residues from each aliquot DAC sample obtained after filtration to investigate the particle-dissolution kinetic during solubilization from the general qualitative viewpoint. Imaging was performed by scanning electron microscope analysis of dried samples. The first set of micrographs (Figure 31) shows the particle evolution within solubilization with initial pH of 3.5. It is clearly visible the insolubilized DAC phase maintains its original shape and individual particles can be distinguished even after 7 hours of solubilization. This observation correlates with the macroscopic behaviour (high turbidity) and low solubilized fraction content.

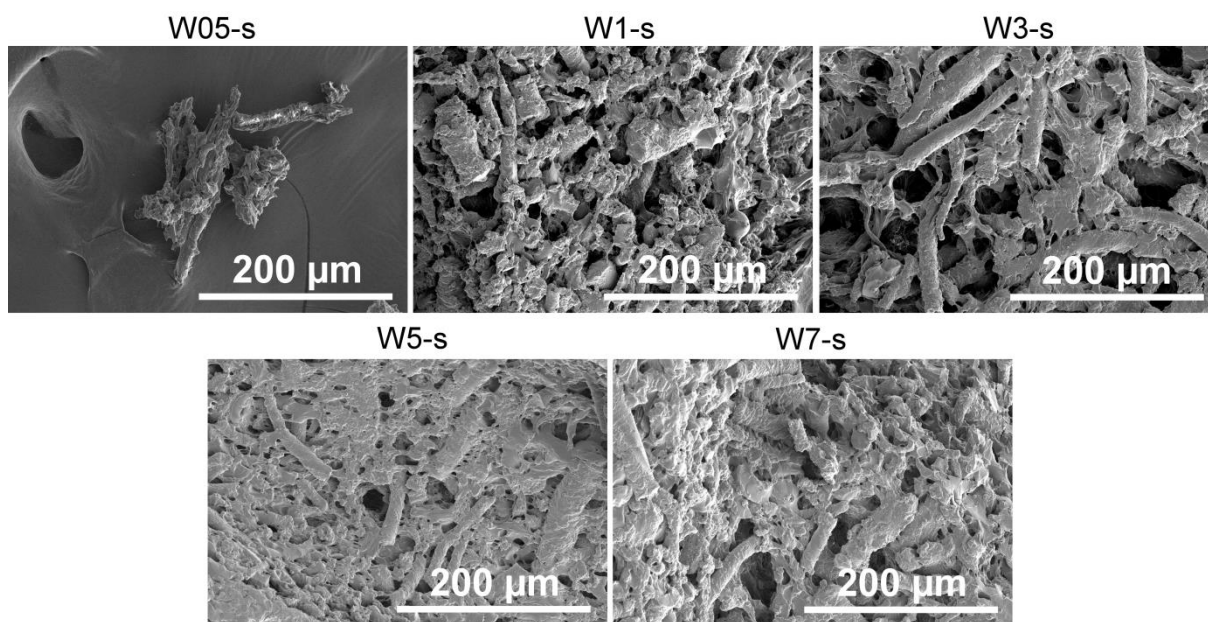


Figure 31 SEM micrographs of solid DAC phase during solubilization (initial pH 3.5).

Another two sets of micrographs (Figures 32 and 33) shows the particle evolution during the solubilization utilizing initial pH of 5 and 6, respectively.

There are visible some minor differences between these two sets of samples. When comparing samples of corresponding sampling time (e.g. X1-s vs. Y1-s), the insolubilized fraction manifested by residual fibrous fragments is visibly present in higher amount in samples solubilized using pH 5. This correlates with previously discussed solubilized content, which is higher in solubilization at initial pH of 6.

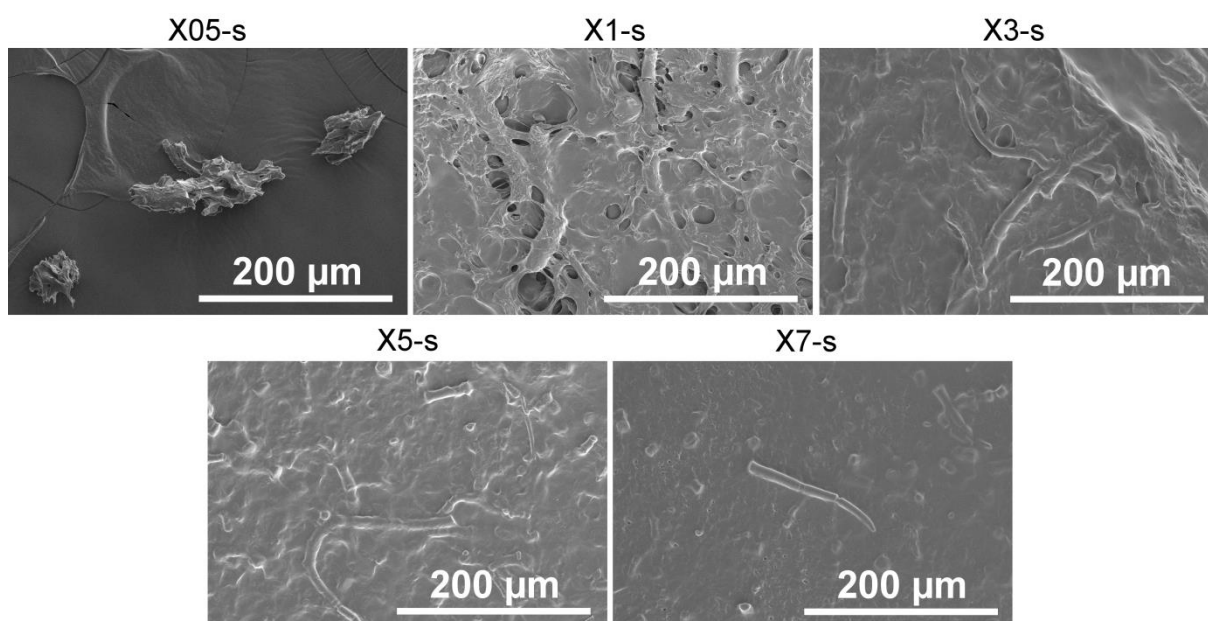


Figure 32 SEM micrographs of solid DAC phase during solubilization (initial pH 5).

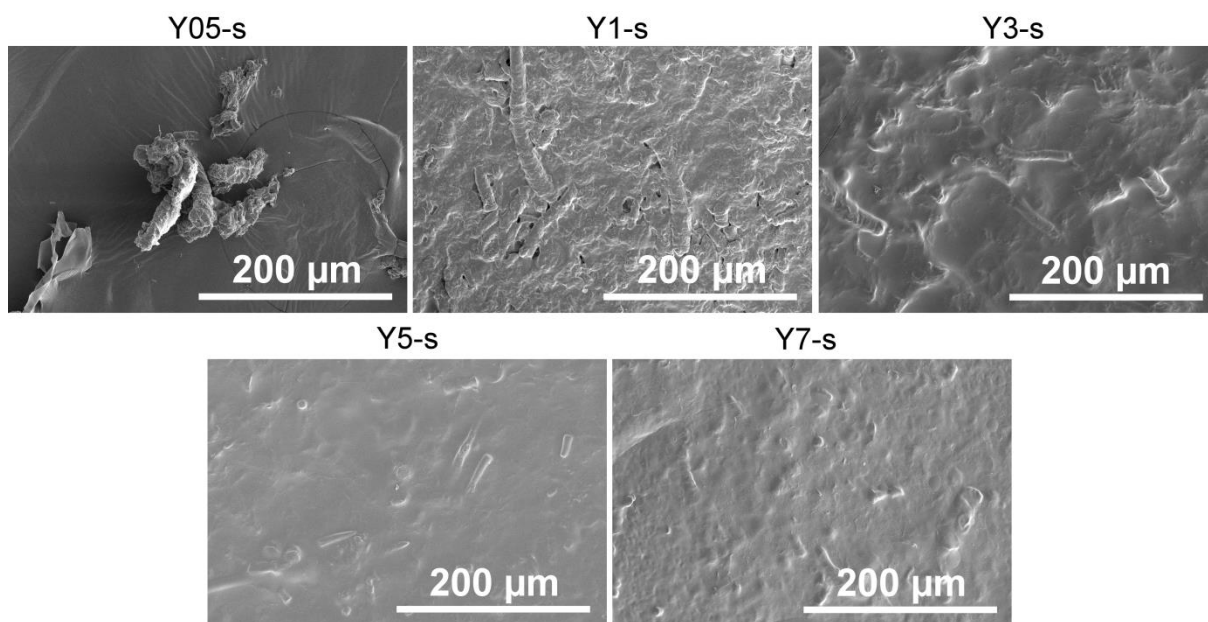


Figure 33 SEM micrographs of solid DAC phase during solubilization (initial pH 6).

The last analysed set of samples solubilized employing initial pH of 7.5 exhibits expected morphology with the respect to identified increase in solubilization rate. The sample Z05-s solubilized for only half an hour is structurally similar to sample X3-s solubilized for 3 hours with starting pH of 5. This gives evidence about the significant role of pH regarding the solubilization. Furthermore, respective filtrates of these samples showed quite similar content of solubilized DAC (see Table 20). As the solubilization at initial pH 7 proceeds, the fibrous residues of insolubilized DAC gradually disappear and are no longer visible in sample Z7-s.

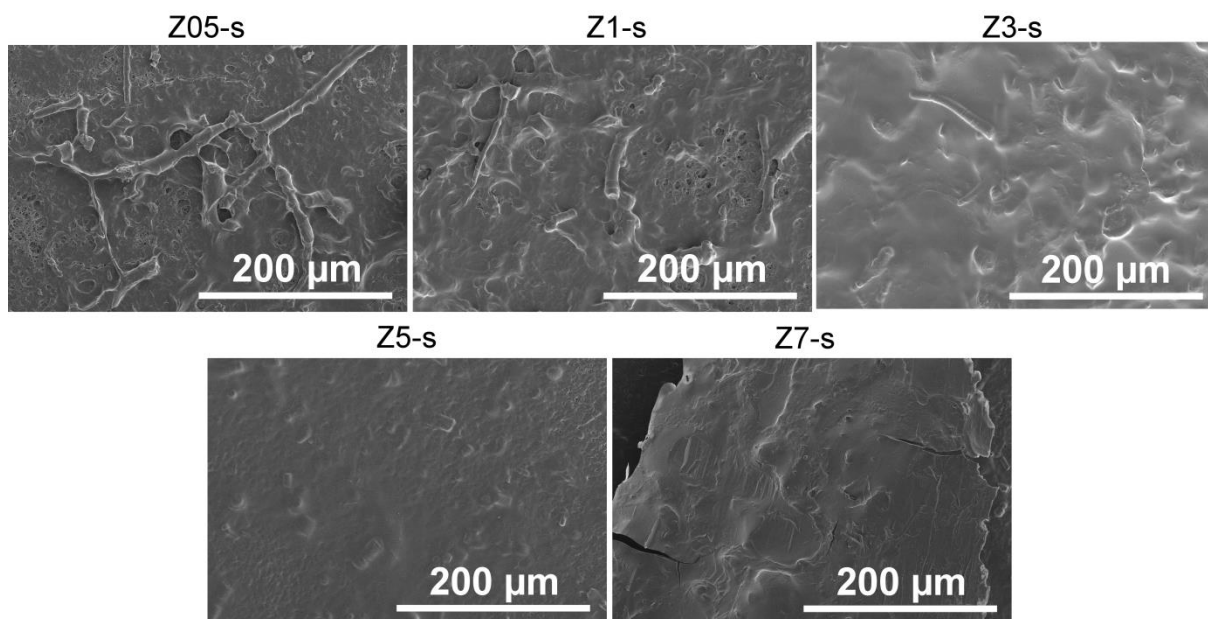


Figure 34 SEM micrographs of solid DAC phase during solubilization (initial pH 7.5).

SEM analysis revealed the particle-dissolution kinetic with high dependence on the used initial pH of solubilization and its time. Moreover, it is in good agreement with the data obtained from these solubilization experiments by other methods in the previous section.

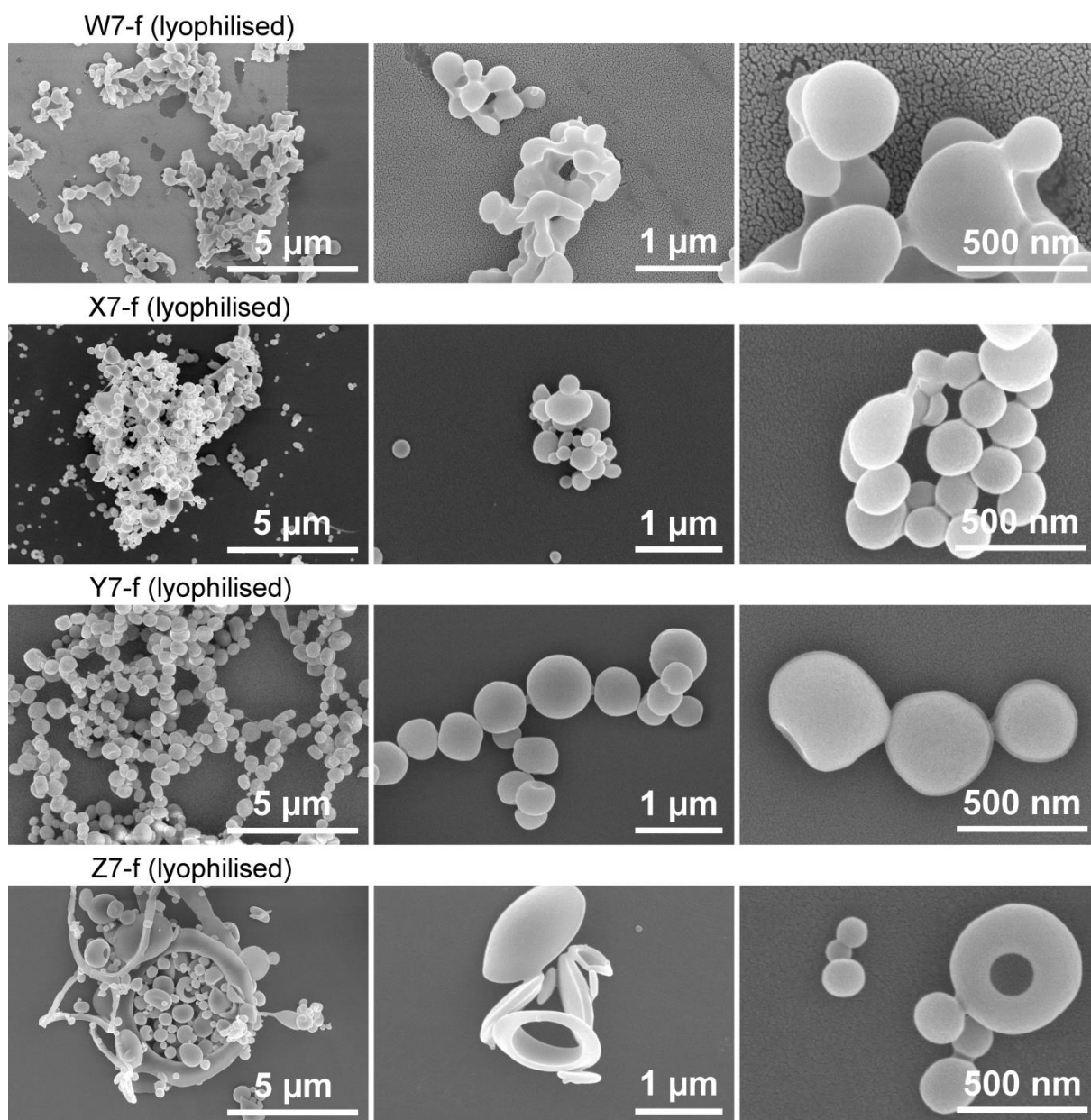


Figure 35 SEM micrographs of lyophilised products of solubilization via conventional heating carried out under different initial pH.

Besides the SEM analysis of solid residues of solubilization, the final solubilized products were freeze-dried and imaged as well. Figure 35 shows lyophilised DAC samples obtained after 7 hours of solubilization under different initial pH conditions. Spherical DAC beads were present in all prepared samples regardless of the solubilization conditions. However, some characteristic

patterns are more frequent for specific initial pH setup. The solubilized DAC under low pH exhibits higher fraction of fused beads (W7-f row of micrographs in Figure 35). Lyophilisation of DAC solubilized using initial pH slightly acidic or close to neutral (pH = 5 or 6) results in more or less perfectly shaped beads (X7-f and Y7-f rows of micrographs in Figure 35). Another imaged material prepared by lyophilisation of DAC solubilized at higher initial pH of 7.5 exhibits larger fraction of imperfect or hollow DAC beads structures (Z7-f row of micrographs in Figure 35).

The last investigated set of lyophilised samples was prepared from DAC solubilized by MWS under different pH (Figure 36). All samples contain fraction of spherical as well as slightly irregular DAC beads.

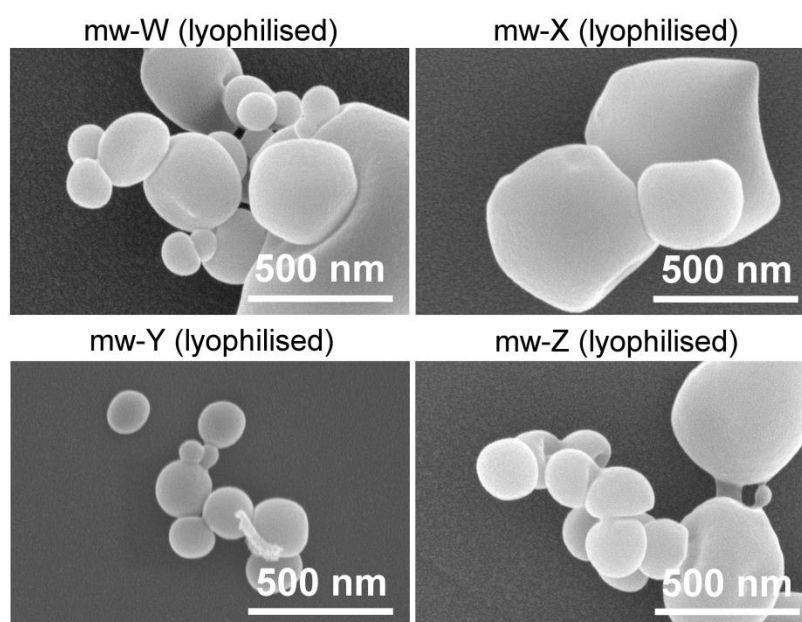


Figure 36 SEM micrographs of lyophilised products of MWS (one hour heating) carried out under different initial pH.

The results of SEM analysis showed the influence of solubilization pH on resulting particle shape, whether it is the insolubilized residues or the solubilized and subsequently lyophilised DAC products (except in the case of MWS utilization). These changes in morphology are most likely caused by the pro-degradative behaviour of higher values of pH, which on the one side speeds up the solubilization process and on the other cause additional DAC chain scission.

The following part of text is focused on the application of solubilized DAC as a crosslinking agent for PVA under different conditions (different catalyst system, DAC age or type of PVA) and evaluation of resulting hydrogel properties.

7.3 Hydrogel study

The main objectives of the hydrogel study are to (i) investigate the crosslinking ability of pH-stabilized DAC during its aging, i.e. prepare and evaluate properties of PVA/DAC hydrogels using fresh and aged DAC; (ib) utilize chemically distinct catalysts of crosslinking reaction of DAC and PVA and (ii) compare crosslinking efficiency of DAC and common crosslinker glutaraldehyde (GA) under equivalent reactive group concentration conditions.

The first part of this study includes preparation of PVA/DAC xerogels using fresh and aged DAC acidic solution and is closely related to role of different catalysts or catalyst systems required to initiate crosslinking reactions. The prepared PVA/DAC xerogels were firstly analysed by TGA, XRD and tensile measurements and subsequently investigated by a more elaborate method of structural analysis defining crosslinked network properties via solid-state NMR analysis. Furthermore, the key functional properties of hydrogels, i.e. network parameters such as swelling capacity, equilibrium water content (EWC) and gel fraction were measured. Based on obtained data, average molecular weight between crosslinks (\bar{M}_c) and crosslink density (ρ_c) were evaluated with the aid of equilibrium swelling theory by Flory and Rehner (1943). [148] Finally, all measured swelling related characteristics of PVA/DAC material were corroborated by their evident correlation with structural and functional properties obtained by the other methods and discussed in a separate section.

The second part of this study aims to prepare PVA hydrogels crosslinked by DAC (PVA/DAC) or GA (PVA/GA) utilizing broad concentration range of these crosslinkers and diluted HCl as catalyst. All prepared hydrogels were compared in the terms of their network parameters and two different types of crosslink topologies were proposed.

7.3.1 Characterization of PVA/DAC

The initial characterization of PVA/DAC materials is focused on evaluation of xerogel properties with the respect to the utilized catalyst system (see Table 12) and the age of used pH-stabilized DAC crosslinker.

TGA analysis. Influence of two different catalyst systems on thermal stability profile was examined for unwashed/washed cross-linked PVA/DAC samples as well as for input materials (untreated PVA and DAC). Figure 37 shows thermogravimetric analysis results of input materials and examples of unwashed/washed PVA/DAC samples prepared using HCl catalyst (A01) and catalyst system composed of H_2SO_4 , CH_3OH and CH_3COOH (B01). Only PVA/DAC samples prepared using fresh DAC are discussed as samples prepared utilizing aged DAC showed similar thermal properties.

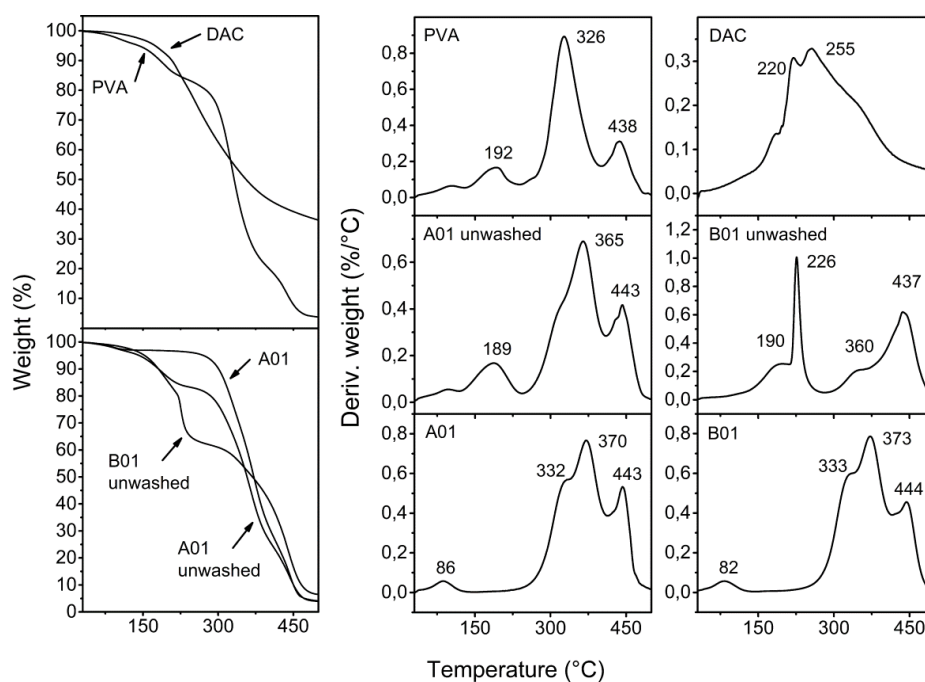


Figure 37 TGA analysis of untreated input PVA (Mowiflex) and examples of PVA/DAC xerogels (washed and unwashed) prepared using fresh DAC and two different types of acidic catalyst.

There is noticeable difference in thermal behaviour between unwashed samples A01 and B01. Unwashed sample A01 showed very similar thermal decomposition patterns as untreated PVA with shift of peak weight loss rate to higher temperatures (PVA/A01 unwashed – 326 °C/365 °C, 438 °C/443 °C, see left part of Figure 37). This upward shift is most likely caused by the presence of PVA/DAC crosslinked network, capable to better withstand higher temperatures compared to untreated PVA. In contrast to this, unwashed sample B01 exhibits strong peak in weight loss rate at 226 °C implying the negative influence of B catalyst system on thermal stability of such xerogel. There is also apparent peak in weight loss rate at around 190 °C in both unwashed PVA/DAC xerogels which can be most likely assigned to low molecular additive. After hydrogel washing step, i.e. removal of uncrosslinked PVA, low molecular additive and catalyst system residues, both A01 and B01 samples show very similar thermal behaviour with negligible differences.

To summarize, the results from TGA analysis revealed the different influence of two catalyst systems residues present in unwashed PVA/DAC xerogels. It is evident, that the presence of HCl catalyst residues does not compromise the thermal stability of such material. Oppose to this, residues of catalyst mixture based on H₂SO₄ considerably lowers the thermal stability. Washed PVA/DAC samples exhibited similar thermal behaviour. In order to define the properties of PVA/DAC xerogels free of possible interference caused by uncrosslinked PVA, additives or catalyst residues, following analyses were conducted only on washed xerogels.

Tensile measurements. Mechanical properties were firstly investigated for untreated PVA and secondly for PVA/DAC samples crosslinked by fresh and aged DAC utilizing different catalyst systems. The examples of stress vs. strain curves of untreated PVA sample and crosslinked PVA/DAC xerogel are shown in the left part of Figure 38 and they represent two diverse cases of mechanical behaviour. In the first case, untreated PVA exhibits typical elastic behaviour of relatively high elongation and lower average values of Young's modulus. In contrast to this, the second case, typical for all of the prepared PVA/DAC xerogels, shows more semi-ductile plastic behaviour in the sense of comparably decreased elongation, yield point and apparent necking during tensile tests. These observations imply presence of crosslinked network within all PVA/DAC xerogels. Here it should be noted, that the second yield point visible in the stress vs. strain curve of PVA/DAC sample shown in the lower left part of Figure 38 is a result of different strain rates during tensile testing. [91]

Figure 38 (right) shows the dependence of Young's modulus (E) of PVA/DAC xerogel samples on DAC solution age and chosen catalyst system (A or B series). Detailed results of mechanical properties from tensile tests are given in Table 22. [91]

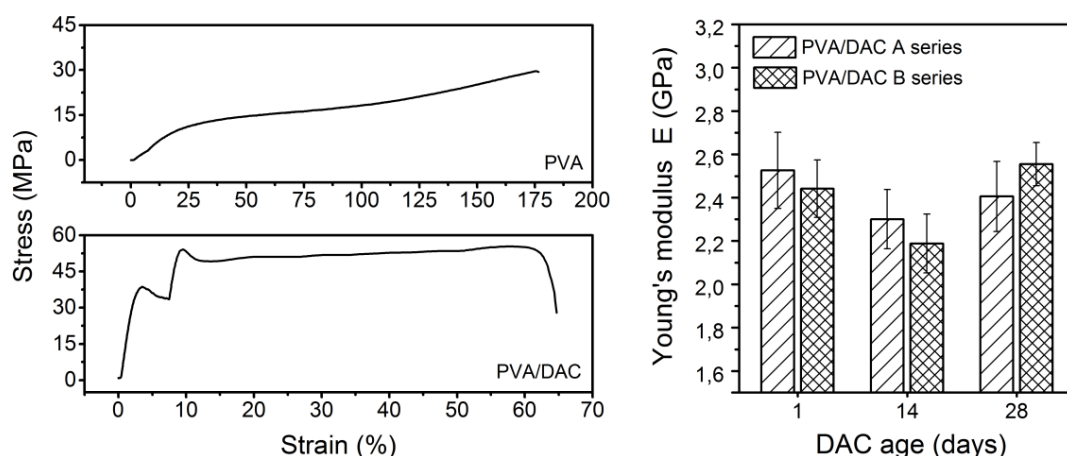


Figure 38 Examples of stress vs. strain curve of untreated input PVA and PVA/DAC, please note the x-axis scale difference between the upper and lower graph panel (left); evolution of Young's modulus E of washed PVA/DAC dependent on DAC age (right). [91]

The presence of crosslinked polymer network within all of the PVA/DAC xerogels results in the significant increase of E to values above 2 GPa, ten times higher compared to untreated PVA (see Table 22). The formed stiff polymer network thus results in much higher Young's modulus than contribution of hydrogen bond structure of untreated PVA. [91]

Table 22 Mechanical properties calculated for untreated input PVA and PVA/DAC crosslinked samples. [91]

#	Young's Modulus E (GPa)	Peak elongation (%)
PVA (Mowiflex)	0.24 ± 0.02	170.9 ± 12.2
A01	2.53 ± 0.18	84.9 ± 17.1
A02	2.30 ± 0.14	66.3 ± 12.4
A03	2.41 ± 0.16	68.3 ± 5.4
B01	2.44 ± 0.13	60.2 ± 15.9
B02	2.19 ± 0.14	59.0 ± 11.9
B03	2.56 ± 0.10	51.2 ± 7.7

As can be seen in Figure 38 (right) and Table 22, PVA/DAC samples prepared using 14 days old DAC (A02 and B02) exhibit the lowest average values of Young's modulus while the PVA/DAC samples prepared using fresh and 28 days old DAC crosslinking solution (A01, B01 and A03, B03) exhibit slightly higher stiffness. The explanation to this can be found in the change of molecular weight of used DAC crosslinker during its shelf-life, i.e. increase of \bar{M}_n during the first 14 days and its subsequent drop after 28 days of aging. These changes most likely define the distribution of crosslinks in polymer network. In other words, the presence of larger number of smaller DAC macromolecules ($\bar{M}_n \sim 2\,000$ g/mol) presumably forms denser crosslink network, which positively influences stiffness of such PVA/DAC material. [91]

Outlined, tensile measurements (Young's Modulus and peak elongation) indicate presence of crosslinked polymer network with stiffness of all crosslinked PVA/DAC xerogel samples ranging from 2 to 2.5 GPa utilizing 1 wt% of DAC crosslinking agent. Instead of expected decrease of PVA/DAC xerogel mechanical properties with the age of utilized DAC crosslinking agent, the PVA/DAC xerogels crosslinked using the oldest (28 days) DAC solution were capable to retain its relatively high stiffness. Connected to this, the trends in stiffness correlate with the molecular weight evolution of aged pH-stabilized DAC rather than with the weakly manifested trend of reactive aldehyde group content loss. On the other hand, variation of the mechanical properties of xerogels with aging time of stabilized solubilized DAC solution is very small and it can be said, that the stabilized solution is negligibly influenced by aging from the application point of view. However, it must be noted that full variability between these samples will be manifested in fully swollen state, but for the moment, let us proceed with xerogels again. The following XRD analysis further reveals the dependence of DAC age on resulting PVA/DAC xerogels crystallinity.

XRD analysis. Diffractogram examples obtained from XRD analysis for input materials (PVA “Mowiflex”, alpha cellulose and solubilized-dried DAC) and PVA/DAC xerogel samples from B series are shown in Figure 39. Particular results from this analysis are noted in Table 23. In order to compare the input materials, respective diffractograms are shown in the left part of Figure 39. As has been noted earlier (section 7.2.1 “Basic characterization of DAC”, Figure 21), prepared DAC showed significant loss of crystallinity compared to original alpha cellulose as a result of the opening of glucopyranose rings (destruction of ordered macromolecular packing). [97, 99] Utilized untreated PVA “Mowiflex” exhibits lower crystallinity than alpha cellulose used in subsequent production of DAC. The set of diffractograms recorded for samples from B series shown in the right part of Figure 39 illustrates noticeable changes in crystallinity. [91]

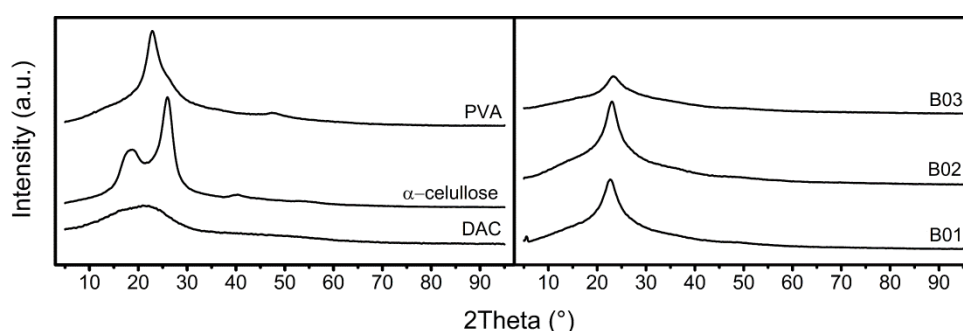


Figure 39 Diffractograms of input materials (left) and PVA/DAC samples from B series (right). [91]

The trends in crystallinity of both PVA/DAC series correspond with trends in Young’s modulus determined by tensile testing (see Figure 38 and Table 22) with close relation to \bar{M}_n of DAC in solution during its aging. It should be also noted, that the crystalline phase is only a minor component within prevailing amorphous crosslinked network and has small contribution to the overall stiffness of PVA/DAC material examined by tensile measurements. The PVA/DAC samples exhibiting slightly larger stiffness (A01, B01 and A03, B03) prepared utilizing larger number of relatively low molecular weight DAC macromolecules present in fresh and 28 days old DAC ($\bar{M}_n \sim 2000$ g/mol) form presumably denser crosslink network which prevents formation of larger crystalline sequences between PVA and DAC crosslinking spots. This leads to decreased crystallinity of these PVA/DAC samples (e.g. $X_{A03} = 13$ %, $X_{B03} = 6$ %). In contrast to this, the PVA/DAC samples A02 and B02 prepared using smaller number of larger DAC macromolecules (14 days old DAC of $\bar{M}_n = 3\ 100$ g/mol) result in xerogels with somewhat lower stiffness and most likely lower crosslink density, which further enables to form more evolved PVA crystallites in sparsely crosslinked PVA/DAC matrix ($X_{A02} = X_{B02} = 16$ %). [91]

Table 23 Crystallinity (X) of input material (α -cellulose, DAC and PVA) and resulting PVA/DAC samples prepared using different catalyst systems and aged DAC. [91]

#	Crystallinity X (%)
α -cellulose	25
DAC (solubilized-dried)	7
PVA (Mowiflex)	18
A01	14
A02	16
A03	13
B01	12
B02	16
B03	6

To summarize, crystallinity reflect mechanical behaviour of prepared PVA/DAC xerogels with correlation to the molecular weight of used DAC crosslinker. As has been mentioned earlier in the part regarding the tensile testing, the properties of PVA/DAC materials seem to be governed not by the decrease of aldehyde group content as it would be normally expected but by the evolution of DAC molecular weight. The correlation of these parameters is further discussed in the 7.3.3 section.

The determined basic properties of PVA/DAC samples are further associated and correlated with structural characteristics determined by solid-state NMR and functional properties expressed by network parameters in the following text.

7.3.2 Structural and functional characterization PVA/DAC

To understand the differences between PVA/DAC xerogels prepared using different catalyst system and utilizing DAC of different age, it is necessary to further investigate the structure of such materials via suitable methods. In connection to this, it is important to evaluate functional properties of formed hydrogels in the terms of network parameters.

Solid-state NMR. In order to study the degree of crosslinking of PVA/DAC xerogel samples prepared using fresh and aged DAC, cross-polarization/magic-angle-spinning (CP/MAS) ^{13}C NMR spectroscopy was employed. [174] The easily recognizable changes in the PVA signals were identified as a result of PVA/DAC xerogel formation (see Figure 40 and Table 24). [91] Unfortunately, the respective DAC resonances located in the range 110–80 ppm for C1–C3 and 80–55 ppm for C4–C6 [175] were extremely weak and partially obscured by the signals of PVA. This observation is not surprising as the ratio between the polymer and crosslinking agent (PVA:DAC) was 99:1 in all PVA/DAC xerogel

samples. Furthermore, the weak DAC signal intensity also arises from the complex composition of DAC in solution which results in the expectation of variety of possible crosslinking modes. [99] Thus, only signals originating from untreated PVA and PVA/DAC samples are discussed in the following text. [91]

In the first place, untreated PVA was characterized using solid-state NMR analysis. The signals depicted in Figure 40 and noted in Table 24 were assigned to the untreated PVA on the base of previously published data. [176, 177] Based on the knowledge of ^{13}C NMR resonance deshielding in PVA spectra caused by the presence of intramolecular hydrogen bonds [174, 176], the steric polymer arrangement (tacticity) can be evaluated. The signal of methine group at 77.1 ppm (marked as **I** in Figure 40) can be attributed to isotactic triad (mm) with two intramolecular hydrogen bonds. Next, the signal found at 71.5 ppm (**II** in Figure 40) belongs to the heterotactic triads (mm and mr) with single intramolecular bond and finally signal observed at 65.4 ppm (**III** in figure 40) corresponds to the syndiotactic triads (mm, mr and rr) without intramolecular hydrogen bonds. Furthermore, only one signal representing CH_2 group (45.3 ppm) was assigned and present in all measured spectra. The last recorded signal at 22.5 ppm present also in all spectra originates from the residual acetate group with corresponding carbonyl resonance at 173.0 ppm (not shown in Figure 40). Based on this, the PVA (Mowiflex) utilized in the crosslinking reactions with DAC possess roughly 16 % of acetate groups and thus it is not fully hydrolysed. [91]

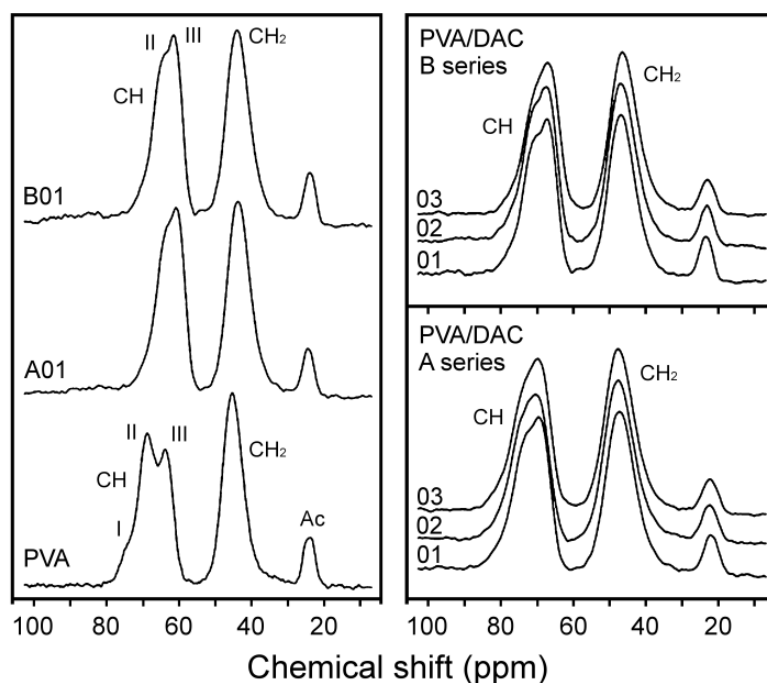


Figure 40 The CP/MAS ^{13}C NMR spectra of PVA and selected PVA/DAC xerogels (left), comparison of PVA/DAC xerogels ^{13}C NMR spectra of samples prepared using various catalyst systems and DAC solution of different age (right). [91]

There are negligible differences between CP/MAS ^{13}C NMR spectra measured for the PVA/DAC xerogels prepared using DAC of different age as well as using different catalyst (see Figure 40 left). However, there are significant noticeable changes when comparing ^{13}C NMR spectra of PVA/DAC xerogels and untreated PVA. From the point of PVA/DAC xerogels, the differences described in Table 24 are manifested by (i) the absence of signal **I**, (ii) the upfield shift of signal **II** from 71.5 to 69.7 ppm resulting in (iii) its complete overlap of somewhat deshielded signal **III** found in the range between 66.6–67.2 ppm (depending on the age of DAC). These changes signify considerable disruption of hydrogen bond network within all PVA/DAC xerogels, which is consistent with observed decrease of PVA/DAC xerogels crystallinity and formation of crosslinks between PVA and DAC. In other words, somewhat bulky DAC crosslinking agent induces larger PVA inter-chain separation and thus most likely disrupts nearby hydrogen bonds. [91]

Table 24 ^{13}C NMR chemical shifts of PVA and PVA/DAC xerogels. [91]

#	CH I (ppm)	CH II (ppm)	CH III (ppm)	CH ₂ (ppm)
PVA (Mowiflex)	77.1	71.5	65.4	45.3
A01	-	69.7	66.6	46.0
A02	-	-	67.2	45.8
A03	-	-	66.9	46.3
B01	-	69.7	66.9	46.3
B02	-	69.6	66.9	46.6
B03	-	-	66.9	46.0

To acquire more information about the structure and properties of PVA/DAC xerogel materials, the changes in NMR chemical shifts were correlated with the results from the $T_{1\rho}(^1\text{H})$ and $T_{1\rho}(^{13}\text{C})$ analyses (see Table 25) offering conclusions in qualitative or semi-qualitative terms.

The $T_{1\rho}(^1\text{H})$ values depend on the nearby spin-reservoirs density with individual spins interaction occurring via $^1\text{H}/^1\text{H}$ dipolar mechanism [167]. Thus, this parameter is not sensitive to motion of individual molecular groups, but it can be treated as a “phase” quantity describing the spin-diffusion processes efficiency in given range around observed nucleus, which is related to the number of neighbouring spins and their individual distances. [174, 177] The obtained $T_{1\rho}(^1\text{H})$ data revealed noticeable increase of this parameter for all of the prepared PVA/DAC xerogel samples, when compared to PVA (see Table 25). This is consistent with the conclusions drawn from the NMR chemical shift study (dilution of nearby ^1H spin reservoirs caused by hydrogen bond network disruption and larger PVA chain separation). Taking into account the

experimental errors, it should be noted, that $T_{1\rho}(^1\text{H})$ values estimated for all of the prepared and investigated PVA/DAC xerogels are more or less comparable. This suggests analogous spin-diffusion efficiency present in all prepared xerogel samples, hence the roughly identical density of hydrogen bond network. The only slight difference can be seen in the case of A03 sample, where $T_{1\rho}(^1\text{H})$ values dropped to 4.1 ± 0.2 ms indicating increased nearby spin density. This observation may be connected to possible partial restoration of hydrogen bond network. [91]

The second evaluated parameter $T_{1\rho}(^{13}\text{C})$ allows to analyse local site-specific motions on kilohertz timescale. [178] It provides information about the local polymer chain dynamics of untreated PVA as well as PVA/DAC crosslinked xerogels. The values of $T_{1\rho}(^{13}\text{C})$ noted in Table 25 show increase in this quantity upon crosslinking, which signify increased flexibility of polymeric domains of PVA/DAC samples (with the exception of B03 sample) in comparison to the untreated PVA. Such observation supports the assumption regarding the dilution of hydrogen bond network in crosslinked PVA/DAC xerogels manifested by the $T_{1\rho}(^1\text{H})$ results. It should be noted, that $T_{1\rho}(^{13}\text{C})$ values are more sensitive to conditions of PVA/DAC sample preparation than $T_{1\rho}(^1\text{H})$. In general, $T_{1\rho}(^{13}\text{C})$ parameter is higher for PVA/DAC samples prepared using 14 days old DAC regardless of the used catalyst system. However, the substantial difference of $T_{1\rho}(^{13}\text{C})$ parameter between catalyst system A and B is noticeable for PVA/DAC samples prepared utilizing the oldest (28 days) DAC crosslinker solution. In this case, sample B03 exhibits even shorter $T_{1\rho}(^{13}\text{C})$ value (4.4 ± 0.2 ms) than one estimated for untreated PVA (7.8 ± 0.5 ms). Such result implies high local molecular motion restriction of B03 sample and loss of chain flexibility. Furthermore, as the $T_{1\rho}(^1\text{H})$ value of this sample remained almost unchanged (see Table 25), the hydrogen bond network was not restored to any significant level and thus such restriction of molecular motion is most likely caused by the increased crosslink density. [91]

Table 25 The $T_{1\rho}(^1\text{H})$ and $T_{1\rho}(^{13}\text{C})$ values for PVA and PVA/DAC samples. [91]

#	$T_{1\rho}(^1\text{H})$ (ms)		$T_{1\rho}(^{13}\text{C})$ (ms)	
	CH III	CH ₂	CH III	CH ₂
PVA (Mowiflex)	3.3 ± 0.2	3.4 ± 0.2	7.8 ± 0.5	5.8 ± 0.5
A01	4.6 ± 0.1	4.7 ± 0.1	12.0 ± 0.9	8.5 ± 0.4
A02	4.6 ± 0.3	4.4 ± 0.3	14.2 ± 0.9	9.0 ± 0.4
A03	4.1 ± 0.2	4.2 ± 0.1	11.0 ± 0.7	5.8 ± 0.3
B01	4.5 ± 0.3	4.5 ± 0.1	11.0 ± 0.5	6.9 ± 0.5
B02	4.8 ± 0.1	4.5 ± 0.1	11.7 ± 0.7	7.3 ± 0.6
B03	4.9 ± 0.1	4.5 ± 0.1	4.4 ± 0.2	2.3 ± 0.1

Obtained results correspond to the previous finding of tensile study and XRD analysis. The dependence of PVA/DAC xerogels structural characteristics expressed by $T_{1\rho}(^1\text{H})$ and $T_{1\rho}(^{13}\text{C})$ on DAC age or more precisely on its molecular weight has been confirmed. The findings imply actual increase of reactivity of aged pH-stabilized DAC solution for crosslinking reactions especially with the use of sulfuric acid as catalyst (B series), [91] instead of expected decrease (accompanied by aldehyde content loss) previously reported for pH neutral DAC solutions. [97, 104]

Network parameters. In order to evaluate PVA/DAC hydrogel functional properties, network parameters were assessed for samples of PVA/DAC prepared using DAC of different age and different catalyst systems. The definitions of network parameters are given in the section 4.2.

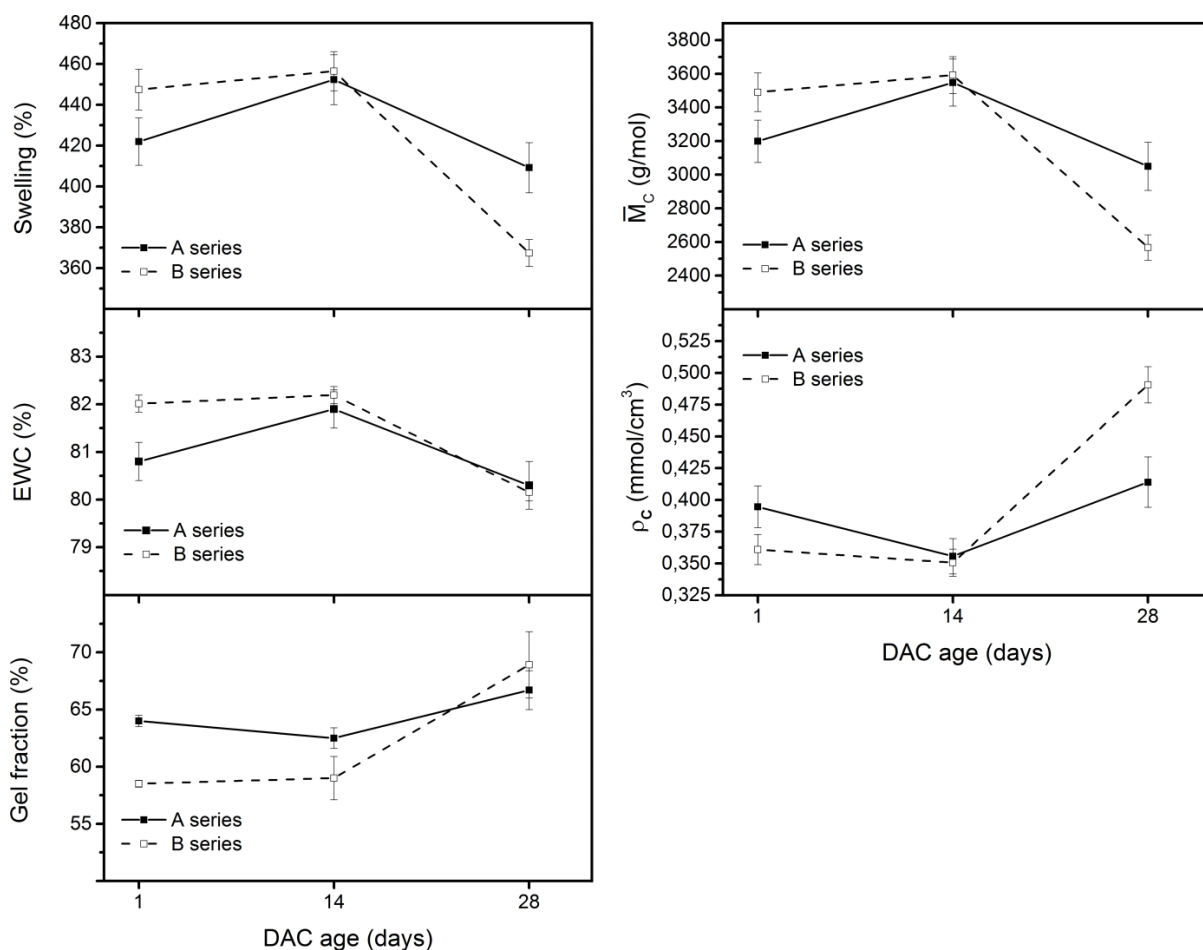


Figure 41 Influence of DAC age used for crosslinking on the network parameters of prepared PVA/DAC hydrogels. The graphs show percentage of swelling, equilibrium water content (EWC), gel fraction, average molecular weight between crosslinks (\bar{M}_c) and crosslink density (ρ_c) of both prepared series of PVA/DAC samples crosslinked by fresh and aged DAC. The lines connecting points in the graphs are only guides for eyes. [91]

The dependence of DAC aging on network parameters, i.e. percentage of swelling, equilibrium water content (EWC), gel fraction, average molecular weight between crosslinks (\bar{M}_c) and crosslink density (ρ_c), of PVA/DAC hydrogels prepared utilizing different catalyst systems (series A and B) are shown in the Figure 41. Several trends can be assigned to the observed quantities of PVA/DAC hydrogels: (i) as the polymer network becomes denser (higher ρ_c), the smaller is the material loss during washing and thus the larger is the amount of gel fraction; (ii) as the amount of gel fraction increases, the swelling capacity, EWC and \bar{M}_c values drop and vice versa. In other words, rise of water uptake goes hand in hand with high swelling capacity because there is more space accessible for water molecules between the longer macromolecular chains segments bonded in sparsely crosslinked network. [91]

Figure 41 shows the similar trends of network parameters dependent on the age of used DAC crosslinking agent evaluated for two catalyst systems utilized in the preparation of PVA/DAC hydrogels. In general, the samples of A series (HCl catalyst) exhibit slightly more uniform behaviour and the properties expressed in the terms of network parameters are less dependent on the DAC age (or more precisely on its molecular weight) than samples of B series (H₂SO₄ catalyst). Taking into account that only 1 wt% of DAC crosslinker was used, the swelling capacity of all PVA/DAC samples (except B03) varied approximately from 400 to 450 % with the respect to age of DAC. The main difference between these two series can be seen in the comparison of network parameters of PVA/DAC samples prepared utilizing the oldest (28 days) DAC crosslinking solution. The sample B03 exhibits relatively steep change in all characteristic features, i.e. lowest swelling capacity (370 %) and EWC (78.6 %), highest amount of gel fraction (68.9 %) and highest crosslink density (0.5 mmol/cm³) of all of the prepared hydrogel samples. This behaviour can be explained by the increased efficiency of sulfuric acid based catalyst system towards the catalysis of crosslinking reactions between low molecular fragments of DAC and PVA. This results in the formation of comparably denser crosslink network exhibiting low swelling capacity and EWC and higher amount of gel fraction. [91]

Similarly to previous structural NMR analysis, XRD analysis and tensile measurements, the network parameters of prepared PVA/DAC hydrogel materials showed noticeable dependence on the molecular weight of used DAC crosslinker as well as the choice of catalyst system. The utilization of diluted hydrochloric acid as catalyst results in uniform behaviour of hydrogels less dependent on the molecular weight of used DAC. In contrast to this, catalyst system based on sulfuric acid seems to be more efficient in the crosslinking reaction of PVA especially in the combination with oldest and thus the most fractioned DAC. [91]

Following text will be focused on the study of correlation between obtained data from particular analyses carried out for PVA/DAC materials and DAC itself and analysis of the role of catalyst system.

7.3.3 Correlation between measured characteristics of PVA/DAC and role of catalyst system

As has been noted in the previous parts of the text regarding the results of tensile measurements, XRD analysis, NMR study and characterization of network parameters, there are distinct trends in the obtained data for PVA/DAC materials which can be closely related to the molecular weight evolution of used DAC crosslinking agent during its aging.

First of all, the evolution of structural properties of DAC during its aging has to be evaluated. Among them, two are most important, i.e. (i) reactive aldehyde content defining the amount of respective functional groups involved in the subsequent crosslinking reactions with PVA and (ii) molecular weight of DAC which is governed by structural changes of DAC via stabilization mechanisms during aging of solubilized DAC stored in acidic media. [99]

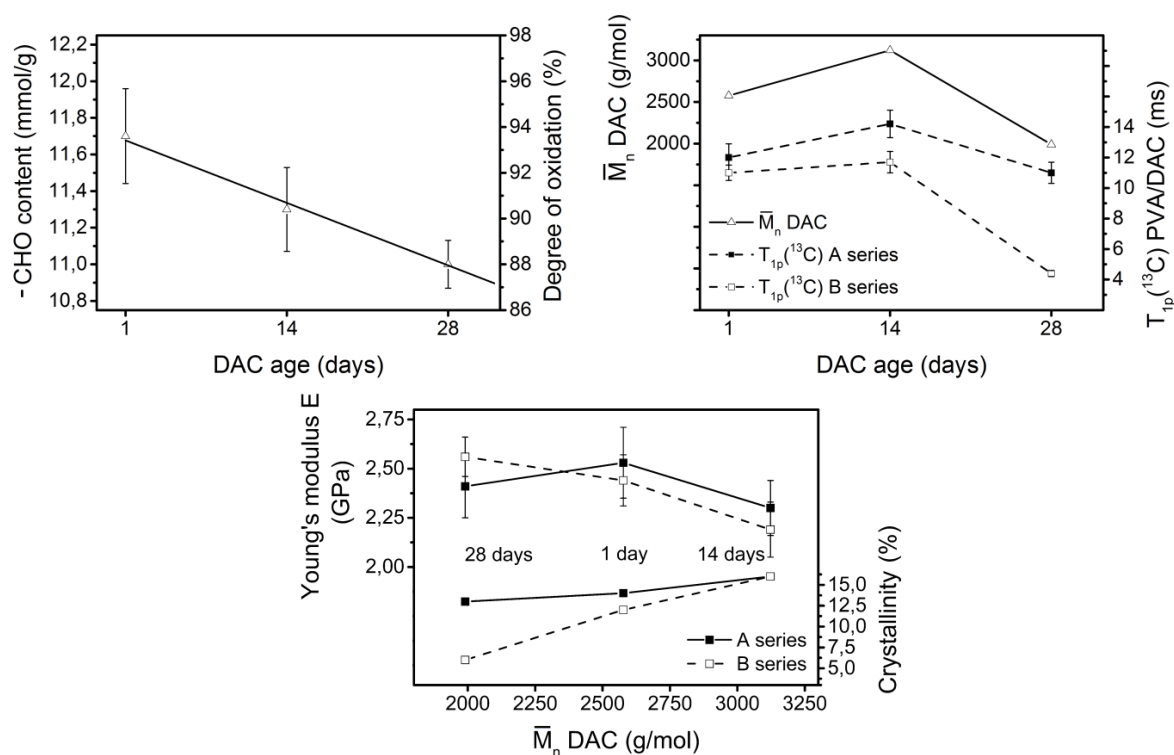


Figure 42 Decrease of reactive aldehyde group with DAC aging (top left); correlation between \bar{M}_n of DAC in solutions of various age (Münster et al., 2017) and $T_{1p}({}^{13}\text{C})$ values of resulting PVA/DAC hydrogels (top right); correlation between \bar{M}_n of DAC and Young's modulus and crystallinity of PVA/DAC xerogels prepared using different catalyst system (A and B series) with marked age of used DAC crosslinker (bottom center). The lines connecting points in the graphs are only guides for eyes. [91, 99]

It has been found, that the total reactive aldehyde group content of pH-stabilized DAC solution decreases only slightly (equivalent to a decrease of the degree of oxidation by less than 10 percentage points after 4 weeks) as noted in

the section 7.2.1. The change in this quantity shows almost linear behaviour as shown in the upper left part of Figure 42. However, the composition of acidic DAC solution changes dramatically during the time of its aging which is further reflected in the evolution of molecular weight of DAC (upper right part of Figure 42). Based on these observations made by NMR and GPC analysis, two competing processes were identified in the acidic DAC solution. The first process dominant during first 14 days favours the formation of intermolecular hemiacetals connecting individual DAC macromolecules and results in the increase of \bar{M}_n roughly about 20 % compared to fresh DAC solution. Next, the second process of DAC chains splitting into smaller molecular fragments prevails after 28 days from DAC preparation over the initial recombination. This results in the noticeable decrease in \bar{M}_n of 28 days aged DAC solution almost by 40 % with the respect to \bar{M}_n of 14 days old DAC which is even below that of fresh solution, see the top curve in the graph depicted in the upper right corner of Figure 42. [91]

These changes in \bar{M}_n of DAC solution in time correlate with $T_{1\rho}(^{13}\text{C})$ results (the upper right graph in Figure 42) implying the direct influence of changes in DAC \bar{M}_n on resulting PVA/DAC hydrogel structure and properties. The consequence of these changes on macromolecular level is more pronounced than decrease of DAC reactive aldehyde group content in time which would otherwise presumably result in increasing trend in this quantity. The explanation can be found in the earlier proposed fact, that smaller number of larger and less mobile fragments present after 14 days do not crosslink PVA polymer matrix as efficiently and densely as larger number of smaller fragments present in 28 days old solution. Therefore, the flexibility of PVA/DAC polymeric domains expressed by the $T_{1\rho}(^{13}\text{C})$ parameter reaches maximum for samples prepared using 14 days old DAC solution (maximum \bar{M}_n), while the most rigid structure is obtained using 28 days old DAC (lowest \bar{M}_n). [91]

Furthermore, these structural conclusions are also reflected in the mechanical properties of prepared PVA/DAC xerogels (top curves in the bottom graph depicted in Figure 42). The linear correlation of \bar{M}_n of used DAC and average values of Young's modulus can be seen for samples prepared utilizing sulfuric acid as catalyst (B series) which supports the assumption of the significant role of molecular weight of used DAC crosslinker over its reactive aldehyde group content. However, this trend is less pronounced in the case of PVA/DAC samples prepared using hydrochloric acid as catalyst (A series). Next, the influence of \bar{M}_n of DAC on crystallinity of PVA/DAC can be seen in the bottom graph in Figure 42. Both of prepared series of PVA/DAC materials exhibit increase in crystallinity values as the \bar{M}_n of DAC increases. Again, the explanation to this can be found in the nature of formed network of crosslinks. The sparsely crosslinked and thus highly flexible PVA matrix crosslinked via smaller number of larger DAC macromolecules present in 14 days old solution results in the presence of (i) region comprised of sizable sections of free PVA

chains bound in the (ii) regions with high crosslink density adjacent to DAC chains. These free PVA macromolecules can presumably form larger crystalline sequences embedded in relatively flexible crosslinked polymer network. This assumption is supported by the correlation of polymeric domain flexibility ($T_{1\rho}(^{13}\text{C})$) and crystallinity of PVA/DAC xerogels as can be seen in the Figure 43. [91]

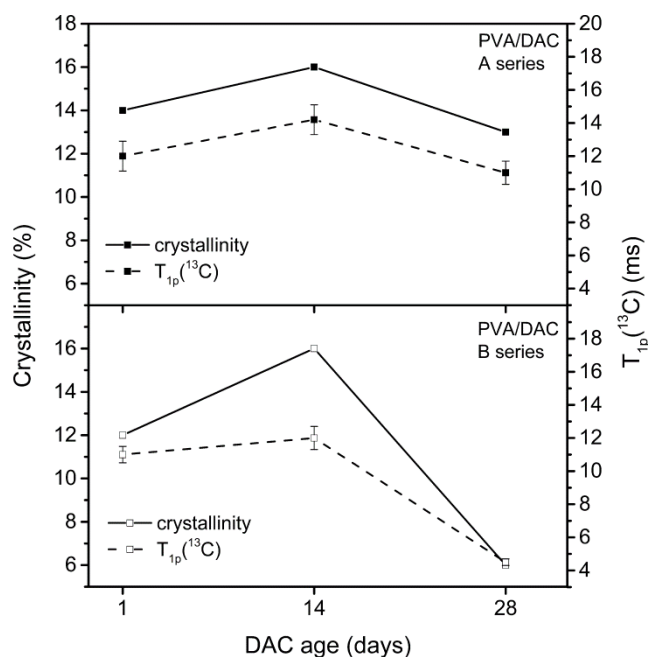


Figure 43 Correlation between crystallinity of PVA/DAC materials prepared using DAC of various age and carbon spin-lattice relaxation time in rotating frame, $T_{1\rho}(^{13}\text{C})$, corresponding to polymeric chain segments flexibility as obtained from NMR study. The lines connecting points in the graphs are only guides for eyes. [91]

These trends are particularly manifested for the B03 sample as its crystallinity drops down to 6 % and it exhibits the lowest $T_{1\rho}(^{13}\text{C})$ value of (4.4 ± 0.2) ms which implies the densest crosslinking of such PVA/DAC sample. Similar, however less pronounced trends are observed for A03 sample. Schematic representation of the two extreme structural situations in xerogels, i.e. PVA/DAC xerogel sample (B02) crosslinked by smaller number of larger DAC macromolecules enabling formation of regions comprising of larger PVA crystallites within the most flexible and thus least rigid crosslinked polymer network on one hand and PVA/DAC sample (B03) crosslinked by larger number of smaller DAC molecular fragments containing less evolved PVA crystallites within most rigid PVA/DAC crosslinked polymer network on the other, is given in Figure 44. The differences between PVA/DAC samples prepared using two chemically distinct catalyst systems is further discussed in the following part of the text. [91]

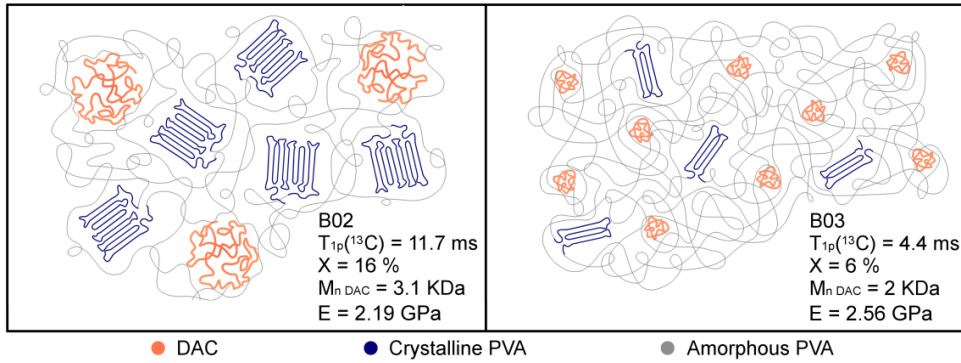


Figure 44 Schematic representation of the structure of the respective xerogels within PVA/DAC series B with their relation between flexibility ($T_{1\rho}(^{13}\text{C})$), crystallinity (X), Young's modulus (E) and number average molecular weight (\bar{M}_n) of DAC. The orange coils correspond to (\bar{M}_n) of DAC, the arrays of blue lines represent polymer chain crystallites, and the grey lines represent the amorphous phase of the polymer with physical entanglements. The size, ratio, and number of depicted features is intentionally exaggerated for better understanding. [91]

Role of catalyst. Characteristics of prepared PVA/DAC materials differing by the age of used DAC crosslinker are correlated to better illustrate the influence of used type of catalyst system (Figure 45).

Almost linear dependence of all characteristic properties of PVA/DAC materials prepared utilizing catalyst system type A is noticeable. There are several quantities increasing with the growing value of \bar{M}_n of used DAC, namely polymeric domain flexibility parameter ($T_{1\rho}(^{13}\text{C})$), graphs III, IV and V in Figure 45) and crystallinity (graphs II and V in Figure 45) of PVA/DAC samples. In contrast to this, PVA/DAC crosslink density (ρ_c , graph I, II, IV and V) exhibit linear decrease with increasing molecular weight of used DAC crosslinker. Moreover, the graph V in Figure 45 shows strong linear correlation between two independent methods characterizing hydrogel network properties, i.e. data obtained from solid-state NMR ($T_{1\rho}(^{13}\text{C})$) and values of (ρ_c) calculated with the aid of equilibrium swelling theory. Regarding graph V, both curves representing samples of series A or B possess apparently the same slope, although the curve belonging to samples of B series is shifted below that of A series samples which indicates slight difference in the distribution of network crosslinks. In general, series A exhibited higher $T_{1\rho}(^{13}\text{C})$ values than series B at the same values of ρ_c which might be a result of more uniform distribution of network crosslinks of samples of B series over samples of A series. Moreover, as the same stock fresh/aged DAC solution was always utilized in the preparation of corresponding samples of both A or B series, there is a presumption that the catalyst system type B (based on sulfuric acid) can be more sensitive towards the low molecular fragments of DAC, or can cause degradation of DAC, or this catalyst system may influence the formation of PVA physical crosslinks by entanglements. Based on the observed properties, there are most likely different

crosslinking mechanisms resulting from the utilization two chemically distinct catalyst systems producing principally different networking. Furthermore, there are some non-linear trends in the correlation of several properties of B series samples, such as of ρ_c vs. crystallinity of xerogels or vs. \bar{M}_n of used DAC crosslinker. This presumably arises from the overall complexity of catalyst system composition (methanol as volatile quencher, sulfuric and acetic acid as catalyst and buffer, respectively) and further complicates interpretation. In other words, although this crosslinking system (DAC + B type catalyst) works well and results in the formation of crosslinked PVA/DAC material, it is advisable to favour the simpler hydrochloric acid catalyst as properties of such prepared PVA/DAC hydrogels exhibit better coherence and predicable trends. Therefore, the next part of the study focusing on comparison of crosslinking effectivity and efficiency of DAC vs. GA was conducted using only HCl as the catalyst. [91]

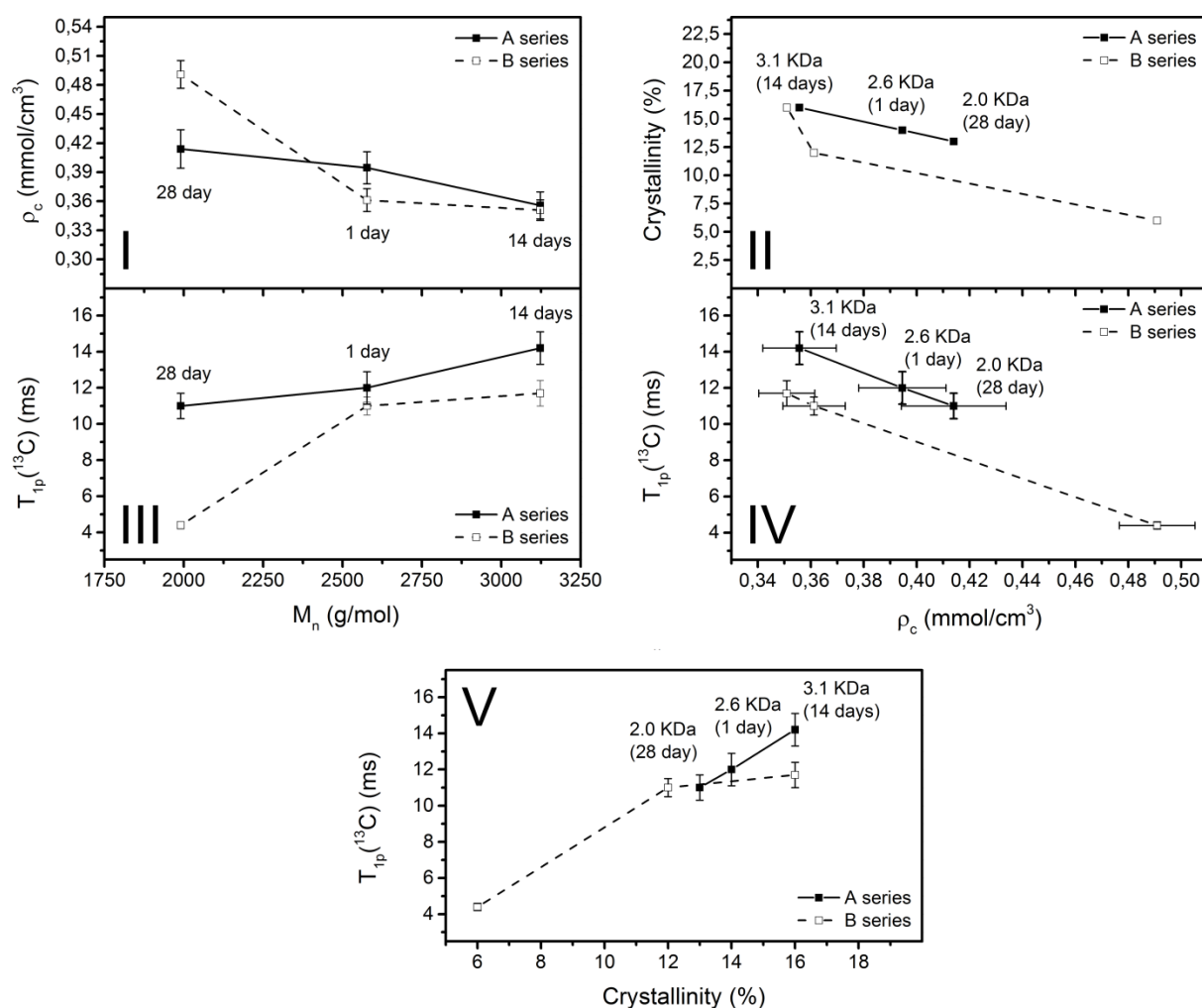


Figure 45 Correlation between data measured by various methods for PVA/DAC prepared using aged DAC and different catalyst system. The lines connecting points in the graphs are only guides for eyes. The data points are labelled by corresponding age and number average molecular weight for one series (A) only in each graph. The second series (B) has the same order of data points from left to right always. [91]

7.3.4 Comparative PVA crosslinking study of DAC and GA

The last part of this research objectives is focused on the comparison of network parameters of PVA hydrogels crosslinked by DAC (PVA/DAC) and by GA (PVA/GA) prepared utilizing broad range respective crosslinkers under equivalent conditions (drying temperature, amount of catalyst and amount of crosslinkers aldehyde groups per sample etc.). Such approach enables evaluation of the crosslinking effectivity and efficiency of the newly introduced macromolecular DAC crosslinking agent with respect to its low molecular counterpart GA which is one of the most commonly utilized PVA crosslinkers [179–181]. Based on the observations and conclusions made in previous chapter, diluted hydrochloric acid was used as the catalyst of crosslinking reactions between PVA and DAC as well as GA crosslinker.

It should be stressed out that only fresh solubilized DAC was utilized toward this purpose with the concentration ranging from 0.0625 to 5 wt% relative to amount of used PVA. According to the experimentally obtained value of reactive aldehyde content (via oxime reaction) of fresh DAC solution (11.7 ± 0.3 mmol/g), the exact chemical amount of crosslinkers aldehyde groups (n_{CHO}) per sample were calculated. The designation of the PVA/DAC samples prepared using PVA type “Mowiflex” and their measured network parameters are noted in the Table 26.

As can be seen in this table, DAC was found to be effective crosslinking agent for PVA type “Mowiflex” in the whole range of used concentrations (5–0.0625 wt%) when using hydrochloric acid as catalyst. The network parameters exhibit expected trends, i.e. as the amount of used DAC crosslinker decreases, the swelling capacity, equilibrium water content (EWC) and average molecular weight between crosslinks (\bar{M}_c) increase while gel fraction and crosslink density (ρ_c) decrease. Swelling capacity, as one of the most characteristic features of hydrogels, exhibits values ranging from approximately 100 % to 6 500 %. Next, closely related to the swelling capacity is the gel fraction, which gradually decreases from roughly 84 to 14 %. These values of specific network parameters are mentioned for the two extreme cases of used crosslinker concentration of 5 and 0.0625 wt%, respectively. The explanation to this behaviour as well as to previously described trends and correlations between network parameters is simple; as the concentration of the crosslinker decreases, the polymer network becomes sparsely crosslinked and thus the average length of PVA chains between crosslinks grows. On the one side, such sparsely crosslinked network possesses more space for water uptake by swelling and on the other it leaves more free uncrosslinked PVA macromolecules only physically entangled in the hydrogel matrix which increases the material weight loss during washing process. [91] The model of the structure of PVA/DAC hydrogel will be further refined and compared with that of PVA/GA.

Table 26 Network parameters (percentage of swelling, equilibrium water content EWC, gel fraction, average molecular weight between crosslinks \bar{M}_c and crosslink density ρ_c) of PVA/DAC (DTC) samples prepared using different concentrations of DAC crosslinking agent and “Mowiflex” type of PVA. Different concentrations are also expressed by crosslinker reactive aldehyde groups (n_{CHO}) per sample. [91]

#	DTC-						
	A	B	C	D	E	F	G
DAC (wt%)	5	3	1.5	1	0.25	0.125	0.0625
n_{CHO} per sample (μmol)	2 920 \pm 60	1 750 \pm 40	877 \pm 19	585 \pm 13	146 \pm 3	73.1 \pm 1.6	36.6 \pm 0.8
Swelling (%)	107.7 \pm 0.8	150.4 \pm 1.3	276 \pm 4	422 \pm 12	2 330 \pm 50	4 300 \pm 200	6 500 \pm 400
EWC (%)	51.9 \pm 0.2	60.1 \pm 0.2	73.4 \pm 0.3	80.8 \pm 0.4	95.9 \pm 0.1	97.7 \pm 0.1	98.5 \pm 0.1
Gel frac. (%)	83.9 \pm 0.1	81.4 \pm 0.1	73.5 \pm 0.7	64.0 \pm 0.5	28.7 \pm 0.2	19.2 \pm 0.6	13.5 \pm 1.8
\bar{M}_c (g/mol)	272 \pm 4	504 \pm 8	1 560 \pm 40	3 200 \pm 130	10 810 \pm 30	11 430 \pm 30	11 594 \pm 15
ρ_c (mmol/cm ³)	4.63 \pm 0.06	2.50 \pm 0.04	0.81 \pm 0.02	0.395 \pm 0.017	0.1170 \pm 0.0004	0.1100 \pm 0.0003	0.1090 \pm 0.0001

The comparative study continues with the evaluation of the network parameters of the PVA hydrogels prepared using GA and PVA of the type “Mowiflex”.

The calculated network parameters for PVA/GA hydrogel samples are noted in the Table 27. It should be stressed, that these hydrogels were prepared using volumes of GA crosslinker containing equivalent amount of reactive aldehyde groups (n_{CHO}) per sample as in the case of PVA/DAC hydrogel samples preparation (for details see section “6.2.iii Hydrogel study”).

Table 27 Network parameters of PVA/GA (GTC) samples prepared using different concentrations of GA crosslinking agent defined by chemical amount of reactive aldehyde groups (n_{CHO}) per sample and “Mowiflex” type of PVA. [91]

#	GTC-						
	A	B	C	D	E	F	G
n_{CHO} per sample (μmol)	2 920 \pm 60	1 750 \pm 40	877 \pm 19	585 \pm 13	146 \pm 3	73.1 \pm 1.6	36.6 \pm 0.8
Swelling (%)	136.8 \pm 1.5	178 \pm 4	291.7 \pm 1.6	384 \pm 6	1 640 \pm 30	-	-
EWC (%)	57.8 \pm 0.3	64.0 \pm 0.5	74.5 \pm 0.1	79.4 \pm 0.2	94.3 \pm 0.1	-	-
Gel frac. (%)	86.9 \pm 0.1	83.8 \pm 0.6	80.2 \pm 0.5	76.5 \pm 1.8	44.9 \pm 0.7	-	-
\bar{M}_c (g/mol)	422 \pm 8	690 \pm 30	1 730 \pm 17	2 760 \pm 70	10 050 \pm 50	-	-
ρ_c (mmol/cm ³)	2.99 \pm 0.06	1.83 \pm 0.07	0.729 \pm 0.007	0.456 \pm 0.011	0.1250 \pm 0.0006	-	-

The ‘-’ sign means that the prepared material disintegrated in water.

In contrast to the previous case of hydrogel preparation by utilizing macromolecular DAC as the crosslinking agent, low molecular crosslinker GA exhibited its crosslinking effectivity only at relatively high concentrations compared to DAC. Data on network parameters of PVA/GA hydrogel samples designated as GTC-F and GTC-G prepared utilizing concentrations of the lower part of investigated range (crosslinker reactive groups per sample $n_{CHO} = 73.1$ and $36.6 \mu\text{mol}$, respectively) are not included in the Table 27 as these parameters were impossible to measure. Such PVA/GA samples teared apart, disintegrated or even dissolved during the washing process. The observed poor crosslinking effectivity of GA crosslinker at low concentrations (amounts of n_{CHO} per sample) while maintaining identical preparation conditions (drying temperature, amount of catalyst, type of PVA etc.) was the main difference in comparison to DAC crosslinker. The next most pronounced difference was the significantly lower swelling ability of PVA/GA in comparison with PVA/DAC samples prepared with the use of low crosslinker concentrations. Utilizing higher concentrations of GA led to formation of PVA/GA hydrogels exhibiting similar trends in network parameters as of PVA/DAC ones. [91]

Figure 46 shows direct comparison of network parameters of PVA/DAC (DTC series, DAC crosslinker, see Table 26) and PVA/GA (GTC series, GA crosslinker, see Table 27) hydrogels prepared utilizing PVA type “Mowiflex” and diluted HCl as catalyst. Regardless of the chosen crosslinking agent, hydrogel samples noted as A–E possess comparable swelling capacity, although samples prepared using DAC in concentrations between 5–1.5 wt% exhibit slightly lower values of swelling capacity. The reason to this can be found in somewhat higher crosslinking efficiency of DAC over GA in this concentration range. An important observation is embodied into the graphs on the right side of the Figure 46. While there is no difference in \bar{M}_c for the two gels, the values of ρ_c differ with increasing concentrations. This must have implication towards the crosslinking network topology. The difference between EWC of the two hydrogels shows opposite trend. [91]

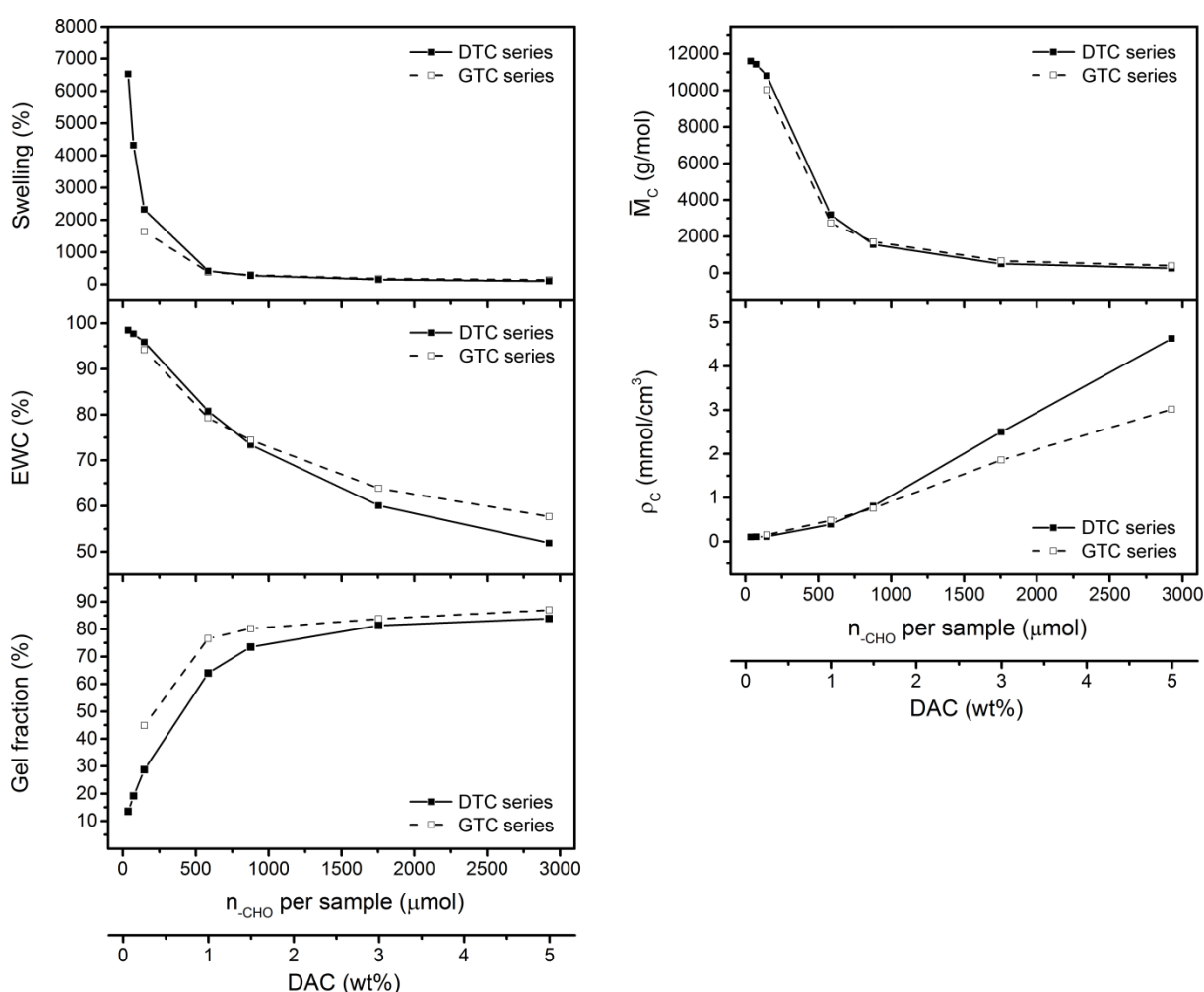


Figure 46 The results from comparative crosslinking study showing dependence of PVA/DAC (DTC) and PVA/GA (GTC) hydrogels network parameters on the used DAC or GA crosslinker amount defined by chemical amount of reactive aldehyde groups per sample and “Mowiflex” type of PVA. The equivalency between DAC and GA reactive group concentrations is expressed by the two bottom x-axes. The lines connecting points in the graphs are only guides for eyes. [91]

The last evaluated network parameter is the gel fraction. In general, the gel fraction of PVA/GA samples is of higher value than of PVA/DAC samples (86.9–44.9 % and 83.9–28.7 %, A–E hydrogel samples, respectively).

The most probable explanation to all these observations lies in the different distribution of crosslinks within network of hydrogels prepared by distinct crosslinking agents with defined molecular weight. In the first case, the low molecular weight crosslinkers such as GA form polymer network with approximately homogeneous distribution of crosslinks. In the second case, the macromolecular crosslinking agent such as DAC principally forms substantially different network of crosslinks composed of (i) regions with high local crosslink density adjacent to the DAC macromolecules which contain large amount of reactive aldehyde groups responsible in crosslink formation and (ii) regions constituted of sizable sections of free or possibly physically entangled PVA chains. Some of these chains linking the densely crosslinked regions together are responsible for the preservation of PVA hydrogel integrity. Other chains can be joined to one densely crosslinked region only. A single PVA chain may be attached to one DAC macromolecule more than on one site forming thus circles. This diverse crosslink distribution gives rise to “two-phase” and homogeneous “single-phase” network topology schematically depicted in the Figure 47. [91]

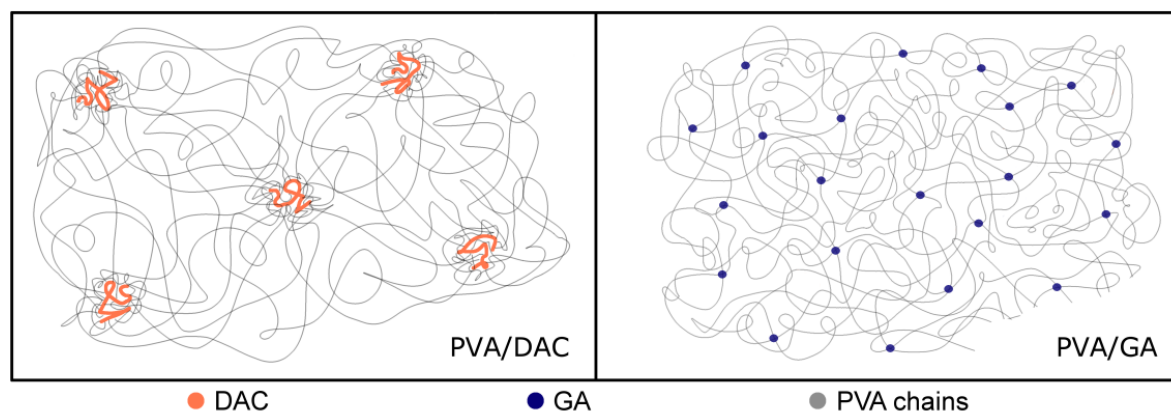


Figure 47 Network topology of PVA/DAC is shown in the left part. It is composed of (i) regions containing high local crosslink density adjacent to DAC macromolecules (orange) embedded in (ii) larger regions comprised of free, chemically unbound, PVA chains (grey) which can be only physically entangled. Some of these chains link the regions (i) together. The right part of the figure shows the homogeneous network topology of PVA/GA crosslinked by GA (blue). The size, ratio, and number of depicted features are intentionally exaggerated for better understanding. [91]

The same experimental procedure of PVA crosslinking via two distinct crosslinking agents and diluted hydrochloric acid as catalyst was applied on different type of PVA (“Mowiol”). It exhibits roughly similar properties (84–86% hydrolysis, $\rho_p = 1.3 \text{ g/cm}^3$, $\bar{M}_n = 27\,500 \text{ g/mol}$) as PVA type “Mowiflex” (~83% hydrolysis, $\rho_p = 1.3 \text{ g/cm}^3$, $\bar{M}_n = 23\,500 \text{ g/mol}$). The Tables 28 and 29

summarize the network parameters of PVA “Mowiol” hydrogels prepared using DAC (DSA series) and GA (GSA series), respectively.

Table 28 Network parameters of PVA/DAC (DSA) samples prepared using different concentrations of DAC crosslinking agent and “Mowiol” type of PVA.

#	DSA-						
	A	B	C	D	E	F	G
DAC (wt%)	5	3	1.5	1	0.25	0.125	0.0625
n_{-CHO} per sample (μmol)	2 920 \pm 60	1 750 \pm 40	877 \pm 19	585 \pm 13	146 \pm 3	73.1 \pm 1.6	36.6 \pm 0.8
Swelling (%)	115.7 \pm 0.5	177.8 \pm 0.2	360 \pm 7	533 \pm 9	2 720 \pm 80	4 900 \pm 200	-
EWC (%)	53.6 \pm 0.1	64.0 \pm 0.1	78.2 \pm 0.3	84.2 \pm 0.2	96.4 \pm 0.1	98.0 \pm 0.1	-
Gel frac. (%)	91.1 \pm 0.1	86.7 \pm 0.1	72.6 \pm 0.6	62.5 \pm 0.6	25.7 \pm 3.0	15.6 \pm 2.8	-
\bar{M}_c (g/mol)	311 \pm 3	697 \pm 2	2 560 \pm 80	4 710 \pm 110	12 780 \pm 50	13 410 \pm 30	-
ρ_c (mmol/cm ³)	4.05 \pm 0.03	1.81 \pm 0.01	0.49 \pm 0.01	0.269 \pm 0.006	0.0986 \pm 0.0004	0.0940 \pm 0.0002	-

The previously observed trends in the correlation between network parameters are the same. However, the crosslinking efficiency of DAC is slightly lower for PVA type “Mowiol” compared to the previous case of PVA type “Mowiflex”. This fact is manifested by shift of several parameters such as swelling capacity, EWC and \bar{M}_c toward higher and ρ_c towards lower average values. Furthermore, DAC crosslinker is comparably worse (loss of hydrogel integrity) at very low concentration (0.0625 wt% or 36.6 μmol of n_{-CHO} crosslinker groups per sample) utilized for PVA type “Mowiol” than in the case of PVA type “Mowiflex”.

However, DAC still exhibits superior crosslinking effectivity over GA at low concentrations even for the PVA type “Mowiol” as can be seen in the comparison of Tables 28 and 29. As in the case of the utilization of different type of PVA, the exceptional crosslinking efficiency of hydrogels formed by

DAC is most likely caused by its macromolecular character which imparts the “two-phase” topology of polymer crosslink network although this effect is not so well pronounced as in the previous case.

Table 29 Network parameters of PVA/GA (GSA) samples prepared using different concentrations of GA crosslinking agent defined by chemical amount of reactive aldehyde groups per sample and “Mowiol” type of PVA.

#	GSA-						
	A	B	C	D	E	F	G
n_{CHO} per sample (μmol)	2 920 \pm 60	1 750 \pm 40	877 \pm 19	585 \pm 13	146 \pm 3	73.1 \pm 1.6	36.6 \pm 0.8
Swelling (%)	139.3 \pm 1.9	187 \pm 3	250 \pm 3	343 \pm 2	4 660 \pm 160	-	-
EWC (%)	58.2 \pm 0.3	65.1 \pm 0.3	71.4 \pm 0.3	77.4 \pm 0.1	97.9 \pm 0.1	-	-
Gel frac. (%)	94.3 \pm 0.1	94.7 \pm 0.2	89.9 \pm 0.1	84.2 \pm 0.1	31.3 \pm 1.8	-	-
\bar{M}_c (g/mol)	437 \pm 11	760 \pm 20	1 300 \pm 30	2 300 \pm 30	11 500 \pm 20	-	-
ρ_c (mmol/cm ³)	2.89 \pm 0.07	1.66 \pm 0.05	0.97 \pm 0.02	0.549 \pm 0.006	0.1098 \pm 0.0002	-	-

Figure 48 shows the dependence of crosslinking agent concentration on the resulting characteristics of prepared “Mowiol” type of PVA hydrogels expressed by the network parameters. The main difference from the “Mowiflex” type of gels can be seen in the two graphs on the right side of Figure 48. The difference between \bar{M}_c for the two gels (DSA and GSA) has just opposite trend that the difference between ρ_c for those gels. This most likely means, that the “two-phase” crosslinking network topology was not developed to such extent as in the case of DTC samples. Alternative explanation based on worsening of the homogeneity of the distribution of GA crosslinking seems not to be reasonable. However, even for these series of samples, the high effectivity of DAC (namely using very low concentrations) is proven and the properties of PVA/DAC (DSA series) are better or comparable with PVA/GA (GSA series).

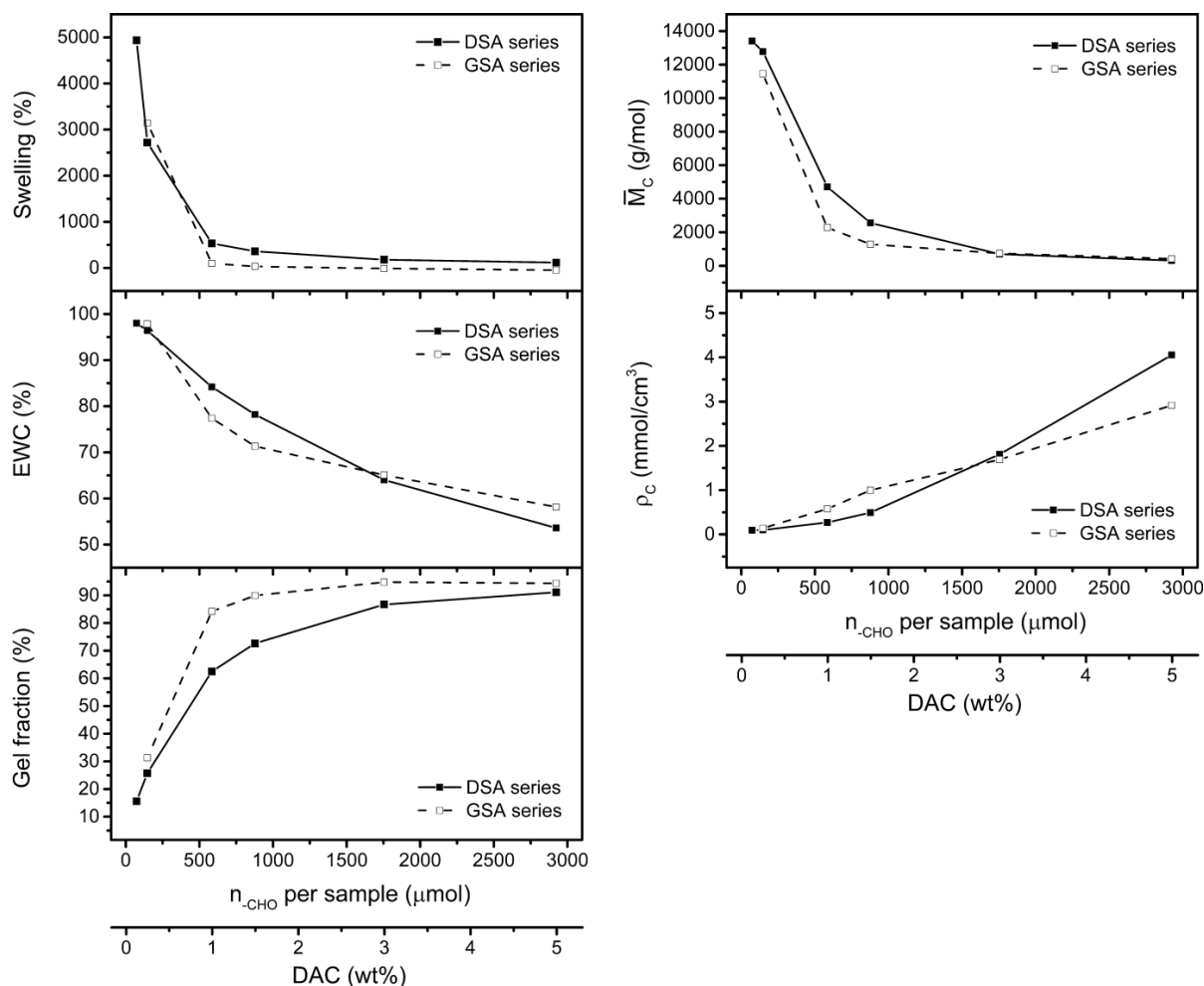


Figure 48 The results from comparative crosslinking study showing dependence of PVA/DAC (DSA) and PVA/GA (GSA) hydrogels network parameters on the used DAC or GA crosslinker amount defined by chemical amount of reactive aldehyde groups per sample and “Mowiol” type of PVA. The equivalency between DAC and GA reactive group concentrations is expressed by the two bottom x-axes. The lines connecting points in the graphs are only guides for eyes.

To summarize, samples prepared using higher concentrations of DAC and GA crosslinking agents showed relatively comparable network parameters for both utilized types of PVA. However, slightly increased crosslink density was observed for PVA/DAC samples in the span of used DAC concentration from 1.5 to 5 wt% when “Mowiflex” type of PVA employed in the hydrogel preparation. The second investigated type of PVA “Mowiol” exhibited more or less comparable network parameters to those measured for PVA/GA (GSA series). The common feature regardless of utilized PVA matrix is better crosslinking efficiency of DAC at very low crosslinker concentrations. This observation is likely connected to the macromolecular character of DAC which enables its use at very low concentrations (0.0625 wt%, i.e. 36.6 μmol or 0.125 wt%, i.e. 73.2 μmol of $-\text{CHO}$ groups per sample in DTC or DSA series, respectively) compared to GA, allowing to prepare hydrogels with very high swelling capacity.

8. CONCLUDING SUMMARY

The concluding summary can be divided into three key parts following the structure of the Thesis:

(i) Initially, the pilot study demonstrated the possibility of solubilized DAC utilization as a crosslinking agent for PVA. It was found that one of the key factors defining the resulting PVA/DAC material properties is the optimization of process parameters such as catalyst system concentration and drying temperature. Within this pilot study, the crosslinking of PVA matrix was achieved in all hydrogel samples prepared by employing 2 wt% of DAC crosslinking agent, both concentrations of catalyst system based on sulfuric acid and whole set of drying temperatures. Resulting materials showed different thermal behaviour and possessed different network parameters based on the variation of these process parameters. However, in order to obtain degradation-free hydrogel material, the optimal parameters for the preparation of the PVA/DAC crosslinked material should include drying temperatures below 60 °C and utilize lower concentration of catalyst system.

(ii) The next part focused on the process of DAC preparation, analysis and detailed investigation of its solubilization process. The initial characterization of prepared DAC confirmed presence of reactive aldehyde groups and disruption of ordered macromolecular packing manifested by decrease in crystallinity compared to original cellulose. In the subsequent step, it was found that the DAC solubilization process causes severe degradation of the material regardless of heating method or initial pH. Thus the contradictions in literature between the studies of Kim *et al.* (2004) [97] and Sulaeva *et al.* (2015) [98] were decided in the favour of progressive deterioration of DAC macromolecules during its solubilization. The resulting product of solubilization exhibited approximately one tenth of the original cellulose polymerization degree. Disregarding this molecular weight determining step, obtained solubilized DAC retained its characteristic features, namely content of reactive aldehyde groups. These reactive substituents present on the polymer chain enable DAC utilization in the crosslinking applications for hydroxyl group containing polymers and thus can be further considered as an alternative to common used aldehyde-based low molecular crosslinkers. Main benefit of DAC as a crosslinker lies in its bio-macromolecular character, which makes it less toxic in comparison to its low molecular counterparts.

Next, the aging of DAC solution was studied in the terms of its functional group content, structure and molecular weight distribution. Due to known DAC sensitivity towards alkalic environment, the DAC solution was kept under acidic condition in current study. Initially, the composition of fresh acidic DAC

solution was investigated by NMR and the main forms of solubilized DAC identified for the first time. The most abundant forms are intra- and intermolecular DAC hemiacetals. As the aging of DAC proceeded, no new NMR signals were detected. The only observable changes were in the population of particular DAC forms. This observation can be assigned to the low pH conditions which increased the stability of the system in comparison with previous investigations reported by other authors. The low pH presumably suppresses the degradation processes described as β -elimination and further preserves the reactive aldehyde group content in time of DAC aging. The indirect alkalimetric titration showed less than a half decrease of reactive aldehyde content after four compared to previous studies on this topic. The results from NMR and GPC study were interpreted as several characteristic processes taking place during DAC aging. The first process occurs immediately after DAC preparation and comprises of internal stabilization by the formation of intramolecular DAC hemiacetals. The second process was noticed after 14 days after DAC preparation and is manifested by reactions between DAC macromolecules resulting in the formation of intermolecular hemiacetals. This recombination process is also reflected in the increased values of all momentums of molecular weight estimated by GPC. The third process, DAC chain fragmentation, becomes dominant with increasing time of DAC aging. The significant increase in PDI and decrease in values of certain momentums of molecular weight (\bar{M}_n , \bar{M}_w and M_p) testifies presence of such process in 28 days old solutions. However, low pH of the solution suppresses this fragmentation process (β -elimination) for the first 14 days of DAC aging. Hence, the evolution and accumulation of smaller DAC fragments evolution and accumulation is apparent after 28 days.

It should be stressed out, that the processes of recombination and fragmentation run concurrently during entire solubilized acidic DAC aging timeframe. This fact is supported by the changes in the PDI values as well as in the monotonous increase of \bar{M}_z values during DAC aging. The practical outcome of the investigation on the structural arrangements and properties of solubilized acidic DAC solutions during its shelf-life is the promising potential to be conveniently utilized for various purposes (such as crosslinking agent or intermediate in the preparation of other derivatives) without the need to prepare fresh DAC every time as it retains its functional properties at least for 28 days from its preparation.

(iii) The suitability of solubilized acidic DAC as a crosslinking agent for PVA was investigated along the utilization of different catalyst systems. The effects of catalyst systems based on the sulfuric or hydrochloric acid and the role of the age of pH-stabilized DAC solution on resulting properties of PVA crosslinked hydrogels were studied. Furthermore, the comparative crosslinking study of PVA utilizing DAC or GA crosslinkers in broad range of concentrations under

equivalent conditions was conducted. The results of this study were expressed and compared in the terms of network parameters of prepared hydrogels.

The applicability of the acidic DAC solution as a crosslinking agent for PVA was confirmed even after 28 days from its preparation. Moreover, DAC was found to be effective crosslinker with both chosen catalyst systems. It was revealed, that the properties of prepared PVA/DAC hydrogels are governed by the molecular weight of solubilized acidic DAC and selected catalyst rather than by the reactive aldehyde content. The functional DAC groups content responsible for the formation of crosslinks in PVA matrix decrease linearly in the course of 4 weeks. Thus the resulting properties of prepared hydrogels, such as swelling capacity, should exhibit linearly increasing trend as the crosslinking agent becomes less efficient over time. However, this was not observed. Instead, the trends of hydrogel properties follow the evolution of DAC molecular weight. There is about 20 % increase in its \bar{M}_n after 14 days caused by intermolecular hemiacetal formation (DAC recombination) followed by decrease of this quality about 40 % after 28 days from crosslinker preparation (DAC fragmentation). Similar trends were observed in number of measured properties of prepared PVA/DAC xerogels and hydrogels such as polymeric domain flexibility ($T_{1\rho}(^{13}\text{C})$), crosslink density (ρ_c), swelling capacity, equilibrium water content (EWC), average molecular weight between crosslinks (\bar{M}_c), amount of crystalline phase and average values of Young's modulus. The fact, that crosslinkers molecular weight is the key factor in hydrogel preparation implies potential possibility of "tuning" of hydrogel properties without need for other additives.

The properties of PVA/DAC hydrogels prepared using fresh/aged DAC exhibit similar quantitative trends when different catalyst systems were employed. However, there are noticeable differences in material properties of hydrogels prepared using the oldest and thus the most fractioned DAC and different catalyst. Based on the data obtained from NMR, tensile testing and network parameters evaluation, sulfuric acid accompanied by methanol and acetic acid seem to be (a) more efficient catalyst or (b) may induce DAC degradation or (c) influence physical PVA entanglements. All of these possibilities result in the formation of PVA hydrogel with increased crosslink density and other related network parameters. The downside of the utilization of this catalyst system lies in non-linear behaviour of several correlated properties arising from the complexity of this specific catalyst system. Comparatively, the utilization of fairly simple catalyst based on diluted hydrochloric acid produces PVA hydrogels of predicable, structurally stable and less DAC molecular weight-dependent properties.

The last part of this research was devoted to the comparison of macromolecular DAC to low molecular GA crosslinker. The exceptional crosslinking efficiency of DAC at very low concentrations outperforms GA and enables to form hydrogels with extreme swelling capacity. Such crosslinking

capability of DAC can be explained as a result of its macromolecular character, which forms “two-phase” crosslink network topology composed of regions with high crosslink density adjacent to the DAC macromolecule embedded in a chemically uncrosslinked matrix comprised of sizable sections of free PVA chains, which are physically entangled only. Some of these chains linking the densely crosslinked regions together are responsible for the preservation of PVA hydrogel integrity. Other chains can be joined to one densely crosslinked region only. A single PVA chain may be attached to one DAC macromolecule more than on one site forming thus circles hypothetically allowing concatenation. Relatively sparse distribution separation of high-density crosslink regions results is responsible for the large swelling ability of PVA/DAC hydrogels. On the other side of the crosslinker concentration range, DAC enables formation of highly crosslinked hydrogels of comparable or even better material characteristics that those obtained by utilizing GA. Furthermore, due to presumably lower toxicity of DAC compared to GA, this cellulose derivative is promising compound for the application in medicine and pharmacy.

9. SUMMARY OF CONTRIBUTIONS TO SCIENCE AND PRAxis

The main contributions of this research to science and praxis include following achievements (i) preparation and characterization of solubilized dialdehyde cellulose (DAC) and its use as a poly(vinyl alcohol) (PVA) crosslinker, (ii) investigation of the solubilization effects on the properties of DAC (iii) analysis of DAC structure in acidic media during its aging, (iv) utilization of fresh/aged solubilized DAC as a PVA crosslinker with evaluation of its crosslinking abilities and finally (v) comparison of network parameters of PVA hydrogels prepared using DAC and glutaraldehyde (GA) crosslinker in wide range of concentrations.

Periodate oxidation does not influence molecular weight. However, subsequent solubilization was proven to cause severe degradation of resulting solubilized DAC.

Significant improvement of DAC stability in comparison to the previous studies and thus prolongation of its shelf-life and applicability was achieved via our originally developed low pH procedure. DAC is initially stabilized by intramolecular and subsequently intermolecular hemiacetal formation as confirmed by NMR and GPC. Fragmentation occurs during observed DAC aging as well as minor decrease in reactive aldehyde group content.

It was found that DAC molecular weight influences the properties of PVA/DAC hydrogels more than its reactive aldehyde group content. The changes in molecular weight or functional group content did not compromise DAC crosslinking ability even 28 days from its preparation.

It was demonstrated that solubilized and stabilized DAC exceeds crosslinking efficiency of GA at very low concentrations. Moreover, it forms denser network at high concentrations and principally different network topology compared to GA. This enables to prepare hydrogels with wide range of properties. Furthermore, arising from its macromolecular character, it is considerably less toxic than low molecular crosslinkers. Preliminary results confirmed low toxicity and biocompatibility of PVA/DAC hydrogels. Future work will focus on hydrogels loading with active compounds such as platinum based complexes, their subsequent release kinetic and biological testing.

Besides DAC utilization as crosslinker, it can serve as an intermediate in the preparation of dicarboxy cellulose (DCC) which is another promising drug carrier. Our recent study showed DCC high loading efficiency (90 %) and capacity (60 % w/w) of platinum based anticancer drugs. Furthermore, it allows adjustable and pH sensitive drug-release kinetics.

To generalize, the results embodied in this Thesis open a new field for applications of DAC and its derivatives, namely in medical sector and pharmacy as promised by ongoing research.

REFERENCES

- [1] THOMAS, S., DURAND, D., CHASSENIEUX, Ch. and JYOTISHKUMAR, P. (eds.). *Handbook of biopolymer-based materials: from blends and composites to gels and complex networks*. Weinheim : Wiley-VCH, 2013. ISBN 978-3-527-32884-0.
- [2] WICHTERLE, O. and LÍM, D. Hydrophilic Gels for Biological Use. *Nature*. 1960. Vol. 185, no. 4706, p. 117–118. DOI 10.1038/185117a0.
- [3] PEPPAS, N. A. Hydrogels in pharmaceutical formulations. *European Journal of Pharmaceutics and Biopharmaceutics*. 2000. Vol. 50, no. 1, p. 27–46. DOI 10.1016/S0939-6411(00)00090-4.
- [4] CHEN, R. and HUNT, J. A. Biomimetic materials processing for tissue-engineering processes. *Journal of Materials Chemistry*. 2007. Vol. 17, no. 38, p. 3974–3979. DOI 10.1039/b706765h.
- [5] MA, P. X. Biomimetic materials for tissue engineering. *Advanced Drug Delivery Reviews*. 2008. Vol. 60, no. 2, p. 184–198. DOI 10.1016/j.addr.2007.08.041.
- [6] TIBBITT, M. W. and ANSETH, K. S. Hydrogels as extracellular matrix mimics for 3D cell culture. *Biotechnology and Bioengineering*. 2009. Vol. 103, no. 4, p. 655–663. DOI 10.1002/bit.22361.
- [7] LIU, L. S., KOST, J., YAN, F. and SPIRO, R. C. Hydrogels from Biopolymer Hybrid for Biomedical, Food, and Functional Food Applications. *Polymers*. 2012. Vol. 4, no. 4, p. 997–1011. DOI 10.3390/polym4020997.
- [8] QIU, Y. and PARK, K. Environment-sensitive hydrogels for drug delivery. *Advanced Drug Delivery Reviews*. 2001. Vol. 53, no. 3, p. 321–339. DOI 10.1016/S0169-409X(01)00203-4.
- [9] CARPI, A. (ed.). *Progress in Molecular and Environmental Bioengineering - From Analysis and Modeling to Technology Applications*. InTech, 2011. ISBN 978-953-307-268-5.
- [10] BAKER, M. I., WALSH, S. P., SCHWARTZ, Z. and BOYAN, B. D. A review of polyvinyl alcohol and its uses in cartilage and orthopedic applications. *Journal of Biomedical Materials Research Part B: Applied Biomaterials*. 2012. Vol. 100, no. 5, p. 1451–1457. DOI 10.1002/jbm.b.32694.

- [11] KAMOUN, E. A., CHEN, X., MOHY ELDIN, M. S. and KENAWY, E.-R. S. Crosslinked poly(vinyl alcohol) hydrogels for wound dressing applications: A review of remarkably blended polymers. *Arabian Journal of Chemistry*. 2015. Vol. 8, no. 1, p. 1–14. DOI 10.1016/j.arabjc.2014.07.005.
- [12] BOLTO, B., TRAN, T., HOANG, M. and XIE, Z. Crosslinked poly(vinyl alcohol) membranes. *Progress in Polymer Science*. 2009. Vol. 34, no. 9, p. 969–981. DOI 10.1016/j.progpolymsci.2009.05.003.
- [13] LEE, K. Y. and MOONEY, D. J. Hydrogels for Tissue Engineering. *Chemical Reviews*. 2001. Vol. 101, no. 7, p. 1869–1880. DOI 10.1021/cr000108x.
- [14] MIYAZAKI, T., TAKEDA, Y., AKANE, S., ITOU, T., HOSHIKO, A. and EN, K. Role of boric acid for a poly(vinyl alcohol) film as a cross-linking agent: Melting behaviors of the films with boric acid. *Polymer*. 2010. Vol. 51, no. 23, p. 5539–5549. DOI 10.1016/j.polymer.2010.09.048.
- [15] BISPO, V. M., MANSUR, A. A. P., BARBOSA-STANCIOLI, E. F. and MANSUR, H. S. Biocompatibility of Nanostructured Chitosan/Poly(Vinyl Alcohol) Blends Chemically Crosslinked with Genipin for Biomedical Applications. *Journal of Biomedical Nanotechnology*. 2010. Vol. 6, no. 2, p. 166–175. DOI 10.1166/jbn.2010.1110.
- [16] OTT, E., SPURLIN, H. M. and GRAFFLIN, M. W. (eds.). *Cellulose and cellulose derivatives, Part I*. New York : Interscience Publishers, 1954. ISBN 978-0-470-39007-8.
- [17] MÜNSTER, L. and KUŘITKA, I. Vliv koncentrace katalyzačního systému a teploty sušení na síťování PVA/DAC směsi. In : *PLASTKO 2016*. Zlín, 2016. p. 507–515. ISBN 978-80-7454-590-0.
- [18] CHANG, J. Y. (ed.). *Biopolymers, PVA hydrogels, anionic polymerisation, nanocomposites*. Berlin : Springer, 2000. ISBN 978-3-540-67313-2.
- [19] ZUGENMAIER, P. *Crystalline cellulose and cellulose derivatives: characterization and structures*. Berlin : Springer, 2008. ISBN 978-3-540-73933-3.
- [20] SJÖSTRÖM, E. *Wood chemistry: fundamentals and applications*. New York : Academic Press, 1993. ISBN 978-0-08-092589-9.
- [21] ZHAO, Y. and LI, J. Excellent chemical and material cellulose from tunicates: diversity in cellulose production yield and chemical and

- morphological structures from different tunicate species. *Cellulose*. 2014. Vol. 21, no. 5, p. 3427–3441. DOI 10.1007/s10570-014-0348-6.
- [22] SACUI, I. A., NIEUWENDAAL, R. C., BURNETT, D. J., STRANICK, S. J., JORFI, M., WEDER, C., FOSTER, E. J., OLSSON, R. T. and GILMAN, J. W. Comparison of the Properties of Cellulose Nanocrystals and Cellulose Nanofibrils Isolated from Bacteria, Tunicate, and Wood Processed Using Acid, Enzymatic, Mechanical, and Oxidative Methods. *ACS Applied Materials & Interfaces*. 2014. Vol. 6, no. 9, p. 6127–6138. DOI 10.1021/am500359f.
- [23] WERTZ, J.-L., BÉDUÉ, O. and MERCIER, J. P. *Cellulose science and technology*. Lausanne : EPFL Press, 2010. ISBN 978-1-4200-6688-3.
- [24] PIZZI, A. and EATON, N. The Structure of Cellulose by Conformational Analysis. 2. The Cellulose Polymer Chain. *Journal of Macromolecular Science: Part A - Chemistry*. 1985. Vol. 22, no. 1, p. 105–137. DOI 10.1080/00222338508063300.
- [25] NEVELL, T. P. and ZERONIAN, S. H. (eds.). *Cellulose chemistry and its applications*. New York : Halsted Press, 1985. ISBN 978-0-85312-463-4.
- [26] BAKER, A. A., HELBERT, W., SUGIYAMA, J. and MILES, M. High-Resolution Atomic Force Microscopy of Native Valonia Cellulose I Microcrystals. *Journal of Structural Biology*. 1997. Vol. 119, no. 2, p. 129–138. PMID: 9245753.
- [27] SIQUEIRA, G., BRAS, J. and DUFRESNE, A. Cellulosic Bionanocomposites: A Review of Preparation, Properties and Applications. *Polymers*. 2010. Vol. 2, no. 4, p. 728–765. DOI 10.3390/polym2040728.
- [28] CHANZY, H., IMADA, K. and VUONG, R. Electron diffraction from the primary wall of cotton fibers. *Protoplasma*. 1978. Vol. 94, no. 3–4, p. 299–306. DOI 10.1007/BF01276778.
- [29] KROON-BATENBURG, L. M. J., BOUMA, B. and KROON, J. Stability of Cellulose Structures Studied by MD Simulations. Could Mercerized Cellulose II Be Parallel? *Macromolecules*. 1996. Vol. 29, no. 17, p. 5695–5699. DOI 10.1021/ma9518058.
- [30] FRENCH, A. D., BROWN, R. M., CHANZY, H., GRAY, D., HATTORI, K. and GLASSER, W. Cellulose. In : *Encyclopedia of Polymer Science and Technology*. Hoboken : John Wiley & Sons, Inc., 2003. ISBN 978-0-471-44026-0.

- [31] KRÄSSIG, H. A. *Cellulose: structure, accessibility, and reactivity*. Yverdon : Gordon and Breach Science, 1993. ISBN 978-2-88124-798-9.
- [32] GILBERT, R. D. (ed.). *Cellulosic polymers, blends, and composites*. Munich : Hanser Publishers, 1994. ISBN 978-1-56990-166-3.
- [33] KLEMM, D. (ed.). *Comprehensive cellulose chemistry*. Weinheim : Wiley-VCH, 1998. ISBN 978-3-527-29413-8.
- [34] BAYER, E. A., CHANZY, H., LAMED, R. and SHOHAM, Y. Cellulose, cellulases and cellulosomes. *Current Opinion in Structural Biology*. 1998. Vol. 8, no. 5, p. 548–557. PMID: 9818257.
- [35] KENNEDY, J. F., PHILLIPS, G. O. and WILLIAMS, P. A. (eds.). *Cellulose sources and exploitation: industrial utilization, biotechnology, and physico-chemical properties*. New York : Ellis Horwood, 1990. ISBN 978-0-13-121955-7.
- [36] KRÄSSIG, H., SCHURZ, J., STEADMAN, R. G., SCHLIEFER, K. and ALBRECHT, W. Cellulose. In : ELVERS, B. (ed.), *Ullmann's Encyclopedia of Industrial Chemistry*. Weinheim : Wiley-VCH, 2000. ISBN 978-3-527-30673-2.
- [37] MAEKAWA, E. and KOSHIJIMA, T. Properties of 2,3-dicarboxy cellulose combined with various metallic ions. *Journal of Applied Polymer Science*. 1984. Vol. 29, no. 7, p. 2289–2297. DOI 10.1002/app.1984.070290705.
- [38] EPSTEIN, J. A. and LEWIN, M. Kinetics of the oxidation of cotton with hypochlorite in the pH range 5–10. *Journal of Polymer Science*. 1962. Vol. 58, no. 166, p. 991–1008. DOI 10.1002/pol.1962.1205816661.
- [39] LEWIN, M. and EPSTEIN, J. A. Functional groups and degradation of cotton oxidized by hypochlorite. *Journal of Polymer Science*. 1962. Vol. 58, no. 166, p. 1023–1037. DOI 10.1002/pol.1962.1205816663.
- [40] KATO, K., VASILETS, V. N., FURSA, M. N., MEGURO, M., IKADA, Y. and NAKAMAE, K. Surface oxidation of cellulose fibers by vacuum ultraviolet irradiation. *Journal of Polymer Science Part A: Polymer Chemistry*. 1999. Vol. 37, no. 3, p. 357–361.
- [41] LEWIN, M. and ETTINGER, A. Oxidation of cellulose by hydrogen peroxide. *Cellulose Chemistry and Technology*. 1969. Vol. 3, no. 1, p. 9–20.
- [42] NEVELL, T. P. and ZERONIAN, S. H. The Effect of Periodate Oxidation and of Subsequent Borohydride Reduction on the Tensile Strength of Cotton.

Journal of the Textile Institute Proceedings. 1962. Vol. 53, no. 2, p. 175–176.
DOI 10.1080/19447016208688667.

- [43] SAITO, T., KIMURA, S., NISHIYAMA, Y. and ISOGAI, A. Cellulose Nanofibers Prepared by TEMPO-Mediated Oxidation of Native Cellulose. *Biomacromolecules*. 2007. Vol. 8, no. 8, p. 2485–2491. DOI 10.1021/bm0703970.
- [44] CLODE, D. M. and HORTON, D. Synthesis of the 6-aldehyde derivative of cellulose, and a mass-spectrometric method for determining position and degree of substitution by carbonyl groups in oxidized polysaccharides. *Carbohydrate Research*. 1971. Vol. 19, no. 3, p. 329–337. DOI 10.1016/S0008-6215(00)86163-7.
- [45] YACKEL, E. C. and KENYON, W. O. The Oxidation of Cellulose by Nitrogen Dioxide. *Journal of the American Chemical Society*. 1942. Vol. 64, no. 1, p. 121–127. DOI 10.1021/ja01253a032.
- [46] PAINTER, T. J. Preparation and periodate oxidation of C-6-oxycellulose: conformational interpretation of hemiacetal stability. *Carbohydrate Research*. 1977. Vol. 55, no. 1, p. 95–103. DOI 10.1016/S0008-6215(00)84446-8.
- [47] CHANG, P. S. and ROBYT, J. F. Oxidation of Primary Alcohol Groups of Naturally Occurring Polysaccharides with 2,2,6,6-Tetramethyl-1-Piperidine Oxoammonium Ion. *Journal of Carbohydrate Chemistry*. 1996. Vol. 15, no. 7, p. 819–830. DOI 10.1080/07328309608005694.
- [48] DE NOOY, A. E. J., BESEMER, A. C. and VAN BEKKUM, H. Highly selective TEMPO mediated oxidation of primary alcohol groups in polysaccharides. *Recueil des Travaux Chimiques des Pays-Bas*. 2010. Vol. 113, no. 3, p. 165–166. DOI 10.1002/recl.19941130307.
- [49] BOSSO, C., DEFAYE, J., GADELLE, A., WONG, Ch. Ch. and PEDERSEN, Ch. Homopolysaccharides interaction with the dimethyl sulphoxide-paraformaldehyde cellulose solvent system. Selective oxidation of amylose and cellulose at secondary alcohol groups. *Journal of the Chemical Society, Perkin Transactions 1*. 1982. No. 0, p. 1579–1585. DOI 10.1039/P19820001579.
- [50] ZHANG, H. and PARK, S.-M. Kinetic studies on the oxidation of cellulose and its model compounds by Mn(III). *Carbohydrate Research*. 1995. Vol. 266, no. 1, p. 129–142. DOI 10.1016/0008-6215(94)00259-I.
- [51] PIERCE, A., WILSON, D. and WIEBKIN, O. Surgicel®: Macrophage processing of the fibrous component. *International Journal of Oral and*

Maxillofacial Surgery. 1987. Vol. 16, no. 3, p. 338–345. DOI 10.1016/S0901-5027(87)80156-X.

- [52] DOMB, A. J., KOST, J. and WISEMAN, D. M. (eds.). *Handbook of biodegradable polymers*. Amsterdam : Harwood Academic Publishers, 1997. ISBN 978-90-5702-153-4.
- [53] BOGAN, D., MOORE, J. and SCHMIDT, R. Use of oxidized cellulose as free radical scavenger. EP1153618A1. 2001.
- [54] WATT, P. W., HARVEY, W., WISEMAN, D., LIGHT, N., SAFERSTEIN, L. and CINI, J. Use of oxidized cellulose and complexes thereof for chronic wound healing. EP0918548. 2003.
- [55] MILICHOVSKY, M. and MILICHOVSKA, S. Characterization of oxidized cellulose with ultraviolet-visible spectroscopy. *Journal of Applied Polymer Science*. 2008. Vol. 107, no. 3, p. 2045–2052. DOI 10.1002/app.27232.
- [56] BANKER, G. S. and KUMAR, V. Microfibrillated oxycellulose. US5405953A. 1995.
- [57] CULLEN, B., WATT, P. W., LUNDQVIST, Ch., SILCOCK, D., SCHMIDT, R. J, BOGAN, D. and LIGHT, N. D. The role of oxidised regenerated cellulose/collagen in chronic wound repair and its potential mechanism of action. *The International Journal of Biochemistry & Cell Biology*. 2002. Vol. 34, no. 12, p. 1544–1556. DOI 10.1016/S1357-2725(02)00054-7.
- [58] SCHONAUER, C., TESSITORE, E., BARBAGALLO, G., ALBANESE, V. and MORACI, A. The use of local agents: bone wax, gelatin, collagen, oxidized cellulose. *European Spine Journal*. 2004. Vol. 13, no. 1, p. 89–96. DOI 10.1007/s00586-004-0727-z.
- [59] BAJEROVÁ, M., KREJČOVÁ, K., RABIŠOVÁ, M., GAJDZIOK, J. and MASTEIKOVÁ, R. Oxycellulose: Significant characteristics in relation to its pharmaceutical and medical applications. *Advances in Polymer Technology*. 2009. Vol. 28, no. 3, p. 199–208. DOI 10.1002/adv.20161.
- [60] HART, J., SILCOCK, D., GUNNIGLE, S., CULLEN, B., LIGHT, N. D. and WATT, P. W. The role of oxidised regenerated cellulose/collagen in wound repair: effects in vitro on fibroblast biology and in vivo in a model of compromised healing. *The International Journal of Biochemistry & Cell Biology*. 2002. Vol. 34, no. 12, p. 1557–1570. DOI 10.1016/S1357-2725(02)00062-6.

- [61] JESCHKE, M. G., SANDMANN, G., SCHUBERT, T. and KLEIN, D. Effect of oxidized regenerated cellulose/collagen matrix on dermal and epidermal healing and growth factors in an acute wound. *Wound Repair and Regeneration*. 2005. Vol. 13, no. 3, p. 324–331. DOI 10.1111/j.1067-1927.2005.130316.x.
- [62] JELÍNKOVÁ, M., BRIESTENSKÝ, J., SANTAR, I. and ŘÍHOVÁ, B. In vitro and in vivo immunomodulatory effects of microdispersed oxidized cellulose. *International Immunopharmacology*. 2002. Vol. 2, no. 10, p. 1429–1441. DOI 10.1016/S1567-5769(02)00087-5.
- [63] SHELEG, S. V., KOROTKEVICH, E. A., ZHAVRID, Edvard A., MURAVSKAYA, G. V., SMEYANOVICH, A. F., SHANKO, Y. G., YURKSHTOVICH, T. L., BYCHKOVSKY, P. B. and BELYAEV, S. A. Local chemotherapy with cisplatin-depot for glioblastoma multiforme. *Journal of Neuro-Oncology*. 2002. Vol. 60, no. 1, p. 53–59. PMID: 12416546.
- [64] GERT, E. V., TORGASHOV, V. I., ZUBETS, O. V. and KAPUTSKII, F. N. Combination of oxidative and hydrolytic functions of nitric acid in production of enterosorbents based on carboxylated microcrystalline cellulose. *Russian Journal of Applied Chemistry*. 2006. Vol. 79, no. 11, p. 1896–1901. DOI 10.1134/S1070427206110309.
- [65] TURKOVÁ, J., VAJČNER, J., VANČUROVÁ, D. and ŠTAMBERG, J. Immobilization on cellulose in bead form after periodate oxidation and reductive alkylation. *Collection of Czechoslovak Chemical Communications*. 1979. Vol. 44, no. 11, p. 3411–3417. DOI 10.1135/cccc19793411.
- [66] VALENTOVÁ, O., MAREK, M., ŠVEC, F., ŠTAMBERG, J. and VODRÁŽKA, Z. Comparison of different methods of glucose oxidase immobilization: Glucose oxidase immobilization. *Biotechnology and Bioengineering*. 1981. Vol. 23, no. 9, p. 2093–2104. DOI 10.1002/bit.260230913.
- [67] BALA, K., GUHA, S. K. and VASUDEVAN, P. p-Amino salicylic acid — oxidized cellulose system: a model for long term drug delivery. *Biomaterials*. 1982. Vol. 3, no. 2, p. 97–100. DOI 10.1016/0142-9612(82)90041-2.
- [68] KUMAR, V. and YANG, D. Oxidized cellulose esters: I. Preparation and characterization of oxidized cellulose acetates — a new class of biodegradable polymers. *Journal of Biomaterials Science, Polymer Edition*. 2002. Vol. 13, no. 3, p. 273–286. DOI 10.1163/156856202320176529.

- [69] ZHU, L., KUMAR, V. and BANKER, G. S. Examination of aqueous oxidized cellulose dispersions as a potential drug carrier. I. Preparation and characterization of oxidized cellulose-phenylpropanolamine complexes. *American Association of Pharmaceutical Scientists*. 2004. Vol. 5, no. 4, p. 138–144. DOI 10.1208/pt050469.
- [70] ZIMNITSKY, D. S., YURKSHTOVICH, T. L. and BYCHKOVSKY, P. M. Multilayer adsorption of amino acids on oxidized cellulose. *Journal of Colloid and Interface Science*. 2005. Vol. 285, no. 2, p. 502–508. DOI 10.1016/j.jcis.2004.12.021.
- [71] MATSUMURA, S., NISHIOKA, M., SHIGENO, H., TANAKA, T. and YOSHIKAWA, S. Builder performance in detergent formulations and biodegradability of partially dicarboxylated cellulose and amylose containing sugar residues in the backbone. *Macromolecular Materials and Engineering*. 1993. Vol. 205, no. 1, p. 117–129. DOI 10.1002/apmc.1993.052050110.
- [72] ROWEN, J. W., FORZIATI, F. H. and REEVES, R. E. Spectrophotometric Evidence for the Absence of Free Aldehyde Groups in Periodate-oxidized Cellulose. *Journal of the American Chemical Society*. 1951. Vol. 73, no. 9, p. 4484–4487. DOI 10.1021/ja01153a535.
- [73] SPEDDING, H. Infrared spectra of periodate-oxidised cellulose. *Journal of the Chemical Society (Resumed)*. 1960. P. 3147–3152. DOI 10.1039/jr9600003147.
- [74] CREMONESI, P., DANGIURO, L. and FOCHER, B. Cellulose fibers modification by synthetic polymers grafting. *Chimica & L Industria*. 1972. Vol. 54, no. 10, p. 871.
- [75] BOBBITT, J. M. Periodate Oxidation of Carbohydrates. In : *Advances in Carbohydrate Chemistry*. New York : Academic Press, 1956. ISBN 978-0-12-007211-8.
- [76] WHISTLER, R. L., WOLFROM, M. L. and BEMILLER, J. N. (eds.). *Cellulose*. New York : Academic Press, 1963. ISBN 978-0-12-746203-5.
- [77] HEATH, H. D., HOFREITER, B. T. and ERNST, A. J. Method of making nongelling aqueous cationic dialdehyde starch compositions. US4001032A. 1977.
- [78] YU, J., CHANG, P. R. and MA, X. The preparation and properties of dialdehyde starch and thermoplastic dialdehyde starch. *Carbohydrate Polymers*. 2010. Vol. 79, no. 2, p. 296–300. DOI 10.1016/j.carbpol.2009.08.005.

- [79] KIM, U.-J., KUGA, S., WADA, M., OKANO, T. and KONDO, T. Periodate oxidation of crystalline cellulose. *Biomacromolecules*. 2000. Vol. 1, no. 3, p. 488–492. DOI 10.1021/bm0000337.
- [80] RAHN, K. and HEINZE, T. New cellulosic polymers by subsequent modification of 2,3-dialdehyde cellulose. *Cellulose Chemistry and Technology*. 1998. Vol. 32, no. 3–4, p. 173–183.
- [81] POMMERENING, K., REIN, H., BERTRAM, D. and MÜLLER, R. Estimation of dialdehyde groups in 2,3-dialdehyde bead-cellulose. *Carbohydrate Research*. 1992. Vol. 233, p. 219–223. DOI 10.1016/S0008-6215(00)90933-9.
- [82] MAEKAWA, E. and KOSHIJIMA, T. Preparation and structural consideration of nitrogen-containing derivatives obtained from dialdehyde celluloses. *Journal of Applied Polymer Science*. 1991. Vol. 42, no. 1, p. 169–178. DOI 10.1002/app.1991.070420120.
- [83] PRINCI, E., VICINI, S., PEDEMONTE, E., PROIETTI, N., CAPITANI, D., SEGRE, A. L., D’ORAZIO, L., GENTILE, G., POLCARO, C. and MARTUSCELLI, E. Physical and Chemical Characterization of Cellulose Based Textiles Modified by Periodate Oxidation. *Macromolecular Symposia*. 2001. Vol. 169, no. 1, p. 343–352. DOI 10.1002/masy.200451435.
- [84] VICINI, S., PRINCI, E., LUCIANO, G., FRANCESCHI, E., PEDEMONTE, E., OLDAK, D., KACZMAREK, H. and SIONKOWSKA, A. Thermal analysis and characterisation of cellulose oxidised with sodium metaperiodate. *Thermochimica Acta*. 2004. Vol. 418, no. 1–2, p. 123–130. DOI 10.1016/j.tca.2003.11.049.
- [85] JANJIĆ, S., KOSTIĆ, M., ŠKUNDRIĆ, P., LAZIĆ, B. and PRASKALO, J. Antibacterial fibers based on cellulose and chitosan. *Contemporary Materials*. 2013. Vol. 2, no. 3. DOI 10.7251/COMEN1202207J.
- [86] VARMA, A. J. and KULKARNI, M. P. Oxidation of cellulose under controlled conditions. *Polymer Degradation and Stability*. 2002. Vol. 77, no. 1, p. 25–27. DOI 10.1016/S0141-3910(02)00073-3.
- [87] HON, D. N.-S. (ed.). *Chemical modification of lignocellulosic materials*. New York : M. Dekker, 1996. ISBN 978-0-8247-9472-9.
- [88] CALVINI, P., CONIO, G., PRINCI, E., VICINI, S. and PEDEMONTE, E. Viscometric determination of dialdehyde content in periodate oxycellulose Part II. Topochemistry of oxidation. *Cellulose*. 2006. Vol. 13, no. 5, p. 571–579. DOI 10.1007/s10570-005-9035-y.

- [89] PAINTER, T. J. Control of depolymerisation during the preparation of reduced dialdehyde cellulose. *Carbohydrate Research*. 1988. Vol. 179, p. 259–268. DOI 10.1016/0008-6215(88)84123-5.
- [90] LINDH, J., CARLSSON, D. O., STRØMME, M. and MIHRANYAN, A. Convenient One-Pot Formation of 2,3-Dialdehyde Cellulose Beads via Periodate Oxidation of Cellulose in Water. *Biomacromolecules*. 2014. Vol. 15, no. 5, p. 1928–1932. DOI 10.1021/bm5002944.
- [91] MÜNSTER, L., VÍCHA, J., KLOFÁČ, J., MASAR, M., HURAJOVÁ, A. and KUŘITKA, I. Dialdehyde Cellulose Crosslinked Poly(vinyl alcohol) Hydrogels: Influence of Catalyst and Crosslinker Shelf Life. *Carbohydrate Polymers*. 2018. under review
- [92] LIIMATAINEN, H., SIRVIÖ, J. A., PAJARI, H., HORMI, O. and NIINIMÄKI, J. Regeneration and Recycling of Aqueous Periodate Solution in Dialdehyde Cellulose Production. *Journal of Wood Chemistry and Technology*. 2013. Vol. 33, no. 4, p. 258–266. DOI 10.1080/02773813.2013.783076.
- [93] KOPRIVICA, S., SILLER, M., HOSOYA, T., ROGGENSTEIN, W., ROSENAU, T. and POTTHAST, A. Regeneration of Aqueous Periodate Solutions by Ozone Treatment: A Sustainable Approach for Dialdehyde Cellulose Production. *ChemSusChem*. 2016. Vol. 9, no. 8, p. 825–833. DOI 10.1002/cssc.201501639.
- [94] LISTER, M. W. and ROSENBLUM, P. The Oxidation of Nitrite and Iodate Ions by Hypochlorite Ions. *Canadian Journal of Chemistry*. 1961. Vol. 39, no. 8, p. 1645–1651. DOI 10.1139/v61-211.
- [95] SIRVIÖ, J. A., HYVAKKO, U., LIIMATAINEN, H., NIINIMÄKI, J. and HORMI, O. Periodate oxidation of cellulose at elevated temperatures using metal salts as cellulose activators. *Carbohydrate Polymers*. 2011. Vol. 83, no. 3, p. 1293–1297. DOI 10.1016/j.carbpol.2010.09.036.
- [96] SIRVIÖ, J. A., LIIMATAINEN, H., NIINIMÄKI, J. and HORMI, O. Dialdehyde cellulose microfibers generated from wood pulp by milling-induced periodate oxidation. *Carbohydrate Polymers*. 2011. Vol. 86, no. 1, p. 260–265. DOI 10.1016/j.carbpol.2011.04.054.
- [97] KIM, U.-J., WADA, M. and KUGA, S. Solubilization of dialdehyde cellulose by hot water. *Carbohydrate Polymers*. 2004. Vol. 56, no. 1, p. 7–10. DOI 10.1016/j.carbpol.2003.10.013.

- [98] SULAEVA, I., KLINGER, K. M., AMER, H., HENNIGES, U., ROSENAU, T. and POTTHAST, A. Determination of molar mass distributions of highly oxidized dialdehyde cellulose by size exclusion chromatography and asymmetric flow field-flow fractionation. *Cellulose*. 2015. Vol. 22, no. 6, p. 3569–3581. DOI 10.1007/s10570-015-0769-x.
- [99] MÜNSTER, L., VÍCHA, J., KLOFÁČ, J., MASAŘ, M., KUCHARCZYK, P. and KUŘITKA, I. Stability and aging of solubilized dialdehyde cellulose. *Cellulose*. 2017. Vol. 24, no. 7, p. 2753–2766. DOI 10.1007/s10570-017-1314-x.
- [100] VEELAERT, S., DE WIT, D., GOTLIEB, K.F. and VERHÉ, R. Chemical and physical transitions of periodate oxidized potato starch in water. *Carbohydrate Polymers*. June 1997. Vol. 33, no. 2–3, p. 153–162. DOI 10.1016/S0144-8617(97)00046-5.
- [101] KIM, U.-J. and KUGA, S. Thermal decomposition of dialdehyde cellulose and its nitrogen-containing derivatives. *Thermochimica Acta*. 2001. Vol. 369, no. 1–2, p. 79–85. DOI 10.1016/S0040-6031(00)00734-6.
- [102] JAIN, R. K., LAL, K. and BHATNAGAR, H. L. Thermal, morphological and spectroscopic studies on cellulose modified with phosphorus, nitrogen, sulphur and halogens. *Journal of Applied Polymer Science*. 1987. Vol. 33, no. 2, p. 247–282. DOI 10.1002/app.1987.070330201.
- [103] NADA, A. M. A. and HASSAN, M. L. Thermal behavior of cellulose and some cellulose derivatives. *Polymer Degradation and Stability*. 2000. Vol. 67, no. 1, p. 111–115. DOI 10.1016/S0141-3910(99)00100-7.
- [104] SIRVIÖ, J. A., LIIMATAINEN, H., VISANKO, M. and NIINIMÄKI, J. Optimization of dicarboxylic acid cellulose synthesis: reaction stoichiometry and role of hypochlorite scavengers. *Carbohydrate Polymers*. 2014. Vol. 114, p. 73–77. DOI 10.1016/j.carbpol.2014.07.081.
- [105] POTTHAST, A., SCHIEHSER, S., ROSENAU, T. and KOSTIC, M. Oxidative modifications of cellulose in the periodate system – Reduction and beta-elimination reactions. *Holzforschung*. 2009. Vol. 63, p. 12–17. DOI 10.1515/HF.2008.109.
- [106] BOEDEN, H.-F., POMMERENING, K., BECKER, M., RUPPRICH, C., HOLTZHAUER, M., LOTH, F., MÜLLER, R. and BERTRAM, D. Bead cellulose derivatives as supports for immobilization and chromatographic purification of proteins. *Journal of Chromatography A*. 1991. Vol. 552, p. 389–414. DOI 10.1016/S0021-9673(01)95956-4.

- [107] KIM, U.-J. and KUGA, S. Ion-exchange chromatography by dicarboxyl cellulose gel. *Journal of Chromatography A*. 2001. Vol. 919, no. 1, p. 29–37. DOI 10.1016/S0021-9673(01)00800-7.
- [108] KIM, U.-J. and KUGA, S. Ion-exchange separation of proteins by polyallylamine-grafted cellulose gel. *Journal of Chromatography A*. 2002. Vol. 955, no. 2, p. 191–196. DOI 10.1016/S0021-9673(02)00246-7.
- [109] CRESCENZI, V., DENTINI, M., MEOLI, C., CASU, B., NAGGI, A. and TORRI, G. Dicarboxyamyllose and dicarboxycellulose, stereoregular polyelectrolytes: binding of calcium and magnesium ions. *International Journal of Biological Macromolecules*. 1984. Vol. 6, no. 3, p. 142–144. DOI 10.1016/0141-8130(84)90055-2.
- [110] TAPLEY, K. N. and LEWIS, D. M. Periodate oxidized cellulose for dyeing with alkylamino dyes. *Textile Chemist and Colorist*. 1999. Vol. 5, p. 20–26.
- [111] SIRVIÖ, J. A., HONKA, A., LIIMATAINEN, H., NIINIMÄKI, J. and HORMI, O. Synthesis of highly cationic water-soluble cellulose derivative and its potential as novel biopolymeric flocculation agent. *Carbohydrate Polymers*. 2011. Vol. 86, no. 1, p. 266–270. DOI 10.1016/j.carbpol.2011.04.046.
- [112] GURVICH, A. E. and LECHTZIND, E. V. High capacity immunoadsorbents based on preparations of reprecipitated cellulose. *Molecular Immunology*. 1982. Vol. 19, no. 4, p. 637–640. DOI 10.1016/0161-5890(82)90233-4.
- [113] VARAVINIT, S., CHAOKASEM, N. and SHOBSNGOB, S. Covalent immobilization of a glucoamylase to bagasse dialdehyde cellulose. *World Journal of Microbiology and Biotechnology*. 2001. Vol. 17, no. 7, p. 721–725. DOI 10.1023/A:1012984802624.
- [114] ANIULYTE, J., LIESIENE, J. and NIEMEYER, B. Evaluation of cellulose-based biospecific adsorbents as a stationary phase for lectin affinity chromatography. *Journal of Chromatography B*. 2006. Vol. 831, no. 1–2, p. 24–30. DOI 10.1016/j.jchromb.2005.11.016.
- [115] WOLF, B. and FINKE, I. The use of bead celluloses as carrier for controlled liberation of drugs . Part 5: Binding of benzocaine as a model-drug to dialdehyde bead cellulose and its invitro liberation. *Pharmazie*. 1992. Vol. 47, no. 2, p. 121–125. PMID: 1635919.

- [116] LIU, X. D., NISHI, N., TOKURA, S. and SAKAIRI, N. Chitosan coated cotton fiber: preparation and physical properties. *Carbohydrate Polymers*. 2001. Vol. 44, no. 3, p. 233–238. DOI 10.1016/S0144-8617(00)00206-X.
- [117] DASH, R. and RAGAUSKAS, A. J. Synthesis of a novel cellulose nanowhisiker-based drug delivery system. *RSC Advances*. 2012. Vol. 2, no. 8, p. 3403–3409. DOI 10.1039/c2ra01071b.
- [118] LI, J., WAN, Y., LI, L., LIANG, H. and WANG, J. Preparation and characterization of 2,3-dialdehyde bacterial cellulose for potential biodegradable tissue engineering scaffolds. *Materials Science and Engineering: C*. 2009. Vol. 29, no. 5, p. 1635–1642. DOI 10.1016/j.msec.2009.01.006.
- [119] DASH, R., ELDER, T. and RAGAUSKAS, A. J. Grafting of model primary amine compounds to cellulose nanowhiskers through periodate oxidation. *Cellulose*. 2012. Vol. 19, no. 6, p. 2069–2079. DOI 10.1007/s10570-012-9769-2.
- [120] KIM, U.-J., LEE, Y. R., KANG, T. H., CHOI, J. W., KIMURA, S. and WADA, M. Protein adsorption of dialdehyde cellulose-crosslinked chitosan with high amino group contents. *Carbohydrate Polymers*. 2017. Vol. 163, p. 34–42. DOI 10.1016/j.carbpol.2017.01.052.
- [121] KIM, U.-J., KIM, H. J., CHOI, J. W., KIMURA, S. and WADA, M. Cellulose-chitosan beads crosslinked by dialdehyde cellulose. *Cellulose*. 2017. Vol. 24, no. 12, p. 5517–5528. DOI 10.1007/s10570-017-1528-y.
- [122] CASU, B., NAGGI, A., TORRI, G., ALLEGRA, G., MEILLE, S. V., COSANI, A. and TERBOJEVICH, M. Stereoregular acyclic polyalcohols and polyacetates from cellulose and amylose. *Macromolecules*. 1985. Vol. 18, no. 12, p. 2762–2767. DOI 10.1021/ma00154a068.
- [123] MAEKAWA, E. Analysis of oxidized moiety of partially periodate-oxidized cellulose by NMR spectroscopy. *Journal of Applied Polymer Science*. 1991. Vol. 43, no. 3, p. 417–422. DOI 10.1002/app.1991.070430301.
- [124] HOU, Q. X., LIU, W., LIU, Z. H. and BAI, L. L. Characteristics of Wood Cellulose Fibers Treated with Periodate and Bisulfite. *Industrial & Engineering Chemistry Research*. 2007. Vol. 46, no. 23, p. 7830–7837. DOI 10.1021/ie0704750.
- [125] WEBER, V., ETTENAUER, M., LINSBERGER, I., LOTH, F., THÜMMLER, K., FELDNER, A., FISCHER, S. and FALKENHAGEN, D. Functionalization and Application of Cellulose Microparticles as Adsorbents

- in Extracorporeal Blood Purification. *Macromolecular Symposia*. 2010. Vol. 294, no. 2, p. 90–95. DOI 10.1002/masy.200900042.
- [126] HOU, Q., LIU, W., LIU, Z., DUAN, B. and BAI, L. Characteristics of antimicrobial fibers prepared with wood periodate oxycellulose. *Carbohydrate Polymers*. 2008. Vol. 74, no. 2, p. 235–240. DOI 10.1016/j.carbpol.2008.02.010.
- [127] FARRIS, S., SCHAICH, K. M., LIU, L., PIERGIOVANNI, L. and YAM, K. L. Development of polyion-complex hydrogels as an alternative approach for the production of bio-based polymers for food packaging applications: a review. *Trends in Food Science & Technology*. 2009. Vol. 20, no. 8, p. 316–332. DOI 10.1016/j.tifs.2009.04.003.
- [128] GULREZ, S. K. H., AL-ASSAF, S. and PHILLIPS, Glyn O. Hydrogels: Methods of Preparation, Characterisation and Applications. In : CARPI, A. (ed.), *Progress in Molecular and Environmental Bioengineering - From Analysis and Modeling to Technology Applications*. InTech, 2011. ISBN 978-953-307-268-5.
- [129] QUEIROZ, A. Adsorption and release studies of sodium ampicillin from hydroxyapatite and glass-reinforced hydroxyapatite composites. *Biomaterials*. 2001. Vol. 22, no. 11, p. 1393–1400. DOI 10.1016/S0142-9612(00)00296-9.
- [130] LIM, F. and SUN, A. M. Microencapsulated islets as bioartificial endocrine pancreas. *Science*. 1980. Vol. 210, no. 4472, p. 908–910. PMID: 6776628.
- [131] YANNAS, I. V., BURKE, J. F., ORGILL, D. P. and SKRABUT, E. M. Method of Promoting the Regeneration of Tissue at a Wound. US4418691A. 1983.
- [132] PEPPAS, N. A. (ed.). *Hydrogels in medicine and pharmacy*. Boca Raton : CRC Press, 1986. ISBN 978-0-8493-5546-2.
- [133] PEPPAS, N. A. and MERRILL, E. W. Poly(vinyl alcohol) hydrogels: Reinforcement of radiation-crosslinked networks by crystallization. *Journal of Polymer Science: Polymer Chemistry Edition*. 1976. Vol. 14, no. 2, p. 441–457. DOI 10.1002/pol.1976.170140215.
- [134] ROSIAK, J. M. and YOSHII, F. Hydrogels and their medical applications. *Nuclear Instruments and Methods in Physics Research Section B: Beam Interactions with Materials and Atoms*. 1999. Vol. 151, no. 1–4, p. 56–64. DOI 10.1016/S0168-583X(99)00118-4.

- [135] HENNINK, W. E. and VAN NOSTRUM, C. F. Novel crosslinking methods to design hydrogels. *Advanced Drug Delivery Reviews*. 2002. Vol. 54, no. 1, p. 13–36. PMID: 11755704.
- [136] YAHIA, L. History and Applications of Hydrogels. *Journal of Biomedical Sciences*. 2015. Vol. 4, no. 2. DOI 10.4172/2254-609X.100013.
- [137] FAZEL, R. (ed.). *Biomedical Engineering - Frontiers and Challenges*. InTech, 2011. ISBN 978-953-307-309-5.
- [138] HICKEY, A. S. and PEPPAS, N. A. Mesh size and diffusive characteristics of semicrystalline poly(vinyl alcohol) membranes prepared by freezing/thawing techniques. *Journal of Membrane Science*. 1995. Vol. 107, no. 3, p. 229–237. DOI 10.1016/0376-7388(95)00119-0.
- [139] KATZ, M. G. and WYDEVEN, T. Selective permeability of PVA membranes. II. Heat-treated membranes. *Journal of Applied Polymer Science*. 1982. Vol. 27, no. 1, p. 79–87. DOI 10.1002/app.1982.070270109.
- [140] CHEN, C. T., CHANG, Y. J., CHEN, M. C. and TOBOLSKY, A. V. Formalized poly(vinyl alcohol) membranes for reverse osmosis. *Journal of Applied Polymer Science*. 1973. Vol. 17, no. 3, p. 789–796. DOI 10.1002/app.1973.070170311.
- [141] BOLTO, B. A., EPPINGER, K., MACPHERSON, A. S., SIUDAK, R., WEISS, D. E. and WILLIS, D. An ion exchange process with thermal regeneration IX. A new type of rapidly reacting ion-exchange resin. *Desalination*. 1973. Vol. 13, no. 3, p. 269–285. DOI 10.1016/S0011-9164(00)80056-9.
- [142] JIAN, S. and XIAO MING, S. Crosslinked PVA-PS thin-film composite membrane for reverse osmosis. *Desalination*. 1987. Vol. 62, p. 395–403. DOI 10.1016/0011-9164(87)87040-6.
- [143] HAN, B., LI, J., CHEN, C., XU, C. and WICKRAMASINGHE, S.R. Effects of Degree of Formaldehyde Acetal Treatment and Maleic Acid Crosslinking on Solubility and Diffusivity of Water in PVA Membranes. *Chemical Engineering Research and Design*. 2003. Vol. 81, no. 10, p. 1385–1392. DOI 10.1205/026387603771339609.
- [144] URAGAMI, T., OKAZAKI, K., MATSUGI, H. and MIYATA, T. Structure and Permeation Characteristics of an Aqueous Ethanol Solution of Organic-Inorganic Hybrid Membranes Composed of Poly(vinyl alcohol) and Tetraethoxysilane. *Macromolecules*. 2002. Vol. 35, no. 24, p. 9156–9163. DOI 10.1021/ma020850u.

- [145] DICK, R. and NICOLAS, L. Membranes composites preparees a partir d'alcool polyvinylique et de diisocyanate de toluylene destinees a l'osmose inverse. *Desalination*. 1975. Vol. 17, no. 3, p. 239–255. DOI 10.1016/S0011-9164(00)84059-X.
- [146] MATEESCU, M. A., SCHELL, H. D., DIMONIE, M., TODIREANU, S. and MAIOR, O. Some peculiar properties of cross-linked polyvinyl alcohol (CL-PVA) related to the reticulation degree. *Polymer Bulletin*. 1984. Vol. 11, no. 5, p. 421–427. DOI 10.1007/BF00265481.
- [147] XIAO, S., HUANG, R. Y.M. and FENG, X. Preparation and properties of trimesoyl chloride crosslinked poly(vinyl alcohol) membranes for pervaporation dehydration of isopropanol. *Journal of Membrane Science*. 2006. Vol. 286, no. 1–2, p. 245–254. DOI 10.1016/j.memsci.2006.09.042.
- [148] FLORY, P. J. and REHNER, J. Statistical Mechanics of Crosslinked Polymer Networks II. Swelling. *The Journal of Chemical Physics*. 1943. Vol. 11, no. 11, p. 521–526. DOI 10.1063/1.1723792.
- [149] TIGHE, B. J. The Role of Permeability and Related Properties in the Design of Synthetic Hydrogels for Biomedical Applications. *British Polymer Journal*. 1986. Vol. 18, no. 1, p. 8–13. DOI 10.1002/pi.4980180104.
- [150] PEPPAS, N. A., HUANG, Y., TORRES-LUGO, M., WARD, J. H. and ZHANG, J. Physicochemical foundations and structural design of hydrogels in medicine and biology. *Annual Review of Biomedical Engineering*. 2000. Vol. 2, p. 9–29. DOI 10.1146/annurev.bioeng.2.1.9. PMID: 11701505.
- [151] OMIDIAN, H., HASHERNI, S.-A., ASKARI, F. and NAFISI, S. Swelling and Crosslink Density Measurements for Hydrogels. *Iranian Journal of Polymer Science and Technology*. 1994. Vol. 3, no. 2, p. 115–119.
- [152] GONZALEZ, J. S., LUDUEÑA, L. N., PONCE, A. and ALVAREZ, V. A. Poly(vinyl alcohol)/cellulose nanowhiskers nanocomposite hydrogels for potential wound dressings. *Materials Science and Engineering: C*. 2014. Vol. 34, p. 54–61. DOI 10.1016/j.msec.2013.10.006.
- [153] KAMOUN, E. A., KENAWY, E.-R. S., TAMER, T. M., EL-MELIGY, M. A. and MOHY ELDIN, M. S. Poly (vinyl alcohol)-alginate physically crosslinked hydrogel membranes for wound dressing applications: Characterization and bio-evaluation. *Arabian Journal of Chemistry*. 2015. Vol. 8, no. 1, p. 38–47. DOI 10.1016/j.arabjc.2013.12.003.
- [154] ZHANG, D., ZHOU, W., WEI, B., WANG, X., TANG, R., NIE, J. and WANG, J. Carboxyl-modified poly(vinyl alcohol)-crosslinked chitosan

- hydrogel films for potential wound dressing. *Carbohydrate Polymers*. 2015. Vol. 125, p. 189–199. DOI 10.1016/j.carbpol.2015.02.034.
- [155] TANG, J., BAO, L., LI, X., CHEN, L. and HONG, F. F. Potential of PVA-doped bacterial nano-cellulose tubular composites for artificial blood vessels. *Journal of Materials Chemistry B*. 2015. Vol. 3, no. 43, p. 8537–8547. DOI 10.1039/C5TB01144B.
- [156] LI, C., SHE, M., SHE, X., DAI, J. and KONG, L. Functionalization of polyvinyl alcohol hydrogels with graphene oxide for potential dye removal. *Journal of Applied Polymer Science*. 2014. Vol. 131, no. 3, p. 39872–39880. DOI 10.1002/app.39872.
- [157] HUI, B., ZHANG, Y. and YE, L. Structure of PVA/gelatin hydrogel beads and adsorption mechanism for advanced Pb(II) removal. *Journal of Industrial and Engineering Chemistry*. 2015. Vol. 21, p. 868–876. DOI 10.1016/j.jiec.2014.04.025.
- [158] HUI, B., ZHANG, Y. and YE, L. Preparation of PVA hydrogel beads and adsorption mechanism for advanced phosphate removal. *Chemical Engineering Journal*. 2014. Vol. 235, p. 207–214. DOI 10.1016/j.cej.2013.09.045.
- [159] TOU, Z. Q., KOH, T. W. and CHAN, C. C. Poly(vinyl alcohol) hydrogel based fiber interferometer sensor for heavy metal cations. *Sensors and Actuators B: Chemical*. 2014. Vol. 202, p. 185–193. DOI 10.1016/j.snb.2014.05.006.
- [160] SPOLJARIC, S., SALMINEN, A., LUONG, N. D. and SEPPÄLÄ, J. Stable, self-healing hydrogels from nanofibrillated cellulose, poly(vinyl alcohol) and borax via reversible crosslinking. *European Polymer Journal*. 2014. Vol. 56, p. 105–117. DOI 10.1016/j.eurpolymj.2014.03.009.
- [161] CHEN, Y.-N., PENG, L., LIU, T., WANG, Y., SHI, S. and WANG, H. Poly(vinyl alcohol)–Tannic Acid Hydrogels with Excellent Mechanical Properties and Shape Memory Behaviors. *ACS Applied Materials & Interfaces*. 2016. Vol. 8, no. 40, p. 27199–27206. DOI 10.1021/acsami.6b08374.
- [162] QI, X., YAO, X., DENG, S., ZHOU, T. and FU, Q. Water-induced shape memory effect of graphene oxide reinforced polyvinyl alcohol nanocomposites. *Journal of Materials Chemistry A*. 2014. Vol. 2, no. 7, p. 2240–2249. DOI 10.1039/C3TA14340F.

- [163] ZAMANI PEDRAM, M., OMIDKHAH, M. and EBADI AMOOGHIN, A. Synthesis and characterization of diethanolamine-impregnated cross-linked polyvinylalcohol/glutaraldehyde membranes for CO₂/CH₄ separation. *Journal of Industrial and Engineering Chemistry*. 2014. Vol. 20, no. 1, p. 74–82. DOI 10.1016/j.jiec.2013.04.024.
- [164] ENGEL, P., HEIN, L. and SPIESS, A. C. Derivatization-free gel permeation chromatography elucidates enzymatic cellulose hydrolysis. *Biotechnology for Biofuels*. 2012. Vol. 5, no. 1, p. 77. DOI 10.1186/1754-6834-5-77.
- [165] BOUZKOVÁ, K., BABINSKÝ, M., NOVOSADOVÁ, L. and MAREK, R. Intermolecular Interactions in Crystalline Theobromine as Reflected in Electron Deformation Density and ¹³C NMR Chemical Shift Tensors. *Journal of Chemical Theory and Computation*. 2013. Vol. 9, no. 6, p. 2629–2638. DOI 10.1021/ct400209b.
- [166] CAPITANI, D., DE ANGELIS, A. A., CRESCENZI, V., MASCI, G. and SEGRE, A. L. NMR study of a novel chitosan-based hydrogel. *Carbohydrate Polymers*. 2001. Vol. 45, no. 3, p. 245–252. DOI 10.1016/S0144-8617(00)00255-1.
- [167] VOELKEL, R. High-Resolution Solid-State¹³C-NMR Spectroscopy of Polymers. *Angewandte Chemie International Edition in English*. 1988. Vol. 27, no. 11, p. 1468–1483. DOI 10.1002/anie.198814681.
- [168] MESTER, L. The Formazan Reaction in Proving the Structure of Periodate Oxidized Polysaccharides. *Journal of the American Chemical Society*. 1955. Vol. 77, no. 20, p. 5452–5453. DOI 10.1021/ja01625a097.
- [169] BIKALES, N. M. and SEGAL, L. *Cellulose and cellulose derivatives Part IV*. New York : Wiley-Interscience, 1971. ISBN 978-0-471-39038-1.
- [170] FAN, Q. G., LEWIS, D. M. and TAPLEY, K. N. Characterization of cellulose aldehyde using Fourier transform infrared spectroscopy. *Journal of Applied Polymer Science*. 2001. Vol. 82, no. 5, p. 1195–1202. DOI 10.1002/app.1953.
- [171] RÖHRLING, J., POTTHAST, A., LANGE, T., ROSENAU, T., ADORJAN, I., HOFINGER, A. and KOSMA, P. Synthesis of oxidized methyl 4-O-methyl-β-d-glucopyranoside and methyl β-d-glucopyranosyl-(1→4)-β-d-glucopyranoside derivatives as substrates for fluorescence labeling reactions. *Carbohydrate Research*. 2002. Vol. 337, no. 8, p. 691–700. DOI 10.1016/S0008-6215(02)00048-4.

- [172] KONO, H., HASHIMOTO, H. and SHIMIZU, Y. NMR characterization of cellulose acetate: Chemical shift assignments, substituent effects, and chemical shift additivity. *Carbohydrate Polymers*. 2015. Vol. 118, p. 91–100. DOI 10.1016/j.carbpol.2014.11.004.
- [173] SILLER, M., AMER, H., BACHER, M., ROGGENSTEIN, W., ROSENAU, T. and POTTHAST, A. Effects of periodate oxidation on cellulose polymorphs. *Cellulose*. 2015. Vol. 22, no. 4, p. 2245–2261. DOI 10.1007/s10570-015-0648-5.
- [174] LAI, S., LOCCI, E., SABA, G., HUSU, I., MASCI, G., CRESCENZI, V. and LAI, A. Solid-state ¹³C and ¹²⁹Xe NMR study of poly(vinyl alcohol) and poly(vinyl alcohol)/lactosilated chitosan gels. *Journal of Polymer Science Part A: Polymer Chemistry*. 2003. Vol. 41, no. 20, p. 3123–3131. DOI 10.1002/pola.10899.
- [175] VARMA, A. J., CHAVAN, V. B., RAJMOHANAN, P. R. and GANAPATHY, S. Some observations on the high-resolution solid-state CP-MAS ¹³C-NMR spectra of periodate-oxidised cellulose. *Polymer Degradation and Stability*. 1997. Vol. 58, no. 3, p. 257–260. DOI 10.1016/S0141-3910(97)00049-9.
- [176] TERAOKA, T., MAEDA, S. and SAIKA, A. High-resolution solid-state carbon-13 NMR of poly(vinyl alcohol): enhancement of tacticity splitting by intramolecular hydrogen bonds. *Macromolecules*. 1983. Vol. 16, no. 9, p. 1535–1538. DOI 10.1021/ma00243a022.
- [177] LAI, S., CASU, M., SABA, G., LAI, A., HUSU, I., MASCI, G. and CRESCENZI, V. Solid-state ¹³C NMR study of poly(vinyl alcohol) gels. *Solid State Nuclear Magnetic Resonance*. 2002. Vol. 21, no. 3–4, p. 187–196. DOI 10.1006/snrmr.2002.0059.
- [178] GARBOW, J. R. and STARK, R. E. Nuclear magnetic resonance relaxation studies of plant polyester dynamics. 1. Cutin from limes. *Macromolecules*. 1990. Vol. 23, no. 10, p. 2814–2819. DOI 10.1021/ma00212a037.
- [179] KIM, K.-J., LEE, S.-B. and HAN, N.-W. Kinetics of crosslinking reaction of PVA membrane with glutaraldehyde. *Korean Journal of Chemical Engineering*. 1994. Vol. 11, no. 1, p. 41–47. DOI 10.1007/BF02697513.
- [180] TANG, C., SAQUING, C. D., HARDING, J. R. and KHAN, S. A. In Situ Cross-Linking of Electrospun Poly(vinyl alcohol) Nanofibers. *Macromolecules*. 2010. Vol. 43, no. 2, p. 630–637. DOI 10.1021/ma902269p.

[181] JAMNONGKAN, T., WATTANAKORNSIRI, A., WACHIRAWONGSAKORN, P. and KAEWPIROM, S. Effects of crosslinking degree of poly(vinyl alcohol) hydrogel in aqueous solution: kinetics and mechanism of copper(II) adsorption. *Polymer Bulletin*. 2014. Vol. 71, no. 5, p. 1081–1100. DOI 10.1007/s00289-014-1112-7.

LIST OF FIGURES

Figure 1 Converting operations of cellulose obtained from wood and cotton (adapted from Ott et al. 1954). [16]	8
Figure 2 Representation of cellulose constituted of cellobiose units or AGUs (with atom numbering) via β -1,4-glycosidic bonds, non-reducing and reducing end of polymer. [Own resource.].....	9
Figure 3 Allomorphs Ia and Ib of cellulose polymorph type I, chain arrangements with distances and angles for 100/010 faces. [19, 26].....	10
Figure 4 Cellulose crystal polymorphism and possible conversions between different types (left), [29] cell units for cellulose types Ib, II, III _r , IV _r . The c dimension perpendicular to the drawing is ~10.31–10.38 Å. [30]	11
Figure 5 Possible structures of oxycellulose repeating units. [33]	15
Figure 6 Mechanism of periodate oxidation of cellulose AGU. [91]	18
Figure 7 Possible structures of DAC: A – dialdehyde, B – hydrated dialdehyde, C – hemialdal, D – intramolecular hemiacetal, E – intermolecular hemiacetal.[99].....	19
Figure 8 Schiff base reaction of aldehyde groups of AGU and hydroxylamine hydrochloride with subsequent formation of oxime. [95]	20
Figure 9 Infrared spectra of DAC different degree of oxidation (D.O.). [79] ..	20
Figure 10 Dependence of degree of oxidation on X-ray diffraction profiles (left) and thermal stability. [101]	21
Figure 11 Example of dialdehyde starch degradation by the process of β -elimination. [100]	23
Figure 12 β -elimination degradation mechanism of DAC under alkaline conditions connected to the different degrees of DAC oxidation (left – lower degree of oxidation, right – higher degree of oxidation). [105]	23
Figure 13 Crosslinking reaction of PVA using glutaraldehyde. [128].....	27
Figure 14 FT-IR spectrum (part I) and TGA thermogravimetric curves (parts IIa and IIb) of uncrosslinked PVA (Mowiflex TC 232). [17]	44
Figure 15 FT-IR analysis of PVA/DAC xerogels prepared within pilot study. [17].....	45
Figure 16 TGA analysis of PVA/DAC xerogels prepared within pilot study. [17]	46
Figure 17 PVA/DAC network parameters dependence on drying temperature and used concentration of catalyst system (pilot study). The lines connecting points in the right graph are only guides for eyes.	48

Figure 18 Macroscopic observation of PVA/DAC xerogels prepared within pilot study. [17].....	48
Figure 19 Possible structural arrangements of DAC. A – dialdehyde, B – fully hydrated dialdehyde, C – hemialdal, D – intramolecular hemiacetal with C3–O–C6 bond, E – intramolecular hemiacetal with C2–O–C6 bond, F – intermolecular hemiacetal with C6–O–C3' bond, G – intermolecular hemiacetal with C6–O–C2' bond. Intermolecular hemiacetals F and G may also contain hemialdal unit C in their structure (not shown). [99].....	50
Figure 20 FT-IR spectra of source cellulose, insolubilized and solubilized-dried DAC. [17, 99].....	52
Figure 21 XRD analysis of source cellulose, insolubilized and solubilized-dried DAC. [17, 99].....	53
Figure 22 Thermogravimetric curves recorded for insolubilized DAC sample and aged solubilized-dried DAC samples. [99].....	54
Figure 23 Reactive aldehyde group content and degree of oxidation of prepared solubilized DAC estimated over period of 28 days of DAC aging. The lines connecting points in the right graph are only guides for eyes. [99].....	56
Figure 24 Possible molecular structures of DAC fragments suggested by Veelaert et al. (1997) [100] and Potthast et al. (2009) [105] observed at noted m/z values in HPLC analysis.....	58
Figure 25 Portion of ¹ H– ¹³ C HMBC (pale red) and multiplicity-edited ¹ H– ¹³ C HSQC spectra (CH signals in blue, CH ₂ signals in deep red). The ¹³ C/ ¹ H correlations for D I are highlighted in black, for G in red. [99].....	61
Figure 26 Suggested structures of D I and D II conformational isomers of DAC form D. [99].....	61
Figure 27 GPC chromatograms recorded for solubilized DAC of various age. The distribution curves are vertically shifted for better clarity. [99].....	64
Figure 28 DAC solubilization analysis scheme; step 1 – cellulose periodate oxidation resulting in insolubilized DAC suspension; step 2a – solubilization of insolubilized DAC at different initial pH setup via (i) conventional heating and (ii) microwave assisted solubilization (MWS); step 2b – chlorite oxidation of aliquot part of insolubilized DAC in order to estimate its \bar{M}_w . [99].....	68
Figure 29 Schematic representation of DAC solubilization with the respect to its time, size of insolubilized DAC phase and size of macromolecular fragments.	70
Figure 30 SEM micrographs of original cellulose and insolubilized DAC.	73

Figure 31 SEM micrographs of solid DAC phase during solubilization (initial pH 3.5).....	74
Figure 32 SEM micrographs of solid DAC phase during solubilization (initial pH 5).....	74
Figure 33 SEM micrographs of solid DAC phase during solubilization (initial pH 6).....	75
Figure 34 SEM micrographs of solid DAC phase during solubilization (initial pH 7.5).....	75
Figure 35 SEM micrographs of lyophilised products of solubilization via conventional heating carried out under different initial pH.	76
Figure 36 SEM micrographs of lyophilised products of MWS (one hour heating) carried out under different initial pH.	77
Figure 37 TGA analysis of untreated input PVA (Mowiflex) and examples of PVA/DAC xerogels (washed and unwashed) prepared using fresh DAC and two different types of acidic catalyst.....	79
Figure 38 Examples of stress vs. strain curve of untreated input PVA and PVA/DAC, please note the x-axis scale difference between the upper and lower graph panel (left); evolution of Young's modulus E of washed PVA/DAC dependent on DAC age (right). [91]	80
Figure 39 Diffractograms of input materials (left) and PVA/DAC samples from B series (right). [91]	82
Figure 40 The CP/MAS ^{13}C NMR spectra of PVA and selected PVA/DAC xerogels (left), comparison of PVA/DAC xerogels ^{13}C NMR spectra of samples prepared using various catalyst systems and DAC solution of different age (right). [91].....	84
Figure 41 Influence of DAC age used for crosslinking on the network parameters of prepared PVA/DAC hydrogels. The graphs show percentage of swelling, equilibrium water content (EWC), gel fraction, average molecular weight between crosslinks (\bar{M}_c) and crosslink density (ρ_c) of both prepared series of PVA/DAC samples crosslinked by fresh and aged DAC. The lines connecting points in the graphs are only guides for eyes. [91]	87
Figure 42 Decrease of reactive aldehyde group with DAC aging (top left); correlation between \bar{M}_n of DAC in solutions of various age (Münster et al., 2017) and $T_{1\rho}(^{13}\text{C})$ values of resulting PVA/DAC hydrogels (top right); correlation between \bar{M}_n of DAC and Young's modulus and crystallinity of PVA/DAC xerogels prepared using different catalyst system (A and B series)	

with marked age of used DAC crosslinker (bottom center). The lines connecting points in the graphs are only guides for eyes. [91, 99].....89

Figure 43 Correlation between crystallinity of PVA/DAC materials prepared using DAC of various age and carbon spin-lattice relaxation time in rotating frame, $T_{1\rho}(^{13}\text{C})$, corresponding to polymeric chain segments flexibility as obtained from NMR study. The lines connecting points in the graphs are only guides for eyes. [91].....91

Figure 44 Schematic representation of the structure of the respective xerogels within PVA/DAC series B with their relation between flexibility ($T_{1\rho}(^{13}\text{C})$), crystallinity (X), Young's modulus (E) and number average molecular weight (\bar{M}_n) of DAC. The orange coils correspond to (\bar{M}_n) of DAC, the arrays of blue lines represent polymer chain crystallites, and the grey lines represent the amorphous phase of the polymer with physical entanglements. The size, ratio, and number of depicted features is intentionally exaggerated for better understanding. [91].....92

Figure 45 Correlation between data measured by various methods for PVA/DAC prepared using aged DAC and different catalyst system. The lines connecting points in the graphs are only guides for eyes. The data points are labelled by corresponding age and number average molecular weight for one series (A) only in each graph. The second series (B) has the same order of data points from left to right always. [91]93

Figure 46 The results from comparative crosslinking study showing dependence of PVA/DAC (DTC) and PVA/GA (GTC) hydrogels network parameters on the used DAC or GA crosslinker amount defined by chemical amount of reactive aldehyde groups per sample and "Mowiflex" type of PVA. The equivalency between DAC and GA reactive group concentrations is expressed by the two bottom x-axes. The lines connecting points in the graphs are only guides for eyes. [91].....97

Figure 47 Network topology of PVA/DAC is shown in the left part. It is composed of (i) regions containing high local crosslink density adjacent to DAC macromolecules (orange) embedded in (ii) larger regions comprised of free, chemically unbound, PVA chains (grey) which can be only physically entangled. Some of these chains link the regions (i) together. The right part of the figure shows the homogeneous network topology of PVA/GA crosslinked by GA (blue). The size, ratio, and number of depicted features is intentionally exaggerated for better understanding. [91].....98

Figure 48 The results from comparative crosslinking study showing dependence of PVA/DAC (DSA) and PVA/GA (GSA) hydrogels network parameters on the

used DAC or GA crosslinker amount defined by chemical amount of reactive aldehyde groups per sample and “Mowiol” type of PVA. The equivalency between DAC and GA reactive group concentrations is expressed by the two bottom x-axes. The lines connecting points in the graphs are only guides for eyes..... 101

LIST OF TABLES

Table 1 Cellulose content of naturally occurring species. [19–22]	7
Table 2 Degree of polymerization of selected cellulose sources. [19, 23].....	10
Table 3 X-ray diffraction estimated crystallinity of native and man-made cellulose sources. [31–33].....	12
Table 4 Native cellulose fibres tensile properties. [23].....	12
Table 5 Cellulose thermal properties data. [33, 36]	13
Table 6 DAC prepared by periodate oxidation of spruce pulp (DP = 650) with 0.25 M NaIO ₄ at 60 °C. [33, 80]	17
Table 7 Mass average molecular weight (\bar{M}_w) values of source cellulose material and DAC after defined process of solubilization. [97, 98].....	22
Table 8 Classification of hydrogels based on their properties. [8].....	26
Table 9 Catalyst system composition and volume in different sets of PVA/DAC mixtures.[17]	34
Table 10 PVA/DAC samples designation based on different amount of catalyst system and different drying temperatures.[17].....	34
Table 11 Designation of DAC samples within solubilization study distinguished by the solubilization time, used method of heating and initial pH of raw DAC suspension.....	36
Table 12 Composition and volume per sample of catalyst systems used for crosslinking of PVA using fresh and aged DAC. [91]	37
Table 13 PVA/DAC samples prepared using aged DAC. [91].....	38
Table 14 PVA/DAC and PVA/GA samples prepared using different PVA source and different crosslinker (DAC or GA). Equal conditions are expressed by the amount of reactive group (n_{-CHO}) per sample. [91]	38
Table 15 Network parameters, i.e. swelling capacity, equilibrium water content (EWC), gel fraction, average molecular weight between crosslinks (\bar{M}_c) and crosslink density (ρ_c), calculated for PVA/DAC hydrogel samples prepared within pilot study.	47
Table 16 Viscosity and density values of fresh and aged DAC solutions. [99]..	57
Table 17 Different DAC forms C, D (involving two sub-forms noted as D I and D II) and G with the ¹ H and ¹³ C NMR chemical shift assignment in ppm. [99]	60
Table 18 GPC recorded data for DAC solutions in different aging time, where \bar{M}_n is the number average molecular weight; \bar{M}_w is the weight (mass) average	

<i>molecular weight, M_p is the peak molecular weight, \bar{M}_z is the third moment of molecular weight and PDI is the index of polydispersity (\bar{M}_w/\bar{M}_n). [99].....</i>	<i>65</i>
Table 19 <i>DAC solubilization analysis carried out at initial pH = 6 (standard pH setup). [99].....</i>	<i>69</i>
Table 20 <i>DAC solubilization analysis under different initial pH.....</i>	<i>71</i>
Table 21 <i>DAC MWS solubilization analysis under different initial pH.</i>	<i>72</i>
Table 22 <i>Mechanical properties calculated for untreated input PVA and PVA/DAC crosslinked samples. [91].....</i>	<i>81</i>
Table 23 <i>Crystallinity (X) of input material (α-cellulose, DAC and PVA) and resulting PVA/DAC samples prepared using different catalyst systems and aged DAC. [91].....</i>	<i>83</i>
Table 24 <i>^{13}C NMR chemical shifts of PVA and PVA/DAC xerogels. [91].....</i>	<i>85</i>
Table 25 <i>The $T_{1\rho}(^1\text{H})$ and $T_{1\rho}(^{13}\text{C})$ values for PVA and PVA/DAC samples. [91]</i>	<i>86</i>
Table 26 <i>Network parameters (percentage of swelling, equilibrium water content EWC, gel fraction, average molecular weight between crosslinks \bar{M}_c and crosslink density ρ_c) of PVA/DAC (DTC) samples prepared using different concentrations of DAC crosslinking agent and “Mowiflex” type of PVA. Different concentrations are also expressed by crosslinker reactive aldehyde groups ($n_{\text{-CHO}}$) per sample. [91]</i>	<i>95</i>
Table 27 <i>Network parameters of PVA/GA (GTC) samples prepared using different concentrations of GA crosslinking agent defined by chemical amount of reactive aldehyde groups ($n_{\text{-CHO}}$) per sample and “Mowiflex” type of PVA. [91].....</i>	<i>96</i>
Table 28 <i>Network parameters of PVA/DAC (DSA) samples prepared using different concentrations of DAC crosslinking agent and “Mowiol” type of PVA.</i>	<i>99</i>
Table 29 <i>Network parameters of PVA/GA (GSA) samples prepared using different concentrations of GA crosslinking agent defined by chemical amount of reactive aldehyde groups per sample and “Mowiol” type of PVA.</i>	<i>100</i>

LIST OF ABBREVIATIONS

Alphabetically ordered

AGU	D-anhydroglucopyranose unit
ATR	Attenuated total reflection
BNC	Bacterial nanocellulose
Cell	Cellulose
CNWs	Cellulose nanowhiskers
CP/MAS	Cross-polarization/magic-angle-spinning
D.O.	Degree of oxidation
DAC	Dialdehyde cellulose
DAS	Diadehyde starch
DCC	Dicarboxy cellulose
DEA	Diethanolamine
DP	Degree of polymerization
ELS	Evaporative light scattering
ESI	Electrospray ionization
EWC	Equilibrium water content
FE-SEM	Field-emission scanning electron microscope
FT-IR	Fourier-transform infrared spectroscopy
GA	Glutaraldehyde
GPC	Gel permeation chromatography
HMBC	Heteronuclear multiple bond correlation
HPLC	High-performance liquid chromatography
HSQC	Heteronuclear single quantum coherence
IR	Infrared
insol.	Insolubilized (raw) dialdehyde cellulose
LC	Liquid chromatography
LC-MS	Liquid chromatography–mass spectrometry
LC-QTOF MS	Liquid chromatography quadrupole time-of-flight mass spectrometry
MWS	Microwave assisted solubilization
Na-DCC	Sodium salt of 2,3-dicarboxy cellulose

NFC	Nanofibrillar cellulose
NMR	Nuclear magnetic resonance
PAA	Poly(acrylic acid)
PTFE	Polytetrafluoroethylene
PVA	Poly(vinyl alcohol)
PVA/DAC	Poly(vinyl alcohol) hydrogels crosslinked by dialdehyde cellulose
PVA/GA	Poly(vinyl alcohol) hydrogels crosslinked by glutaraldehyde
Q-TOF	Quadrupole time-of-flight mass spectrometer
RI	Refractive index
ROESY	Rotating-frame Overhauser spectroscopy
SEM	Scanning electron microscopy
sol.	Solubilization/solubilized
TA	Tannic acid (section 4.3)
temp.	Temperature
TGA	Thermogravimetric analysis
TOCSY	Total correlation spectroscopy
UV	Ultraviolet
WoS	Web of Science
XRD	X-ray diffraction analysis

LIST OF SYMBOLS

Alphabetically ordered

a, b, c	Vectors of crystallographic axes
C1–C6	Numbered carbon atoms of D-anhydroglucopyranose unit
E	Young's modulus
g	Gravitational acceleration
J_{H-C}	Indirect spin-spin coupling constant
M	Molarity (molar concentration)
M_0	Weight of washed and dried hydrogel
\bar{M}_c	Average molecular weight between crosslinks
M_i	Molecular weight of particular polymer species
M_{init}	Weight of unwashed dry hydrogel
mm	Isotactic triad
\bar{M}_n	Number average molecular weight
M_p	Peak molecular weight
mr	Heterotactic triad
M_s	Weight of hydrogel at equilibrium conditions
M_t	Weight of swollen polymer at time
\bar{M}_w	Weight (mass) average molecular weight
\bar{M}_z	Z-average (third moment) of molecular weight
N	Normality (equivalent concentration)
n_{-CHO}	Chemical amount of crosslinkers reactive aldehyde groups
N_i	Number of moles of polymer species of particular molecular weight
PDI	Index of polydispersity
pH	Potential of hydrogen
rr	Syndiotactic triad
t	Swelling time
T	Temperature
$T_{1\rho}(^{13}\text{C})$	Carbon spin-lattice relaxation time in rotating frame
$T_{1\rho}(^1\text{H})$	Proton spin-lattice relaxation time in rotating frame
V_l	Molar volume of water

$V_{2,s}$	Polymer volume fraction
vol%	Percentage by volume
wt%	Percentage by weight
X	Crystallinity
α, β, γ	Angles between vectors of crystallographic axes
δ_{st}	Chemical shift of secondary reference
λ	Wavelength
\bar{v}	Specific volume of polymer
ρ_c	Crosslink density
ρ_p	Density of polymer
ρ_w	Density of water
σ	Tensile strength
χ_1	Polymer-solvent interaction parameter

LIST OF UNITS

Alphabetically ordered

$\%/\text{°C}$	weight percentage per degree Celsius
°C	degree Celsius
$\text{°C}/\text{min}$	degree Celsius per minute
$2\theta \text{ °}$	two Theta degree (angle)
Å	ångström
cm	centimetre
cm^{-1}	reciprocal centimetre
cm^3/g	cubic centimetre per gram
g	gram
g/cm^3	gram per cubic centimetre
g/mol	gram per mole
GHz	gigahertz
GPa	gigapascal
h	hour
Hz	hertz
J/g	joule per gram
J/g.K	joule per gram Kelvin
kDa	kilodalton
kHz	kilohertz
kJ/g	kilojoule per gram
kJ/mol	kilojoule per mole
kV	kilovolt
m/z	mass-to-charge ratio
mg	milligram
mg/mL	milligram per millilitre
MHz	megahertz
mL	millilitre
mL/min	millilitre per minute
mm	millimetre
mm/min	millimetre per minute
mm^2/s	square millimetre per second

mmol	millimole
mmol/cm ³	millimole per cubic centimetre
mmol/g	millimole per gram
mol	mole
MPa	megapascal
mPa.s	millipascal second
ms	millisecond
<i>n</i>	average number of monomeric units in one macromolecular chain
nm	nanometre
ppm	parts per million
rpm	revolutions per minute
V	volt
W	watt
W/m.K	watt per meter Kelvin
μL	microliter
μm	micrometre
μmol	micromole

LIST OF PUBLICATIONS

Journal articles relevant to the Doctoral Thesis:

- [1] MÜNSTER, L., VÍCHA, J., KLOFÁČ, J., MASAŘ, M., KUCHARCZYK, P. and KUŘITKA, I. Stability and aging of solubilized dialdehyde cellulose. *Cellulose*. 2017. Vol. 24, no. 7, p. 2753–2766. DOI 10.1007/s10570-017-1314-x.
- [2] MÜNSTER, L., VÍCHA, J., KLOFÁČ, J., MASAŘ, M., HURAJOVÁ, A. and KUŘITKA, I. Dialdehyde Cellulose Crosslinked Poly(vinyl alcohol) Hydrogels: Influence of Catalyst and Crosslinker Shelf Life. *Carbohydrate Polymers*. 2018. accepted.

Other journal articles:

- [1] BAŽANT, P., KUŘITKA, I., MÜNSTER, L., MACHOVSKÝ, M., KOŽÁKOVÁ, Z. and SÁHA, P. Hybrid nanostructured Ag/ZnO decorated powder cellulose fillers for medical plastics with enhanced surface antibacterial activity. *Journal of Materials Science: Materials in Medicine*. 2014. Vol. 25, no. 11, p. 2501–2512. DOI 10.1007/s10856-014-5274-5.
- [2] BAŽANT, P., MÜNSTER, L., MACHOVSKÝ, M., SEDLÁK, J., PASTOREK, M., KOŽÁKOVÁ, Z. and KUŘITKA, I. Wood flour modified by hierarchical Ag/ZnO as potential filler for wood/plastic composites with enhanced surface antibacterial performance. *Industrial Crops and Products*. 2014. Vol. 62, p. 179–187. DOI 10.1016/j.indcrop.2014.08.028.
- [3] BAŽANT, P., KUŘITKA, I., MÜNSTER, L. and KALINA, L. Microwave solvothermal decoration of the cellulose surface by nanostructured hybrid Ag/ZnO particles: a joint XPS, XRD and SEM study. *Cellulose*. 2015. Vol. 22, no. 2, p. 1275–1293. DOI 10.1007/s10570-015-0561-y.
- [4] MÜNSTER, L., BAŽANT, P. and MACHOVSKÝ, M. Microwave-assisted hydrothermal synthesis of Ag/ZnO sub-microparticles. *Materiali in tehnologije*. 2015. Vol. 49, no. 2, p. 281–284. DOI 10.17222/mit.2013.223.
- [5] MATYÁŠ, J., MÜNSTER, L., OLEJNÍK, R., VLČEK, K., SLOBODIAN, P., KRČMÁŘ, P., URBÁNEK, P. and KUŘITKA, I. Antenna of silver nanoparticles mounted on a flexible polymer substrate constructed using inkjet print technology. *Japanese Journal of Applied Physics*. 2016. Vol. 55, no. 2S, p. 02BB13. DOI 10.7567/JJAP.55.02BB13.
- [6] CVEK, M., MRLÍK, M., ILČÍKOVÁ, M., MOSNÁČEK, J., MÜNSTER, L. and PAVLÍNEK, V. Synthesis of Silicone Elastomers Containing Silyl-Based Polymer-Grafted Carbonyl Iron Particles: An Efficient Way To Improve Magnetorheological, Damping, and Sensing Performances. *Macromolecules*. 2017. Vol. 50, no. 5, p. 2189–2200. DOI 10.1021/acs.macromol.6b02041.

- [7] MASAŘ, M., URBÁNEK, P., ŠKODA, D., HANULÍKOVÁ, B., KOŽÁKOVÁ, Z., MACHOVSKÝ, M., MÜNSTER, L. and KUŘITKA, I. Preparation and characterization of expanded g-C 3 N 4 via rapid microwave-assisted synthesis. *Diamond and Related Materials*. 2018. Vol. 83, p. 109–117. DOI 10.1016/j.diamond.2018.01.028.
- [8] ŠKODA, D., URBÁNEK, P., ŠEVČÍK, J., MÜNSTER, L., NADAZDY, V., CULLEN, D. A., BAŽANT, P., ANTOŠ, J. and KUŘITKA, I. Colloidal cobalt-doped ZnO nanoparticles by microwave-assisted synthesis and their utilization in thin composite layers with MEH-PPV as an electroluminescent material for polymer light emitting diodes. *Organic Electronics*. 2018. Vol. 59, p. 337–348. DOI 10.1016/j.orgel.2018.05.037.

Contributions to conference proceedings:

- [1] MÜNSTER, L. and KUŘITKA, I. Vliv koncentrace katalyzačního systému a teploty sušení na síťování PVA/DAC směsi. In : *PLASTKO 2016*. Zlín, 2016. p. 507–515. ISBN 978-80-7454-590-0.
- [2] MÜNSTER, L., VÍCHA, J., KLOFÁČ, J., MASAŘ, M., HURAJOVÁ, A. and KUŘITKA, I. Dialdehydde Cellulose as Crosslinking Agent for Poly(vinyl alcohol) Hydrogels. In : *P.SAHA.18*. Zlín, 2018. ISBN 978-80-7454-729-4.
- [3] MÜNSTER, L., VÍCHA, J., KLOFÁČ, KUCHARCZYK, P., J., MASAŘ and KUŘITKA, I. Investigation of Stability and Aging of Solubilized Dialdehyde Cellulose. In : *P.SAHA.18*. Zlín, 2018. p. ISBN 978-80-7454-729-4.
- [4] KLOFÁČ, J., MÜNSTER, L., BAŽANT, P., SEDLÁK, J. and KUŘITKA, I. Preparation of Flower-Like ZnO Microparticles by Microwave Assisted Synthesis. In : *NANOCON 2012*. Brno, 2012. p. 344–348. ISBN 978-80-87294-35-2.
- [5] MÜNSTER, L., KLOFÁČ, J., SEDLÁK, J., BAŽANT, P., MACHOVSKÝ, M. and KUŘITKA, I. Microwave Assisted Modification of Bio-Template by Ag-ZnO Sub-Microparticles. In : *NANOCON 2012*. Brno, 2012. p. 618–622. ISBN 978-80-87294-35-2.
- [6] MATYÁŠ, J., OLEJNÍK, R., SLOBODIAN, P., MÜNSTER, L., KRČMÁŘ, P. and STEININGER, A. Multiband Antenna Made of Flexible Polymer Substrate Printed with Silver Nanoparticles Using Inkjet Print Technology - A Feasibility Study. In : *NANOCON 2015*. Brno, 2015. p. 377–381. ISBN 978-80-87294-63-5.
- [7] MATYÁŠ, J., OLEJNÍK, R., SLOBODIAN, P., MÜNSTER, L. and URBÁNEK, P. Mikropásková anténa na bázi nanočástic stříbra natištěná na polymerním substrátu. In : *PLASTKO 2016*. Zlín, 2016. p. 340–346. ISBN 978-80-7454-590-0.

CURRICULUM VITAE

Personal information

Name: Lukáš Münster
Date of birth: 17th January 1989
Place of birth: Zlín, Czech Republic
Nationality: Czech
Permanent address: Nevšová 51
763 21 Slavičín
Czech Republic
Affiliation: Centre of Polymer Systems,
Tomas Bata University in Zlín,
Tř. T. Bati 5678, 760 01 Zlín,
Czech Republic
Telephone/E-mail: +420 576 038 128/munster@utb.cz

Education:

2013 – to date
Tomas Bata University in Zlín, Faculty of Technology,
Ph.D., Chemistry and Materials Technology,
Technology of Macromolecular Compounds
2011 – 2013
Tomas Bata University in Zlín, Faculty of Technology,
M.Sc., Chemistry and Materials Technology,
Polymer Engineering
2011/08 – 2011/11
ERASMUS student exchange programme at
Chalmers University of Technology
Chalmersplatsen 4, 412 58 Göteborg,
Sweden
2008 – 2011
Tomas Bata University in Zlín, Faculty of Technology,
B.Sc., Chemistry and Materials Technology,
Polymeric Materials and Technologies
2004 – 2008
Grammar school of Jan Pivečka in Slavičín

Research projects:

NPU I LO1504 – Centre of Polymer Systems plus – research project worker (2015–2020)

GAČR 16-05961S – Advanced Carriers for Platinum Drugs – member of the research team (2016–2018)

GAČR 16-20361Y – Smart systems based on modified graphene oxide particles – member of the research team (2016–2018)

CZ.01.1.02/0.0/0.0/15_019/0005090 – Stenopeic aperture for presbyopia correction – member of the research team (2016–2018)

IGA/FT/2017/007 – Preparation and characterization of nanostructured polymeric and composite systems – member of research team

IGA/FT/2016/006 – Synthesis of functional filler on the basis of metal oxides and sulphides – member of research team

IGA/CPS/2015/005 – Study of synthetic polymer and biopolymer blends – head of research team – project investigator

IGA/FT/2014/008 – Polymer systems with potential medical applications – member of research team

IGA/FT/2013/014 – A new trend in preparation of particles for intelligent systems – member of the research team

IGA/FT/2012/042 – Composite materials with controlled release of active species – member of the research team

Pedagogic activities:

Participated on teaching in laboratory classes of “Preparation and Characterization Methods” and “Nanomaterials and Nanotechnology”.

Trainings:

Summer school of electron microscopy (Brno 2015)

Pharmacokinetic seminary (Pardubice 2016)

Lukáš Münster

**Dialdehyde cellulose preparation, characterization and
utilization as a crosslinking agent for PVA**

Příprava, charakterizace a využití dialdehydu celulózy jako síťovacího činidla
pro PVA

Doctoral Thesis

Published by Tomas Bata University in Zlín,
nám. T. G. Masaryka 5555, 760 01 Zlín.

Print run: printed electronically

Typesetting: Lukáš Münster

This publication did not pass through editorial or stylistic revision.

Year of Publication 2018